Spring 2008

Formation control of car-like mobile robots

Shweta Annapurani Panimadai Ramaswamy

Department:

FORMATION CONTROL OF CAR-LIKE MOBILE ROBOTS

by

SHWETA ANNAPURANI PANIMADAI RAMASWAMY

A THESIS

Presented to the Graduate Faculty of the

MISSOURI UNIVERSITY OF SCIENCE AND TECHNOLOGY

In Partial Fulfillment of the Requirements for the Degree

MASTER OF SCIENCE IN ELECTRICAL ENGINEERING

2008

Approved by

Dr. S.N. Balakrishnan, Co-Advisor
Dr. Donald C. Wunsch II, Co-Advisor
Dr. Ganesh Kumar Venayagamoorthy

ABSTRACT

In literature, leader – follower strategy has been used extensively for formation control of car-like mobile robots with the control law being derived from the kinematics. This work takes it a step further and nonlinear control laws are derived for formation control of car-like mobile robots using robot dynamics.

Firstly, a traditional tracking and control design approach already available in literature is derived and discussed for a car-like mobile robot. It involves a decoupled design involving two separate algorithms, one for velocity control design and another for torque control design. Weak interactions among the algorithms and separate designs make the robot performance optimization and the formation stability difficult to achieve. So, a new tracking and control architecture wherein the conventional elements are replaced by a single component that performs all the functions and hence called the integrated tracking and control scheme is used.

In a novel approach, the integrated tracking and control scheme is used to obtain a nonlinear control law for each follower in the formation. The controllers are obtained using Lyapunov analysis method and State Dependent Algebraic Riccati Equation (SDARE) based optimal control method. To bring robustness into the controller design, unknown quantities like friction, desired accelerations (unmeasured) are computed using an online neural network and the simulations are carried out in the presence of measurement noises. A robust optimal control design is made possible by using the extra control design approach using online neural networks. Simulation results prove the ability of the controllers to effectively stabilize the formation while maintaining the desired relative distance and bearing.

ACKNOWLEDGEMENTS

I would like to thank my advisor Dr. S.N. Balakrishnan for providing me with an opportunity do my Master's degree. With his continued guidance and support, he has been a source of inspiration for me during the past 2 years. He has constantly egged me on to think more, aim higher and never to settle for the ordinary. He helped me identify different ways to solve a research problem and has taught me the importance of analytical thinking, validation and the need to be persistent in accomplishing my goals. He has placed immense confidence in my abilities and made me believe in myself when doubts plagued me. Above all he has always been my well wisher and a person who has supported me in all my endeavors. A special thanks goes to him for helping me with the research and complete the writing of this thesis. I would also like to thank Dr. Donald C. Wunsch and Dr. Ganesh Kumar Venayagamoorthy, for accepting to be on my thesis review committee. I am grateful to my committee members for reviewing my thesis on short notice.

A special thanks goes to all my teachers, colleagues and friends who have made my days in grad school very memorable. If not for grad school, I wouldn’t have met a few of my closet friends that I have made for life now. Before I finish, I thank my mother for all the support that she has provided me over these years and the sacrifices she has made for me. I would not have been able to achieve this degree without her constant encouragement and moral support. Last but not the least, I pray to God to provide me with the strength and courage to face all the challenges that lie ahead in my life and career.

TABLE OF CONTENTS

Page

ABSTRACT iii

ACKNOWLEDGEMENTS iv

LIST OF ILLUSTRATIONS vii

SECTION

1. INTRODUCTION 1
   - 1.1. MOTIVATION 1
   - 1.2. PREVIOUS WORK 1
   - 1.3. CONTRIBUTIONS OF THIS THESIS 3
   - 1.4. ORGANIZATION 5
2. MATHEMATICAL MODEL 6
   - 2.1. KINEMATIC MODEL 6
   - 2.2. DYNAMIC MODEL 8
3. ROBOT PLATFORM, SENSING AND STATE MEASUREMENT 11
4. FORMATION CONTROL PROBLEM AND ERROR DYNAMICS FORMULATION 14
5. TRADITIONAL TRACKING AND CONTROL DESIGN USING LYAPUNOV FUNCTION BASED APPROACH 21
   - 5.1. CONTROLLER DESIGN 21
   - 5.2. WEIGHT UPDATE RULE AND PROOF OF BOUNDED-NESS OF WEIGHTS 25
   - 5.3. FORMATION STABILITY 27
   - 5.4. RESULTS AND DISCUSSION 28
6. ERROR SYSTEM FORMULATION FOR INTEGRATED TRACKING AND CONTROL 40
7. INTGERATED TRACKING AND OPTIMAL CONTROL DESIGN: APPLICATION OF SDARE 42
   - 7.1. OPTIMAL CONTROL PROBLEM AND SDARE APPROACH 42
   - 7.2. CONTROLLER DESIGN 43
   - 7.3. FORMATION STABILITY 54
   - 7.4. RESULTS AND DISCUSSION 55

8. INTEGRATED TRACKING AND ROBUST OPTIMAL CONTROL DESIGN USING ONLINE NEURAL NETWORK AND SDARE APPROACH 65

8.1. PROBLEM DESCRIPTION 65

8.2. OPTIMAL CONTROL DERIVATION FOR THE NOMINAL SYSTEM 66

8.3. UNCERTAINITY MODELING, WEIGHT UPDATES AND EXTRA CONTROL DERIVATION 70

8.4. FORMATION STABILITY 74

8.5. RESULTS AND DISCUSSION 75

9. INTEGRATED TRACKING AND CONTROL DESIGN USING LYAPUNOV FUNCTION BASED APPROACH 101

9.1. CONTROLLER DESIGN 101

9.2. USE OF NEURAL NETWORK FOR CONTROLLER DESIGN, WEIGHT UPDATE RULE AND PROOF OF BOUNDED-NESS OF WEIGHTS 104

9.3. FORMATION STABILITY 108

9.4. RESULTS AND DISCUSSION 109

BIBLIOGRAPHY 119

VITA 122

LIST OF ILLUSTRATIONS

Page

Figure 2.1 Bicycle Model 6
Figure 2.2 Free Body Diagram 9
Figure 3.1 Car-like Mobile Robot..... 11
Figure 3.2 Schematic of the Mobile Robot Platform..... 13
Figure 4.1 Formation Structure..... 16
Figure 5.1 Actual and Desired Position and Orientation of the Follower 30
Figure 5.2 Position and Orientation Errors in Body Coordinates..... 31
Figure 5.3 Drive and Steering Torques..... 32
Figure 5.4 Magnified Plot of Drive and Steering Torques 33
Figure 5.5 Leader and Follower Trajectories..... 34
Figure 5.6 Linear and Angular Velocity Profile of the Follower 35
Figure 5.7 Magnified Plot of Linear and Angular Velocity Profile of the Follower..... 36
Figure 5.8 Velocity and Steering Angle Error Plots..... 37
Figure 5.9 Neural Network Outputs in Comparison with Actual Outputs 38
Figure 5.10 Relative Distance and Relative Bearing of the Follower w.r.t. Leader..... 39
Figure 7.1 Actual and Desired Position and Orientation of the Follower 57
Figure 7.2 Position and Orientation Errors in Body Coordinates..... 58
Figure 7.3 Drive and Steering Torques..... 59
Figure 7.4 Leader and Follower Trajectories..... 60
Figure 7.5 Linear Velocity and Angular Velocity Profile of the Follower..... 61
Figure 7.6 Velocity Error and Steering Angle Error Plots..... 62
Figure 7.7 Relative Distance and Relative Bearing Angle of the Follower w.r.t. Leader 63
Figure 8.1 Actual and Desired Position and Orientation of the Follower 76
Figure 8.2 Position and Orientation Errors of the Follower in Body Coordinates 77
Figure 8.3 Position and Orientation Errors of the Follower in Inertial Coordinates 78
Figure 8.4 Optimal Control Inputs to the Follower Linear and Angular..... 79
Figure 8.5 Magnified Plot of Optimal Control Inputs to the Follower..... 80
Figure 8.6 Magnified Plot of Extra Control Input to the Follower..... 81
Figure 8.7 Extra Control Inputs to the Follower..... 82

Figure 8.8 Drive Torque and Steering Torque of the Follower 83
Figure 8.9 Leader and Follower Trajectories 84
Figure 8.10 Velocity Profile of the Follower 85
Figure 8.11 Velocity and Steering Angle Error Plots 86
Figure 8.12 Neural Network Output 87
Figure 8.13 Neural Network Approximation Error 88
Figure 8.14 Magnified Plot of Noisy Inputs to the Neural Network 89
Figure 8.15 Plots Showing the Bounded-ness of Neural Network Weights 90
Figure 8.16 Relative Distance and Relative Bearing Angle of the Follower w.r.t. Leader 91
Figure 8.17 Actual and Desired Position and Orientation of the follower with $U_{EX} = 0$. 92
Figure 8.18 Magnified Actual and Desired Position and Orientation of the Follower with $U_{EX} = 0$ 93
Figure 8.19 Magnified Position and Orientation Error Plots of the Follower with $U_{EX} = 0$ 94
Figure 8.20 Magnified Position and Orientation Error Plots in Inertial Coordinates with $U_{EX} = 0$ 95
Figure 8.21 Magnified Linear and Angular Velocity Profile of the Follower with $U_{EX} = 0$ 96
Figure 8.22 Magnified Velocity and Steering Angle Error Plots for the Follower with $U_{EX} = 0$ 97
Figure 8.23 Magnified Relative Distance and Bearing Angle of the Follower w.r.t Leader with $U_{EX} = 0$ 98
Figure 8.24 Magnified Optimal Control Inputs to the Follower with $U_{EX} = 0$ 99
Figure 9.1 Actual and Desired Position and Orientation of the Follower 110
Figure 9.2 Leader and Follower Trajectories 111
Figure 9.3 Drive and Steering Torques 112
Figure 9.4 Position and Orientation Errors in Body Coordinates 113
Figure 9.5 Position and Orientation Errors in Inertial Coordinates 114
Figure 9.6 Velocity and Steering Angle Error Plots 115
Figure 9.7 Relative Distance and Relative Bearing of the Follower w.r.t. Leader 116
Figure 9.8 Error Rate Plots 117
Figure 9.9 Linear and Angular Velocity Profile of the Follower 118

1. INTRODUCTION

1.1. MOTIVATION

The use of dynamics coupled with kinematics for control of autonomous mobile robots has been gaining increasing popularity in recent years. The majority of control algorithms available in literature for autonomous mobile robots use only the kinematic model [1]. The kinematic model has its own advantages. It helps in keeping the steering and velocity of the vehicle completely decoupled but in the process, the dynamics of the vehicle is not taken into account and hence remains ignored. The velocity of the car-like robot is very dependant upon the dynamics of the steering system. Hence, in order to control the speed of the vehicle, the dynamics of the vehicle as well as dynamics of the steering must be taken into account.

Automating car-like robot has many advantages which include operating in hazardous environments like mines, data collection and reconnaissance etc. These controllers can be put to use in autonomous armored vehicles (note not tanks) for patrolling the streets to detect improvised explosive devices (IED's). In most of these scenarios the use of a team of robots is advantageous. Employing a team of mobile robots helps in increasing the efficiency with which the task is completed. In case of rescue and search operations, reconnaissance, detection of IED's etc the use of a team helps in faster search of the entire search space and the operation can be carried out in a very systematic and effective way. It is extremely valuable in time critical operations. Hence the focus of research has shifted to the control of a swarm or team of mobile robots in the recent years instead of a single nonholonomic robot.

1.2. PREVIOUS WORK

There are many references available for control of single nonholonomic mobile robots [2]-[8]. The focus of this paper is on the formation control of a team of car-like mobile robots. There are various techniques available in literature for formation control of team of mobile robots. A few of the most commonly used techniques are: leader-

follower [9]-[13], virtual structure based [14] [15] and behavior based approaches [8] [16] [17].

In the virtual structure approach the entire formation is considered as a single virtual rigid structure. A desired motion is assigned to the virtual structure as a whole, which will trace out trajectories for each robot in the formation to follow. The main disadvantage of the virtual structure implementation is centralization, which leads to a single point of failure for the whole system.

In [14] Tan et al. developed a method for motion control of multiple robots using the idea that points in space maintaining fixed geometric relationships behave identically to the points on a rigid body moving through space, hence using the concept of movement inside a virtual structure. Ogren et al. in [15] use control Lyapunov functions to define the formation and in addition use the idea of virtual vehicles to obtain the control for multi agent coordination.

Behavior based approach prescribes several desired behaviors for each robot and the final action of each robot is derived by weighting the relative importance of each behavior. Limitation of this approach is that it is difficult to analyze mathematically, therefore it is hard to guarantee a precise formation control. In [16] [17] Balch et al. and Lawson et al. use the behavior based approach for formation control of multiple robots.

The leader follower approach involves maintaining a desired relative distance and relative bearing between the leader and the follower. The follower robots need to position themselves relative to the leader and maintain a desired relative position which needs to be specified. When the motion of the leader is known, the desired positions of the followers relative to the leader can be achieved by local control law on each follower.

In [1] Shao et al. use the concept of a virtual vehicle and the kinematics to derive the error system for control of multiple Pioneer 3DX vehicles. Li et al. [10] present a kinematics model for the leader following based formation control of tricycle mobile robots and a back stepping based stabilizing controller is derived under the conditions of perfect velocity tracking and no disturbances. Dierks et al. in [10] control a differentially steered robot by backstepping kinematics into dynamics. Desai et al. in [18] use the kinematic model and graph theory to design a controller for multiple mobile robot formations.

1.3. CONTRIBUTIONS OF THIS THESIS

The autonomous mobile robot considered in this work is a front steer, rear drive car-like mobile robot. The focus of this work is on the formation control of a team of car-like mobile robots. The most commonly used technique; the leader follower approach is used in this work.

Unlike other papers, the dynamics of both the drive and the steering system are considered in this study. For the purpose of simulations a single leader single follower scenario is considered but the same can easily be extended to multiple follower scenarios and theoretical proofs are derived to justify the same. The separation-bearing ($l-\psi$) technique is made use of instead of the separation-separation strategy. The objective is to find a toque control input for the follower that will drive the relative distance and relative bearing between the leader and follower to the desired value. Two different schemes are considered;

a) *Traditional tracking and control design* which uses a decoupled design involving two separate algorithms, one for velocity control design and another for torque control design. A lot has already been said about this method in literature. In this work, it has been adapted and simpler equations used for car-like mobile robots. Firstly, a velocity control input is designed for the $l-\psi$ formation control that will drive the relative distance and relative bearing between the leader and follower to the desired value. The dynamics of the leader and the follower are used to derive specific torque control inputs required to achieve the desired velocity profile derived earlier. Imperfect velocity tracking condition is considered. The asymptotic stability of the system is also guaranteed and it is proved that the position tracking errors and the velocity tracking errors go to zero asymptotically. Unknown quantities like friction, desired acceleration (unmeasured) are computed using an online neural network in the presence of measurement noises thereby making the controller robust. Simulation results prove the ability of the controller to effectively stabilize the formation while maintaining the desired relative distance and bearing.

Proofs are derived to guarantee formation stability in case of multiple robot formations with single leader and "*n*" followers.

b) Control law for each follower is obtained using *integrated tracking and control scheme* [19]. Traditional tracking and control designs use a decoupled design involving two separate algorithms, one for velocity control design and another for torque control design. Weak interactions among the algorithms and separate designs make the robot performance optimization and the formation stability difficult to achieve. So a new tracking and control architecture wherein the conventional elements are replaced by a single component that performs all the functions and hence called the integrated tracking and control scheme is used. This results in achieving a level of synergism between robot control and tracking which is extremely difficult to achieve in a decoupled scheme.

Initially, a coupled framework is obtained wherein the follower error equations are combined with follower dynamics. Once the combined framework is obtained, the state space equations thus obtained are used to design torque control inputs for the follower drive system as well as the steering system so that the formation is maintained. The asymptotic stability of the system is also guaranteed. The control inputs are designed using an optimal control approach and Lyapunov analysis approach.

In the Lyapunov approach unknown quantities like friction, desired acceleration (unmeasured) are computed using an online neural network. Simulation results prove the ability of the controller to effectively stabilize the formation while maintaining the desired relative distance and bearing.

A state dependant algebraic Riccati equation (SDARE) method [20]-[25] is used to obtain the optimal control law for the follower to maintain the formation. An *extra control* is used to handle the unmodeled uncertainties of the system [26]. The extra control makes the controller robust to uncertainties due to modeling error or parameter variations. In the design of the extra control an online neural network is used for approximating the unknown quantities and model uncertainties.

Simulation results prove the ability of the controller to effectively stabilize the formation while maintaining the desired relative distance and bearing. Proofs are derived to guarantee formation stability in case of multiple robot formations with single leader and "*n*" followers

1.4. ORGANIZATION

In Section 2 the mathematical model of the car-like mobile robot is derived. Both the kinematic and dynamic model of the robot are derived in this section.

Section 3 presents the details of the mobile robot base along with sensors and architecture of the mobile robot.

In Section 4 the formation control problem is described, various formation schemes presented and the error dynamics to be used in the design of the controller is derived.

The traditional tracking and control design using Lyapunov method is carried out, the simulation results are presented and discussed in Section 5.

The error system formulation required to perform integrated tracking and control is derived in Section 6.

Integrated tracking and control design using optimal control approach with the SDARE method is presented and the simulation results discussed in Section 7.

In Section 8 integrated tracking and robust optimal control of the car-like mobile robot formation is designed using online neural networks and SDARE approach. The simulation results are also presented and discussed.

Section 9 presents robust integrated tracking and control design using Lyapunov function based approach. Also presented in this section are the simulation results for the same.

2. MATHEMATICAL MODEL

This section discusses the mathematical model used for the vehicle. The kinematic and dynamic models of the vehicle are derived in two separate subsections. The controller for the car-like mobile robot is derived using the mathematical model discussed below.

2.1. KINEMATIC MODEL

The kinematic model of the system will be derived taking the nonholonomic constraints into account. Nonholonomic constraints for mobile robots are non-integrable and are related to its velocity. The robot considered in this work is a four wheeled, front-steer, rear drive mobile robot. For very small angles of steering the robot can be modeled as a bicycle (Figure 2.1) .

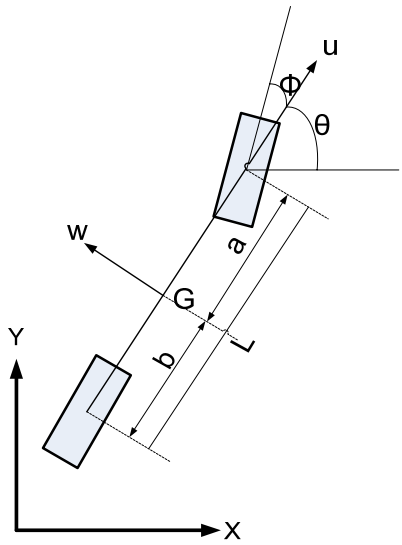

Figure 2.1 Bicycle Model

Consider Figure 2.1. Let (x, y) denote the center of gravity (G) of the robot. The distance from G to the rear and front wheels be a and b respectively. Let θ denote the heading angle of the robot i.e. the orientation of the robot with respect to the $x-axis$ and ϕ denotes the steering angle between the front wheel and the body axis. Let (x_1, y_1) and (x_2, y_2) denote the position of the rear and front wheels. Then from Figure 2.1, (x_1, y_1) and (x_2, y_2) are given by

$$\begin{aligned} x_1 &= x - b\cos(\theta) \quad & x_2 &= x + a\cos(\theta) \\ y_1 &= y - b\sin(\theta) \quad & y_2 &= y + a\sin(\theta) \end{aligned} \tag{1}$$

On differentiation (1) becomes

$$\begin{aligned} \dot{x}_1 &= \dot{x} + b\dot{\theta}\sin(\theta) & \dot{x}_2 &= \dot{x} - a\dot{\theta}\sin(\theta) \\ \dot{y}_1 &= \dot{y} - b\dot{\theta}\cos(\theta) & \dot{y}_2 &= \dot{y} + a\dot{\theta}\cos(\theta) \end{aligned} \tag{2}$$

The nonholonomic constraints for each wheel is given by

$$\begin{aligned} \dot{x}_1\sin(\theta) - \dot{y}_1\cos(\theta) &= 0 \\ \dot{x}_2\sin(\theta+\phi) - \dot{y}_2\cos(\theta+\phi) &= 0 \end{aligned} \tag{3}$$

Substituting (2) in (3) the nonholonomic constraints for the robot are given by

$$\begin{aligned} \dot{x}\sin(\theta) - \dot{y}\cos(\theta) + b\dot{\theta} &= 0 \\ \dot{x}\sin(\theta+\phi) - \dot{y}\cos(\theta+\phi) - a\dot{\theta}\cos(\theta) &= 0 \end{aligned} \tag{4}$$

Let v_u and v_w be the longitudinal and lateral velocities of the vehicle. Using the body coordinates of the vehicle i.e. along the u and w axis $\dot{x}, \dot{y}$ can be written as

$$\begin{aligned} \dot{x} &= v_u\cos(\theta) - v_w\sin(\theta) \\ \dot{y} &= v_u\sin(\theta) + v_w\cos(\theta) \end{aligned} \tag{5}$$

Substituting (5) in (4) and manipulating results in (9)

$$v_u\cos(\theta)\sin(\theta) - v_w\sin^2(\theta) - v_u\sin(\theta)\cos(\theta) - v_w\cos^2(\theta)) + b\dot{\theta} = 0 \tag{6}$$

$$(v_u\cos(\theta) - v_w\sin(\theta))\sin(\theta) - (v_u\sin(\theta) + v_w\cos(\theta))\cos(\theta) + b\dot{\theta} = 0 \tag{7}$$

$$-v_w\sin^2(\theta) - v_w\cos^2(\theta)) = -b\dot{\theta} \tag{8}$$

$$v_w = b\dot{\theta} \tag{9}$$

Also substituting (5) in (4) results in

$$(v_u\cos(\theta) - v_w\sin(\theta))\sin(\theta+\phi) - (v_u\sin(\theta) + v_w\cos(\theta))\cos(\theta+\phi) - a\dot{\theta}\cos(\theta) = 0 \tag{10}$$

Using (9) in (10) and expanding

$$v_u \cos(\theta)\sin(\theta+\phi) - v_w \sin(\theta)\sin(\theta+\phi) - v_u \sin(\theta)\cos(\theta+\phi)$$

$$- v_w \cos(\theta)\cos(\theta+\phi) - a\frac{v_w}{b}\cos(\theta) = 0 \quad (11)$$

Further manipulation results in

$$v_u \sin(\phi) - v_w \cos(\phi) - a\frac{v_w}{b}\cos(\theta) = 0 \quad (12)$$

$$v_u \tan(\phi) = v_w\left(1+\frac{a}{b}\right) \quad (13)$$

$$v_w = \frac{b\tan\phi}{L}v_u \quad (14)$$

From (9) and (14) the heading angle is represented by the differential equation given below

$$\dot{\theta} = \frac{\tan\phi}{L}v_u \quad (15)$$

Using (15) and substituting (14) in (5) the kinematic model of the robot given by

$$\begin{bmatrix}\dot{x}\\ \dot{y}\\ \dot{\theta}\end{bmatrix} = \begin{bmatrix} v_u\cos(\theta) - v_u\frac{b\tan\phi}{L}\sin(\theta) \\ v_u\sin(\theta) + v_u\frac{b\tan\phi}{L}\cos(\theta) \\ \frac{\tan\phi}{L}v_u \end{bmatrix} \quad (16)$$

2.2. DYNAMIC MODEL

Before the dynamic equations are derived, a few assumptions need to be made. The assumptions made are:

(i) There is no slip at the wheel,

(ii) The rear wheels cannot be steered and are always in the same direction as the orientation of the vehicle,

(iii) The drive force and drive torque are assumed to act at the center of the rear wheels [1] [2].

The forces acting on the robot are as shown in Figure 2.2. F_u, F_w, F_d denote the frictional force, the force acting perpendicular to each wheel as a result of the slippage assumption made and the drive force, respectively. Also, m, I denote the mass of the vehicle and the moment of inertia of the vehicle. Balancing the forces acting along the u and w direction as shown in Figure 2.2 results in

$$m(\dot{v}_u - v_w\dot{\theta}) = -F_{uir} - F_{uor} + F_{dir} + F_{dor} - F_{uof}\cos\phi - F_{wof}\sin\phi - F_{uif}\cos\phi - F_{wif}\sin\phi \quad (17)$$

$$\Rightarrow m(\dot{v}_u - v_w\dot{\theta}) = -F_{ur} + F_{dr} - F_{uf}\cos\phi - F_{wf}\sin\phi \quad (18)$$

Similarly,

$$m(\dot{v}_w + v_u\dot{\theta}) = F_{wir} + F_{wor} + F_{wof}\cos\phi + F_{wif}\cos\phi - F_{uif}\sin\phi - F_{uof}\sin\phi \quad (19)$$

$$\Rightarrow m(\dot{v}_w + v_u\dot{\theta}) = F_{wr} - F_{uf}\sin\phi + F_{wf}\cos\phi \quad (20)$$

where $F_{wir} + F_{wor} = F_{wr}$; $F_{uir} + F_{uor} = F_{ur}$; $F_{wif} + F_{wof} = F_{wf}$; $F_{uif} + F_{uof} = F_{uf}$ and $F_{dir} + F_{dor} = F_{dr}$

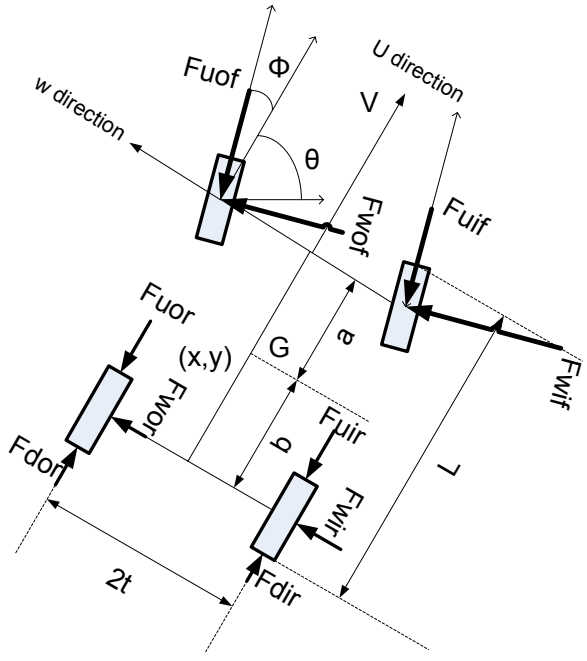

Figure 2.2 Free Body Diagram

Also, from Figure 2.2

$$I\ddot{\theta} = \begin{pmatrix} -b(F_{wir} + F_{wor}) + a(F_{wof} + F_{wif})\cos\phi - a(F_{uif} - F_{uof})\sin\phi \\ +t\left[(F_{wif} - F_{wof})\sin\phi + (F_{uir} - F_{uor}) + (F_{uif} - F_{uof})\cos\phi\right] \end{pmatrix} \tag{21}$$

On manipulation (21) becomes

$$I\ddot{\theta} = \begin{pmatrix} -bF_{wr} + a\left[F_{wf}\cos\phi - (F_{uif} - F_{uof})\sin\phi\right] + t\left[(F_{wif} - F_{wof})\sin\phi + (F_{uir} - F_{uor})\right] \\ +t(F_{uif} - F_{uof})\cos\phi \end{pmatrix} \tag{22}$$

So the dynamical equations of the system are given by(18), (20) and(22). Also steering system dynamics of the robot can be modeled by a first order linear system represented by the differential equation [2]

$$\dot{\phi} = \frac{1}{\tau_s}(u - \phi) \tag{23}$$

where τ_s, u denote the time constant and steering control, respectively.

3. ROBOT PLATFORM, SENSING AND STATE MEASUREMENT

The robot platform consists of a toy Hummer base as the mobile robot base and is shown in Figure 3.1, with the following specifications

- One steering servo motor
- One 12 VDC rear drive motor
- Mass of the vehicle is 7 kgs
- The dimensions of the base are
    a) width = 0.349250 m
    b) length = 0.790575 m
- Drive wheel diameter is 0.28575 m, radius = 0.142875 m

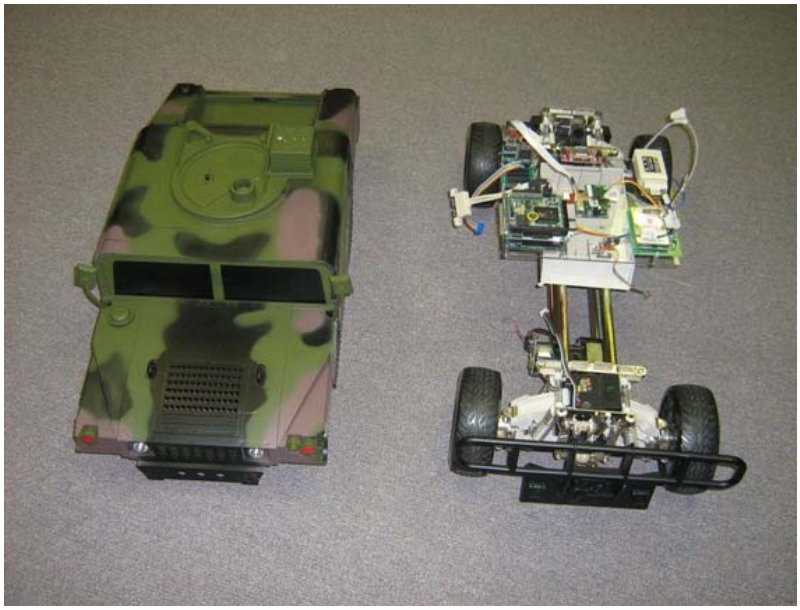

Figure 3.1 Car-like Mobile Robot

The mobile robot base uses a PC104 486 DX2 running at 100 MHz with 32 MB RAM and a 256 MB USB flash drive as the primary processing unit (PPU). The PPU has 16

channels of 16-bit A/D, 4 12-bit D/A channels, 4 serial ports, 1 parallel port, 2 USB ports and 24 DIO lines. Torque control of the DC motors is achieved by using PWM. There is a motor controller mounted on the robot base to provide the servo and drive motors with the desired PWM signals.

A Cirronet radio-modem provides serial communication at 115.2 kbps using the RS-232 COM1 port of the PPU and the base station.

The mobile robot platform also includes the following sensors

- Hewlett Packard wheel encoders HEDS-5500, 500 pulses/rev
- Crossbow INS MNAV 100CA, a calibrated digital sensor system for miniature air and ground robotic navigation. It has the following sensors
    a) Inertial Sensor Array: This is an assembly of three accelerometers, three gyros (rate sensors) with temperature sensors.
    b) Three axis magneto-resistive magnetometers that can be used to compute heading.
    c) A GPS receiver for position and velocity measurement.
    d) Servo Driving Circuit: The integrated circuit that can support up to9 servos.
    e) The R/C Receiver PPM interface that can be used to read the PPM signal from the R/C receiver.
    f) Data processing module, which receives the signals from all the sensors, GPS and PPM interface, and transmits digital data via the serial link, and outputs standard servo signals.

Figure 3.2 shows the schematic of the mobile robot platform. From the schematic it can be seen that the measurements from the sensors are communicated to the PC104 via the serial port. The data thus received by PC104 is filtered using a navigation filter and Kalman filter. The control inputs to drive the motors are obtained by using the filtered data and control algorithms.

The robot platform described above for the implementation of the control algorithm has been built as a part of this work. Real time implementation of the control algorithms to be designed in the sections to come is still in progress.

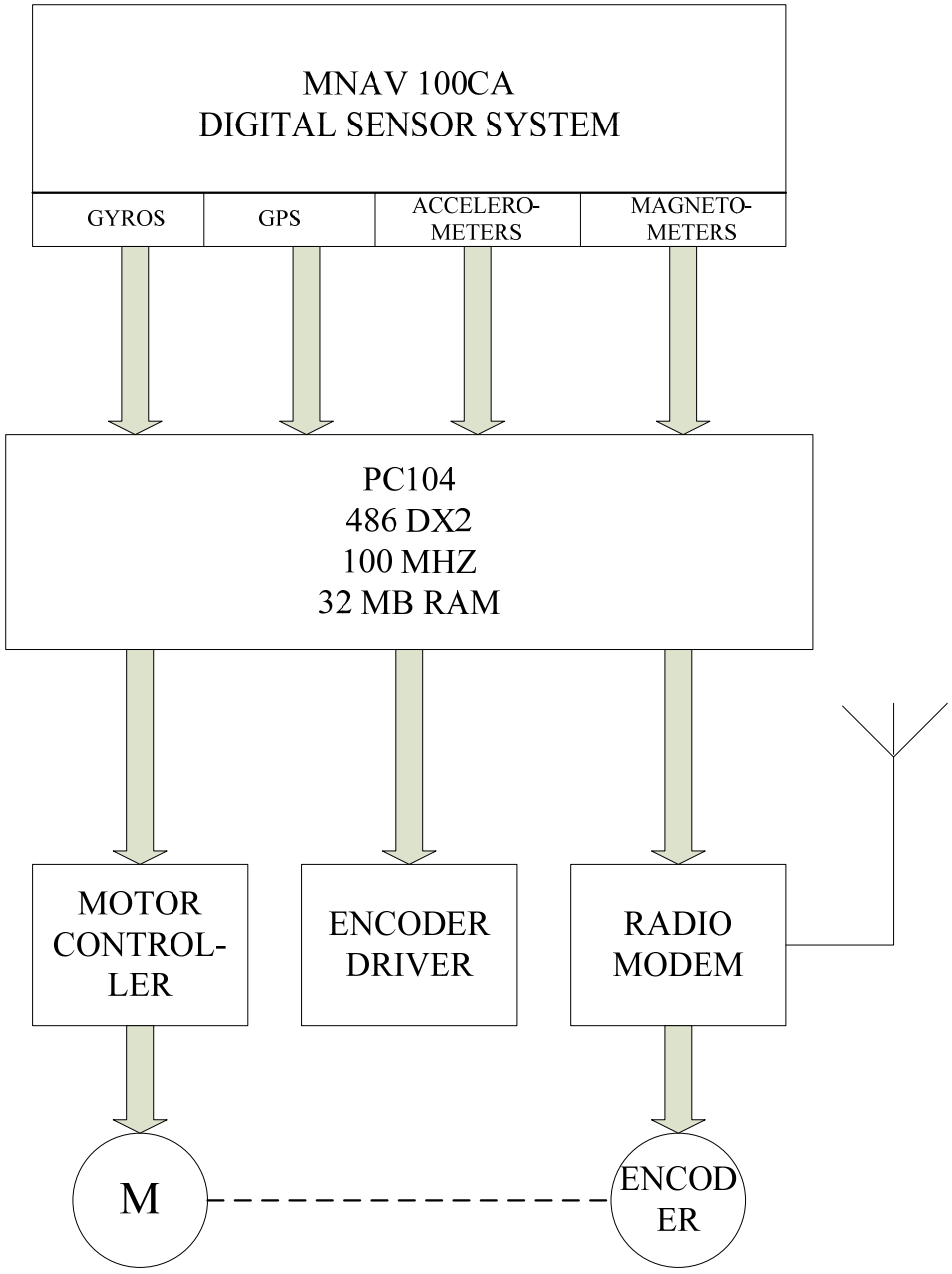

Figure 3.2 Schematic of the Mobile Robot Platform

4. FORMATION CONTROL PROBLEM AND ERROR DYNAMICS FORMULATION

There are various approaches available for formation control. The most common approaches used are the leader follower, virtual structure and behavior based approach. In the virtual structure approach the entire formation is considered as a single virtual rigid structure. A desired motion is assigned to the virtual structure as a whole, which will trace out trajectories for each robot in the formation to follow. The main disadvantage of the virtual structure implementation is centralization, which leads to a single point of failure for the whole system.

In the leader follower approach, one of the robots is designated as the leader with the rest being followers. The follower robots need to position themselves relative to the leader and maintain a desired relative position with respect to the leader. In this formulation the leader's motion and desired relative positions between the leader and the followers needs to be specified. When the motion of the leader is known, the desired positions of the followers relative to the leader can be achieved by local control law on each follower.

Behavior based approach prescribes several desired behaviors for each robot and the final action of each robot is derived by weighting the relative importance of each behavior. Limitation of this approach is that it is difficult to analyze mathematically, therefore it is hard to guarantee a precise formation control.

In this work, the formation control of the robot is achieved using the leader follower approach. The separation-bearing ($l - \psi$) technique is made use of instead of the separation-separation strategy.

The objective is to find a toque control input for the follower that will drive the relative distance and relative bearing between the leader and follower to the desired value. It is assumed that the leader's motion is known i.e. there exists a control law that drives the leader independently to its desired trajectory. Most formation control techniques for car-like robots in the literature involve the kinematics and do not incorporate the dynamics. This issue has been addressed in this work. Two different schemes are addressed:

1) Traditional tracking and control design which uses a decoupled design involving two separate algorithms, one for velocity control design and another for torque control design.

2) A new tracking and control architecture wherein the conventional elements are replaced by a single component that performs all the functions and hence called the integrated tracking and control scheme is used. This results in achieving a level of synergism between robot control and tracking which is extremely difficult to achieve in a decoupled scheme. In this scheme the dynamics is combined along with the error system designed for the formation and the torque control input is designed for the integrated system.

In this section the problem of formation control is modeled as a tracking problem [11] and the goal is to drive the tracking errors to zero. In order to derive the error dynamics for modeling the problem of formation control as a tracking problem, consider the single leader single follower scenario as shown below in Figure 4.1. This can be easily extended to multiple robots in a formation scheme. The subscripts l and f denote the leader and follower respectively. The relative distance L_{LF} is the distance between the rear of the leader (point B) to the front of the follower (point A) and the relative bearing angle ψ_{LF} is the defined as the angle measured from the leader (i.e. the direction of orientation of the leader) to the straight line joining the points A and B. Consider the point A and B in Figure 4.1. They can be written as $[(x_F + d\cos(\theta_F)),(y_F + d\sin(\theta_F))]$ and $[(x_L - d\cos(\theta_L)),(y_L - d\sin(\theta_L))]$ where (x_F, y_F) and (x_L, y_L) indicate the position of the center of mass of the follower and leader respectively. It is assumed that the $a = b = d = L/2$ (refer Figure 2.2 and Figure 4.1), where L is the length of the vehicle and d indicates the distance between the center of mass and the rear and front of the robot.

The relative distance L_{LF} can be expressed in terms of the x and y coordinates of L_{LF} as

$$L_{LF}{}^2 = L_{LFx}{}^2 + L_{LFy}{}^2 \tag{24}$$

where

$$L_{LFx} = x_L - x_F - d(\cos(\theta_L) + \cos(\theta_F)) \tag{25}$$

$$L_{LFy} = y_L - y_F - d(\sin(\theta_L) + \sin(\theta_F)) \tag{26}$$

Also from Figure 4.1, it can be seen that the relative bearing can be expressed in terms of the leader's heading angle and the x and y coordinates of the relative distance as

$$\psi_{LF} = \arctan\left(\frac{L_{LFy}}{L_{LFx}}\right) - \theta_L + \pi \tag{27}$$

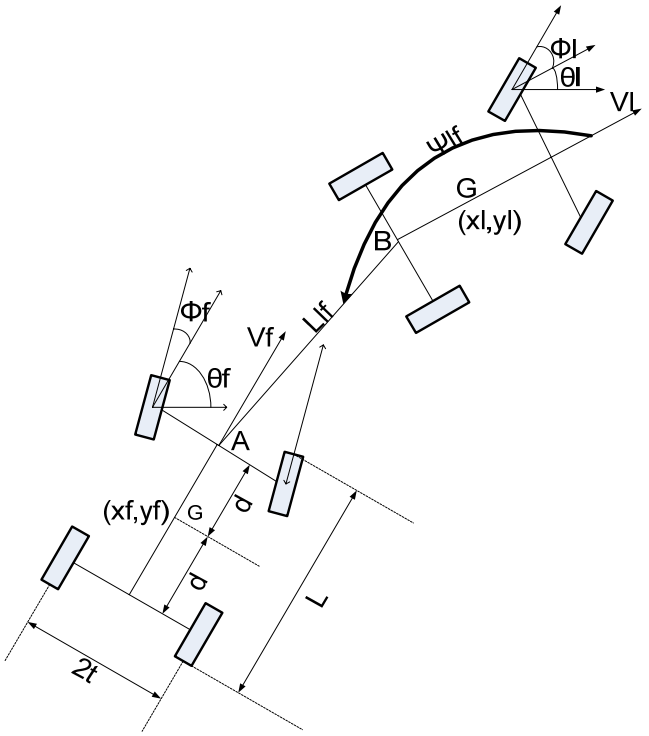

Figure 4.1 Formation Structure

Differentiation of equations (25) and (26) yields

$$\dot{L}_{LFx} = \dot{x}_L - \dot{x}_F + d\dot{\theta}_L \sin(\theta_L) + d\dot{\theta}_F \sin(\theta_F) \tag{28}$$

$$\dot{L}_{LFy} = \dot{y}_L - \dot{y}_F - d\dot{\theta}_L \cos(\theta_L) - d\dot{\theta}_F \cos(\theta_F) \tag{29}$$

The kinematics of the leader and follower from (16) are given by the following equations

$$\begin{bmatrix} \dot{x}_L \\ \dot{y}_L \\ \dot{\theta}_L \end{bmatrix} = \begin{bmatrix} v_L \cos(\theta_L) - d\omega_L \sin(\theta_L) \\ v_L \sin(\theta_L) + d\omega_L \cos(\theta_L) \\ \omega_L \end{bmatrix} \tag{30}$$

$$\begin{bmatrix} \dot{x}_F \\ \dot{y}_F \\ \dot{\theta}_F \end{bmatrix} = \begin{bmatrix} v_F \cos(\theta_F) - d\omega_F \sin(\theta_F) \\ v_F \sin(\theta_F) + d\omega_F \cos(\theta_F) \\ \omega_F \end{bmatrix} \tag{31}$$

where $w_L = \dfrac{v_L \tan(\phi_L)}{L}$ and $w_F = \dfrac{v_F \tan(\phi_F)}{L}$

Substituting (30) and (31) in (28) and (29) , taking $L = 2d$

$$\dot{L}_{LFx} = v_L \cos(\theta_L) - v_F \cos(\theta_F) + v_F \tan(\phi_F) \sin(\theta_F) \tag{32}$$

$$\dot{L}_{LFy} = v_L \sin(\theta_L) - v_F \sin(\theta_F) - v_F \tan(\phi_F) \cos(\theta_F) \tag{33}$$

Differentiation of (24) gives

$$\dot{L}_{LF} = \frac{L_{LFx}}{L_{LF}} \dot{L}_{LFx} + \frac{L_{LFy}}{L_{LF}} \dot{L}_{LFy} \tag{34}$$

From Figure 4.1 it can be seen that

$$\frac{L_{LFx}}{L_{LF}} = \cos(\psi_{LF} + \theta_L - \pi) \tag{35}$$

$$\frac{L_{LFy}}{L_{LF}} = \sin(\psi_{LF} + \theta_L - \pi) \tag{36}$$

Substituting(32), (33), (35) and (36) in (34) results in

$$\dot{L}_{LF} = \begin{pmatrix} -v_L \cos(\psi_{LF} + \theta_L)\cos(\theta_L) + v_F \cos(\theta_F)\cos(\psi_{LF} + \theta_L) - v_L \sin(\theta_L)\sin(\psi_{LF} + \theta_L) \\ +v_F \sin(\theta_F)\sin(\psi_{LF} + \theta_L) - v_F \tan(\phi_F)\sin(\theta_F)\cos(\psi_{LF} + \theta_L) \\ +v_F \tan(\phi_F)\cos(\theta_F)\sin(\psi_{LF} + \theta_L) \end{pmatrix} \tag{37}$$

Define $\gamma_F = \psi_{LF} + \theta_L - \theta_F$ (38)

Consider the trigonometric identities

$$\cos(C - D) = \cos(C)\cos(D) + \sin(C)\sin(D) \tag{39}$$

$$\sin(C - D) = \sin(C)\cos(D) - \cos(C)\sin(D) \tag{40}$$

Using (38) through (40) in (37) $\dot{L}_{LF}$ is given by

$$\dot{L}_{LF} = -v_L \cos(\psi_{LF}) + v_F \tan(\phi_F)\sin(\gamma_F) + v_F \cos(\gamma_F) \tag{41}$$

Differentiation of (27) yields

$$\dot{\psi}_{LF} = \frac{1}{L_{LF}}\left(\frac{L_{LFx}\dot{L}_{LFy}}{L_{LF}} - \frac{L_{LFy}\dot{L}_{LFx}}{L_{LF}} - L_{LF}\dot{\theta}_L\right) \tag{42}$$

Substituting(30), (32) and (33) in (42) results in

$$\dot{\psi}_{LF} = \frac{1}{L_{LF}}\begin{pmatrix} -v_L \sin(\theta_L)\cos(\psi_{LF}+\theta_L) + v_F \sin(\theta_F)\cos(\psi_{LF}+\theta_L) + v_L \cos(\theta_L)\sin(\psi_{LF}+\theta_L) \\ +v_F \tan(\phi_F)\cos(\theta_F)\cos(\psi_{LF}+\theta_L) - L_{LF}\dot{\theta}_L - v_F \cos(\theta_F)\sin(\psi_{LF}+\theta_L) \\ +v_F \tan(\phi_F)\sin(\theta_F)\sin(\psi_{LF}+\theta_L) \end{pmatrix} \tag{43}$$

Using (38) through (40) in (43) $\dot{\psi}_{LF}$ becomes

$$\dot{\psi}_{LF} = \frac{1}{L_{LF}}\left(v_L \sin(\psi_{LF}) + v_F \tan(\phi_F)\cos(\gamma_F)\right) + \frac{1}{L_{LF}}\left(-v_F \sin(\gamma_F) - L_{LF}\dot{\theta}_L\right) \tag{44}$$

Substituting (30) in (44), the simplified expression of $\dot{\psi}_{LF}$ is given by,

$$\dot{\psi}_{LF} = \frac{1}{L_{LF}}\left(v_L \sin(\psi_{LF}) - v_F \sin(\gamma_F)\right) + \frac{1}{L_{LF}}\left(v_F \tan(\phi_F)\cos(\gamma_F)\right) - \frac{v_L \tan(\phi_L)}{L} \tag{45}$$

Also from the Figure 4.1 it can be seen that the actual and desired coordinates of point A can be written in terms of in terms of coordinates of point B, the actual relative distance L_{LF}, the desired relative distance L_{LFD}, the actual relative bearing ψ_{LF} and the desired relative bearing ψ_{LFD} as given below:

$$x_{FD} = x_L - d\cos(\theta_L) + L_{LFD}\cos(\psi_{LFD}+\theta_L) - d\cos(\theta_{FD}) \tag{46}$$

Similarly, y_{FD} can be written as

$$y_{FD} = y_L - d\sin(\theta_L) + L_{LFD}\sin(\psi_{LFD}+\theta_L) - d\sin(\theta_{FD}) \tag{47}$$

$$\theta_{FD} = \theta_L \tag{48}$$

The actual coordinates of the follower can be arrived at in the same way and are given by

$$x_F = x_L - d\cos(\theta_L) + L_{LF}\cos(\psi_{LF}+\theta_L) - d\cos(\theta_F) \tag{49}$$

$$y_F = y_L - d\sin(\theta_L) + L_{LF}\sin(\psi_{LF}+\theta_L) - d\sin(\theta_F) \tag{50}$$

Let the error system be defined as given below

$$\begin{bmatrix} e_1 \\ e_2 \\ e_3 \end{bmatrix} = \begin{bmatrix} x_{FD} - x_F \\ y_{FD} - y_F \\ \theta_L - \theta_F \end{bmatrix} \tag{51}$$

Using equations (46) through (50) in (51) the error system can be expressed as

$$\begin{bmatrix} e_1 \\ e_2 \\ e_3 \end{bmatrix} = \begin{bmatrix} [L_{LFD}\cos(\psi_{LFD}+\theta_L) - d\cos(\theta_{FD}) - L_{LF}\cos(\psi_{LF}+\theta_L) + d\cos(\theta_F)] \\ [L_{LFD}\sin(\psi_{LFD}+\theta_L) - d\sin(\theta_{FD}) - L_{LF}\sin(\psi_{LF}+\theta_L) + d\sin(\theta_F)] \\ [\theta_L - \theta_F] \end{bmatrix} \tag{52}$$

The equation (52) gives the expression for the error system in inertial coordinates. For better intuitive sense they are transformed to body coordinates as shown below:

$$\begin{bmatrix} e_{F1} \\ e_{F2} \\ e_{F3} \end{bmatrix} = T_R \begin{bmatrix} [L_{LFD}\cos(\psi_{LFD}+\theta_L) - d\cos(\theta_{FD}) - L_{LF}\cos(\psi_{LF}+\theta_L) + d\cos(\theta_F)] \\ [L_{LFD}\sin(\psi_{LFD}+\theta_L) - d\sin(\theta_{FD}) - L_{LF}\sin(\psi_{LF}+\theta_L) + d\sin(\theta_F)] \\ [\theta_L - \theta_F] \end{bmatrix} \tag{53}$$

with $T_R = \begin{bmatrix} \cos(\theta_F) & \sin(\theta_F) & 0 \\ -\sin(\theta_F) & \cos(\theta_F) & 0 \\ 0 & 0 & 1 \end{bmatrix}$.

Simplifying equation (53) the expression for the errors in body coordinates is as follows,

$$\begin{bmatrix} e_{F1} \\ e_{F2} \\ e_{F3} \end{bmatrix} = \begin{bmatrix} [L_{LFD}\cos(\psi_{LFD}+e_{F3}) - L_{LF}\cos(\psi_{LF}+e_{F3}) - d\cos(e_{F3}) + d] \\ [L_{LFD}\sin(\psi_{LFD}+e_{F3}) - L_{LF}\sin(\psi_{LF}+e_{F3}) - d\sin(e_{F3})] \\ [\theta_L - \theta_F] \end{bmatrix} \tag{54}$$

Differentiating the expression for e_{F3} from(54), the expression for evolution of e_{F3} over time is obtained as given below,

$$\dot{e}_{F3} = \frac{v_L \tan(\phi_L)}{L} - \frac{v_F \tan(\phi_F)}{L} \tag{55}$$

Similarly, differentiating e_{F1} from (54) and substituting(41), (45) and (55), $\dot{e}_{F1}$ can be expressed as

$$\dot{e}_{F1} = \begin{pmatrix} \frac{-v_L \tan(\phi_L) L_{LFD}\sin(\psi_{LFD}+e_{F3})}{L} + \frac{v_F \tan(\phi_F) L_{LFD}\sin(\psi_{LFD}+e_{F3})}{L} \\ + \frac{v_L \tan(\phi_L) L_{LF}\sin(\gamma_F)}{L} - \frac{v_F \tan(\phi_F) L_{LF}\sin(\gamma_F)}{L} + \frac{v_L \tan(\phi_L) d\sin(e_{F3})}{L} \\ - \frac{v_F \tan(\phi_F) d\sin(e_{F3})}{L} + v_L \cos(\psi_{LF})\cos(\gamma_F) - v_F \cos(\gamma_F)\cos(\gamma_F) \\ - v_F \tan(\phi_F)\sin(\gamma_F)\cos(\gamma_F) + v_L \sin(\psi_{LF})\sin(\gamma_F) - v_F \sin(\gamma_F)\sin(\gamma_F) \\ + v_F \tan(\phi_F)\cos(\gamma_F)\sin(\gamma_F) - \frac{L_{LF}\tan(\phi_L) v_L \sin(\gamma_F)}{L} \end{pmatrix} \tag{56}$$

On simplification (56) becomes

$$\dot{e}_{F1} = v_L \cos(e_{F3}) - v_F + w_L\left[-L_{LF}\sin(\gamma_F) - e_{F2}\right] + w_F e_{F2} \tag{57}$$

Similarly, differentiating e_{F2} from (54) and substituting(41), (45) and (55) , the expression for $\dot{e}_{F2}$ is obtained as given below

$$\dot{e}_{F2} = \begin{pmatrix} \frac{v_L \tan(\phi_L) L_{LFD} \cos(\psi_{LFD} + e_{F3})}{L} - \frac{v_F \tan(\phi_F) L_{LFD} \cos(\psi_{LFD} + e_{F3})}{L} \\ -\frac{v_L \tan(\phi_L) L_{LF} \cos(\gamma_F)}{L} + \frac{v_F \tan(\phi_F) L_{LF} \cos(\gamma_F)}{L} - v_L \sin(\psi_{LF}) \cos(\gamma_F) \\ + v_L \cos(\psi_{LF}) \sin(\gamma_F) - v_F \sin(\gamma_F) \cos(\gamma_F) + v_F \sin(\gamma_F) \cos(\gamma_F) \\ - v_F \tan(\phi_F) \sin(\gamma_F) \sin(\gamma_F) - v_F \tan(\phi_F) \cos(\gamma_F) \cos(\gamma_F) + \frac{L_{LF} \tan(\phi_L) v_L \cos(\gamma_F)}{L} \\ -\frac{v_L \tan(\phi_L) d \cos(e_{F3})}{L} + \frac{v_F \tan(\phi_F) d \cos(e_{F3})}{L} \end{pmatrix} \tag{58}$$

Simplifying(58), $\dot{e}_{F2}$ can be written as

$$\dot{e}_{F2} = v_L \sin(e_{F3}) - L w_F + w_L\left[e_{F1} - d\right] - w_F\left[e_{F1} - d\right] + w_L L_{LF} \cos(\gamma_F) \tag{59}$$

Therefore, the error system is given by equation (60) as given below

$$\begin{bmatrix} \dot{e}_{F1} \\ \dot{e}_{F2} \\ \dot{e}_{F3} \end{bmatrix} = \begin{bmatrix} v_L \cos(e_{F3}) - v_F + w_L\left[-L_{LF}\sin(\gamma_F) - e_{F2}\right] + w_F e_{F2} \\ v_L \sin(e_{F3}) - L w_F + w_L\left[e_{F1} - d\right] + w_L L_{LF}\cos(\gamma_F) - w_F\left[e_{F1} - d\right] \\ w_L - w_F \end{bmatrix} \tag{60}$$

5. TRADITIONAL TRACKING AND CONTROL DESIGN USING LYAPUNOV FUNCTION BASED APPROACH

Objective is to find a velocity control input using kinematics that will drive the relative distance and relative bearing angle between the leader and follower to the desired value to keep the formation. The dynamics of the leader and the follower are used to derive specific torque control inputs required to achieve the desired velocity profile derived using kinematics. The controller design follows a Lyapunov function based approach.

5.1. CONTROLLER DESIGN

To stabilize the kinematic system the velocity control inputs for the follower robot can be designed using Lyapunov analysis. The velocity control inputs thus chosen will help in maintaining the desired relative bearing and distance. Let the Lyapunov candidate function be chosen as

$$V = \frac{K_1 {e_{F1}}^2 + K_2 {e_{F2}}^2}{2} + K_3(1-\cos(e_{F3})) \tag{61}$$

On differentiation of (61) $\dot{V}$ can be expressed as given below,

$$\dot{V} = K_1 e_{F1}\dot{e}_{F1} + K_2 e_{F2}\dot{e}_{F2} + K_3 \sin(e_{F3})\dot{e}_{F3} \tag{62}$$

Substituting (60) in (62) and expanding, $\dot{V}$ can be expressed as

$$\dot{V} = \begin{pmatrix} K_1 e_{F1} v_L \cos(e_{F3}) - K_1 e_{F1} v_F - K_1 e_{F1} w_L L_{LF} \sin(\gamma_F) - K_1 e_{F1} w_L e_{F2} + K_1 e_{F1} w_F e_{F2} \\ + K_2 e_{F2} v_L \sin(e_{F3}) - K_2 e_{F2} L w_F + K_2 e_{F2} w_L e_{F1} - K_2 e_{F2} w_L d + K_2 e_{F2} w_L L_{LF} \cos(\gamma_F) \\ - K_2 e_{F2} w_F e_{F1} + K_2 e_{F2} w_F d + K_3 \sin(e_{F3}) w_L - K_3 \sin(e_{F3}) w_F \end{pmatrix} \tag{63}$$

Let

$$K_1 = K_2 = K \tag{64}$$

Then (63) becomes

$$\dot{V} = \begin{pmatrix} K e_{F1} v_L \cos(e_{F3}) - K e_{F1} w_L L_{LF} \sin(\gamma_F) - K e_{F2} w_L d + K e_{F2} v_L \sin(e_{F3}) \\ + K e_{F2} w_L L_{LF} \cos(\gamma_F) + K_3 \sin(e_{F3}) w_L - K_1 e_{F1} v_F + w_F \left[- K d e_{F2} - K_3 \sin(e_{F3}) \right] \end{pmatrix} \tag{65}$$

Choosing one of the velocity control inputs v_F, the linear velocity of the follower as

$$v_F = K_{vF}\, e_{F1} + v_L \cos(e_{F3}) - w_L L_{LF} \sin(\gamma_F) \tag{66}$$

Substituting (66) in (65) , $\dot{V}$ can be written as

$$\dot{V} = \begin{pmatrix} -KK_{vF}{e_{F1}}^2 - Ke_{F2}d\left[w_L - \dfrac{v_L \sin(e_{F3})}{d} - \dfrac{w_L L_{LF} \cos(\gamma_F)}{d} \right] + K_3 \sin(e_{F3}) w_L \\ + w_F \left[-Kde_{F2} - K_3 \sin(e_{F3}) \right] \end{pmatrix} \tag{67}$$

Now choosing the second velocity control input w_F , the angular velocity of the follower as

$$w_F = \begin{pmatrix} -w_L + \dfrac{(k_v + v_L)\sin(e_{F3})}{d} + \dfrac{w_L L_{LF} \cos(\gamma_F)}{d} + \dfrac{K_{wF} e_{F2}}{d} \\ + \left[\dfrac{2K_3 w_L + \dfrac{K_3 w_L L_{LF}}{d} + \dfrac{K_3 K_{wF} |e_{F2}|}{d} + Kk_V |e_{F2}|}{Kd|e_{F2}| + K_3} \right] \end{pmatrix} \tag{68}$$

and substituting (68) in (67) , $\dot{V}$ can be written as

$$\dot{V} = \begin{pmatrix} -KK_{vF}{e_{F1}}^2 - KK_{wF}{e_{F2}}^2 - \dfrac{K_3(k_V + v_L)\sin^2(e_{F3})}{d} + 2K_3 w_L \sin(e_{F3}) \\ - \dfrac{K_3 \sin(e_{F3}) w_L L_{LF} \cos(\gamma_F)}{d} - \dfrac{K_3 K_{wF} \sin(e_{F3}) e_{F2}}{d} - Kk_V e_{F2} \sin(e_{F3}) \\ - \dfrac{Kde_{F2} + K_3 \sin(e_{F3})}{Kd|e_{F2}| + K_3} \left[2K_3 w_L + \dfrac{K_3 w_L L_{LF}}{d} + \dfrac{K_3 K_{wF} |e_{F2}|}{d} + Kk_V |e_{F2}| \right] \end{pmatrix} \tag{69}$$

Converting the equality in (69) to an inequality results in (70) as given below

$$\dot{V} < \begin{pmatrix} -KK_{vF}{e_{F1}}^2 - KK_{wF}{e_{F2}}^2 - \dfrac{K_3(k_V + v_L)\sin^2(e_{F3})}{d} + 2K_3 w_L + \dfrac{K_3 w_L L_{LF}}{d} + Kk_V |e_{F2}| \\ + \dfrac{K_3 K_{wF} |e_{F2}|}{d} - \dfrac{Kd|e_{F2}| + K_3}{Kd|e_{F2}| + K_3} \left[2K_3 w_L + \dfrac{K_3 w_L L_{LF}}{d} + \dfrac{K_3 K_{wF} |e_{F2}|}{d} + Kk_V |e_{F2}| \right] \end{pmatrix} \tag{70}$$

Therefore, from (70) it can be inferred that

$$\dot{V} < -KK_{vF}{e_{F1}}^2 - KK_{wF}{e_{F2}}^2 - \frac{K_3(k_V + v_L)\sin^2(e_{F3})}{d} \tag{71}$$

Since $v_L \geq 0$, with $K_1 = K_2 = K$ and $K, K_3, K_{vF}, K_{wF}, k_V > 0$, $\dot{V} < 0$. Therefore the velocity control in (66) and (68) provides asymptotic stability to the error system in (60) i.e. $e_F \to 0$ as $t \to \infty$.

In order to track the velocity and the angular velocity derived using Lyapunov analysis, the follower robot dynamics needs to be considered. The torque control inputs

for the drive and steering system which will produce the desired velocity profile need to be obtained. Define a velocity tracking error given by

$$\mathbf{e}_{FD} = \mathbf{Z}_{FD} - \mathbf{Z}_F \tag{72}$$

where

$$\mathbf{Z}_{FD} = \begin{bmatrix} v_{FD} \\ \phi_{FD} \end{bmatrix} \text{ and } \mathbf{Z}_F = \begin{bmatrix} v_F \\ \phi_F \end{bmatrix}. \tag{73}$$

where

$$\phi_{FD} = a\tan\left(\frac{w_{FD}L}{v_{FD}}\right) \tag{74}$$

In (73) v_{FD} and ϕ_{FD} are the desired linear velocity and steering angle profiles derived from the Lyapunov analysis while v_F and ϕ_F denote the actual linear velocity and steering angle of the follower. Substituting (16) and $\tau_F = rF_{dr}$ (where τ_F, r denote the drive torque and wheel radius of the follower) in(18), taking $v_u = v_F$, $\dot{v}_F$ can be expressed as

$$\dot{v}_F = -\frac{F_{uf}\cos\phi_F}{m} - \frac{F_{wf}\sin\phi_F}{m} + \frac{bv_F^2\tan^2\phi_F}{L^2} - \frac{F_{ur}}{m} + \frac{\tau_F}{rm} \tag{75}$$

And the steering dynamics is given by(23).

From (75) and (23), the combined dynamics of the system can be represented as

$$\dot{\mathbf{Z}}_F = -\mathbf{A}\mathbf{Z}_F - \mathbf{B} + \mathbf{E}\mathrm{T} \tag{76}$$

where

$$\mathbf{A}_{11} = \frac{-dv_F\tan^2\phi_F}{L^2}; \quad \mathbf{A}_{12} = 0$$
$$\mathbf{A}_{21} = 0; \qquad \mathbf{A}_{22} = \frac{1}{\tau_s} \tag{77}$$

$$\mathbf{B}_{11} = +\frac{F_{ur}}{m} + \frac{F_{uF}\cos\phi_F}{m} + \frac{F_w\sin\phi_F}{m}; \quad \mathbf{B}_{21} = 0 \tag{78}$$

$$\mathbf{E} = \begin{bmatrix} \frac{1}{rm} & 0 \\ 0 & \frac{1}{\tau_s} \end{bmatrix} \quad \text{and} \quad \mathrm{T} = \begin{bmatrix} \tau_F \\ u \end{bmatrix} \tag{79}$$

Adding and subtracting $\dot{\mathbf{Z}}_{FD}, \mathbf{AZ}_{FD}$ in (76) and simplifying, the expression for $\dot{\mathbf{e}}_{FD}$ is given by

$$\dot{\mathbf{e}}_{FD} = -\mathbf{A}\mathbf{e}_{FD} + \mathbf{AZ}_{FD} + \dot{\mathbf{Z}}_{FD} + \mathbf{B} - \mathbf{E}\mathrm{T} \tag{80}$$

Define

$$\mathbf{f}(\mathbf{x}_{Fnew}) = \mathbf{AZ}_{FD} + \dot{\mathbf{Z}}_{FD} + \mathbf{B} \tag{81}$$

Note that $\mathbf{f}(\mathbf{x}_{Fnew})$ involves friction terms and desired acceleration terms that cannot be computed in a real life accurately. Hence, online neural network will be used to estimate $\mathbf{f}(\mathbf{x}_{Fnew})$ .The error dynamics can now be written as

$$\dot{\mathbf{e}}_{FD} = -\mathbf{A}\mathbf{e}_{FD} + \mathbf{f}(\mathbf{x}_{Fnew}) - \mathbf{E}\mathrm{T} \tag{82}$$

where $\mathbf{x}_{Fnew} = \left[e_{F1}, e_{F2}, e_{F3}, \phi_{FD}, v_{FD}, L_{LF}, \gamma_F\right]$

A torque control given by (83) is designed.

$$\mathrm{T} = \mathbf{E}^{-1}\left[\mathbf{K}_1\mathbf{e}_{FD} + \mathbf{f}(\mathbf{x}_{Fnew})\right] \tag{83}$$

Substituting (83) in (82) results in

$$\dot{\mathbf{e}}_{FD} = -(\mathbf{A} + \mathbf{K}_1)\mathbf{e}_{FD} \tag{84}$$

An appropriate choice of $\mathbf{K}_1$ will result in the system in (84) being asymptotically stable and the velocity tracking error will go to zero. Now consider a new Lyapunov candidate function obtained by appending the one in (61)

$$V_{new} = V_{OLD} + \frac{1}{2}\mathbf{e}^T{}_{FD}\mathbf{e}_{FD} \tag{85}$$

Differentiation of (85) results in

$$\dot{V}_{new} = \dot{V}_{OLD} + \mathbf{e}^T{}_{FD}\dot{\mathbf{e}}_{FD} \tag{86}$$

Substituting (84) in(86), $\dot{V}_{new}$ becomes

$$\dot{V}_{new} = \dot{V}_{OLD} - \mathbf{e}^T{}_{FD}(\mathbf{A} + \mathbf{K}_1)\mathbf{e}_{FD} \tag{87}$$

From earlier derivation and proof it is known that $\dot{V}_{old} < 0$, so to make $\dot{V}_{new} < 0$ the following choice of $\mathbf{K}_1$ is made,

$$\mathbf{K}_1 = \begin{bmatrix} k_1 + \dfrac{dv_F \tan^2 \phi_F}{L^2} & 0 \\ 0 & -\dfrac{1}{\tau_s} + k_4 \end{bmatrix} \tag{88}$$

where $k_1, k_4 > 0$

Substituting (88) in (87), $\dot{V}_{new}$ becomes

$$\dot{V}_{new} = \dot{V}_{OLD} - e_{FD1}^2 k_1 - e_{FD2}^2 k_4 < 0 \tag{89}$$

From (89) it can be inferred that the tracking error system in (82) and the error system given by (60) are asymptotically stable. Since the function $\mathbf{f}(\mathbf{x}_{Fnew})$ is approximated by a neural network a weight update rule is needed for the neural network. In the section below a weight update rule is derived and the bounded-ness of weights is guaranteed. To guarantee the robustness of the controller, measurement noise is added to the inputs given to the neural network.

5.2. WEIGHT UPDATE RULE AND PROOF OF BOUNDED-NESS OF WEIGHTS

A single layer functional link neural network (FLNN) is used for the approximation of $\mathbf{f}(\mathbf{x}_{Fnew})$ [27]. The activation function $\phi(\mathbf{x}_{Fnew})$ can be chosen as a basis set for the universal approximation property to hold for single layer FLNN [20]. Then there exists a weight W such that $\mathbf{f}(\mathbf{x}_{Fnew}) = W^T \phi(\mathbf{x}_{Fnew}) + \varepsilon$ with the estimation error ε bounded. The bound is given by $\|\varepsilon\| < \varepsilon_N$. The ideal approximating weights are unknown and nonunique. So an assumption is made that $\|W\|_F < W_B$ with the bound W_B known. The Forbenius norm is denoted by $\| \ \|_F$. Then an estimate of $\mathbf{f}(\mathbf{x}_{Fnew})$ is given by

$$\hat{\mathbf{f}}(\mathbf{x}_{Fnew}) = \hat{W}^T \phi(\mathbf{x}_{Fnew}) \tag{90}$$

with $\hat{W}$ being neural network weights. Since the function $\mathbf{f}(\mathbf{x}_{Fnew})$ is approximated by a neural network, the expression for torque is given by

$$\mathrm{T} = \mathbf{E}^{-1}\left[\mathbf{K}_1 \mathbf{e}_{FD} + \hat{\mathbf{f}}(\mathbf{x}_{Fnew})\right] \tag{91}$$

where $\hat{\mathbf{f}}(\mathbf{x}_{Fnew})$ is the estimate of $\mathbf{f}(\mathbf{x}_{Fnew})$. Define $\tilde{\mathbf{f}}(\mathbf{x}_{Fnew})$ as

$$\tilde{\mathbf{f}}(\mathbf{x}_{Fnew}) = \mathbf{f}(\mathbf{x}_{Fnew}) - \hat{\mathbf{f}}(\mathbf{x}_{Fnew}) \tag{92}$$

An online weight update rule is now developed to guarantee stable tracking and yet guarantee bounded-ness of weights. The weight estimation error is defined as

$$\tilde{W} = W - \hat{W} \tag{93}$$

Now substituting (91)in (82) and using(92), $\dot{\mathbf{e}}_{FD}$ can be expressed as

$$\dot{\mathbf{e}}_{FD} = -(\mathbf{A} + \mathbf{K}_1)\mathbf{e}_{FD} + \tilde{\mathbf{f}}(\mathbf{x}_{Fnew}) \tag{94}$$

Using (93) and (90) , (94) becomes

$$\dot{\mathbf{e}}_{FD} = -(\mathbf{A} + \mathbf{K}_1)\mathbf{e}_{FD} + \tilde{W}^T\phi(\mathbf{x}_{Fnew}) \tag{95}$$

Choose a Lyapunov candidate function as given below

$$V_W = V_{OLD} + \frac{1}{2}\mathbf{e}_{FD}^T\mathbf{e}_{FD} + \frac{1}{2}tr\left\{\tilde{W}^T F^{-1}\tilde{W}\right\} \tag{96}$$

where F is a user defined tuning matrix and V_{OLD} is given by (61).

Differentiating (96) and substituting (95) $\dot{V}_W$ becomes

$$\dot{V}_W = \dot{V}_{OLD} - \mathbf{e}_{FD}^T(\mathbf{A} + \mathbf{K}_1)\mathbf{e}_{FD} + tr\left\{\tilde{W}^T(F^{-1}\dot{\tilde{W}} + \phi\mathbf{e}^T{}_{FD})\right\} \tag{97}$$

Selecting the weight tuning law as

$$\dot{\hat{W}} = F\phi\mathbf{e}_{FD}^T - kF\|\mathbf{e}_{FD}\|\hat{W} \tag{98}$$

It can be shown that

$$\dot{V} \le \dot{V}_{OLD} - \|\mathbf{e}_{FD}\|\left((\mathbf{A} + \mathbf{K}_1)_{\min}\|\mathbf{e}_{FD}\| + k\left\|\tilde{W}\right\|_F(\left\|\tilde{W}\right\|_F - W_B)\right) \tag{99}$$

where $(.)_{\min}$ denotes the minimum singular value.

The term given by

$$(\mathbf{A} + \mathbf{K}_1)_{\min}\|\mathbf{e}_{FD}\| + k\left\|\tilde{W}\right\|_F(\left\|\tilde{W}\right\|_F - W_B) = k\left(\left\|\tilde{W}\right\|_F - \frac{W_B}{2}\right)^2 - \frac{kW_B^2}{4} + (\mathbf{A} + \mathbf{K}_1)_{\min}\|\mathbf{e}_{FD}\| \tag{100}$$

is guaranteed positive as long as

$$\|\mathbf{e}_{FD}\| \ge \frac{kW_B^2}{4(\mathbf{A} + \mathbf{K}_1)_{\min}} \equiv b_{e_{FD}} or \left\|\tilde{W}\right\|_F > \frac{W_B}{2} + \sqrt{\frac{kW_B^2}{4}} \equiv b_W \tag{101}$$

So, $\dot{V}_W$ is negative outside a compact set. Let the NN function approximation property hold for $\mathbf{f}(\mathbf{x}_{Fnew})$ with an accuracy of ε_N for all $\mathbf{x}_{Fnew}$ in the compact set $S_{Fnew} \equiv \{x_{Fnew} \mid \|x_{Fnew}\| < b_{x_{Fnew}}\}$ with $b_{x_{Fnew}} > Z_{FB}$ where Z_{FB} is the bound on the desired trajectory Z_{FD}.

Define $S_{e_{FD}} \equiv \{e_{FD} \mid \|e_{FD}\| < (b_{x_{Fnew}} - Z_{FB})/(c_0 + c_1)\}$ (102)

Now selecting the gain

$$\left(\mathbf{A} + \mathbf{K}_1\right)_{\min} > \frac{\frac{kW_B^2}{4}(c_0 + c_1)}{(b_{x_{Fnew}} - Z_{FB})} \tag{103}$$

ensures that the compact set defined by $\|e_{FD}\| < b_{e_{FD}}$ is contained in $S_{e_{FD}}$. This guarantees that the error e_{FD} and the NN weight estimates $\hat{W}$ are uniformly ultimately bounded (UUB) [27] with bounds given by (101).

5.3. FORMATION STABILITY

Consider a formation of $N+1$ robots consisting of a leader "l_i" and N followers. Let there be a smooth velocity control input $\begin{bmatrix} v_L & w_L \end{bmatrix}^T$ for the leader and let the torque control inputs $\begin{bmatrix} \tau_L & u_L \end{bmatrix}^T$ be applied to the leader such that the leader tracks a virtual reference robot. The velocity and torque control inputs for the leader can be derived in a similar way as the velocity and torque control inputs for the follower. It is assumed that the leader's motion is known i.e. there exists a control law that drives the leader independently to its desired trajectory. The smooth velocity control inputs $\begin{bmatrix} v_{Fi} & w_{Fi} \end{bmatrix}^T$ for the i^{th} follower are given by (66), (68) and torque control inputs by (91). Then the origin given by $E = \begin{bmatrix} e_{l_1} & e_{l_2} & e_{l_3} & e_{vl} & e_{\phi l} & e_{F1i}^T & e_{F2i}^T & e_{F3i}^T & e_{vFi}^T & e_{\phi Fi}^T \end{bmatrix}^T$ where $E \in \mathbb{R}^{(5(N+1))X1}$, which represents the augmented position , orientation and velocity tracking error systems for the leader "l_i" and N followers, respectively, is asymptotically stable in the presence of uncertainties and noise is proved below.

Consider the following Lyapunov candidate function

$$V_{Formation} = \sum_{1}^{N} V_{Wi} + V_{l_1} \tag{104}$$

where V_{Wi} is given by (96) and

$$V_{l_1} = e_{l_1}^2 + e_{l_2}^2 + e_{l_3}^2 + e_{vl}^2 + e_{\phi l}^2 \tag{105}$$

From (105) and (96) it can be seen that (104) is positive for $E = \begin{bmatrix} e_{l_1} & e_{l_2} & e_{l_3} & e_{vl} & e_{\phi l} & e_{F1i}^T & e_{F2i}^T & e_{F3i}^T & e_{vFi}^T & e_{\phi Fi}^T \end{bmatrix}^T \neq 0$. Differentiating (104) yields

$$\dot{V}_{Formation} = \sum_{1}^{N} \dot{V}_{Wi} + \dot{V}_{l_1} \tag{106}$$

In the previous subsection it has been proved that V_{Wi} for all $i = 1 to N$ individually is negative outside a compact set and that the error e_{FD} and the NN weight estimates $\hat{W}$ are uniformly ultimately bounded (UUB). Hence, when $\dot{V}_{Wi} < 0$ for all $i = 1 to N$, so it automatically follows that $\sum_{1}^{N} \dot{V}_{Wi} < 0$. Also, the torque control and velocity control inputs are designed such that the errors go to zero asymptotically and hence, $\dot{V}_{l_1}$ is negative. Therefore, $\dot{V}_{Formation} < 0$, and the entire formation is asymptotically stable.

5.4. RESULTS AND DISCUSSION

A single leader single follower scenario is considered and the simulations are carried out using MATLAB for the same. The leader executes a circular trajectory with radius = 60 m, linear velocity of 5 m/sec and an angular velocity ~ 0.08 rad/sec. It is desired for the follower to execute a circle of radius = 56 m being parallel to the leader at all times. So the desired relative distance to be maintained is 4.0774 m and a relative bearing angle of 78.8199 degrees. The gains used during simulation are $k_{VF} = .128$, $K_3 = 0.01$, $k_V = 0.0001$, $K = 180$. The constants $k = 0.5$ and $F = 30 * eye(20)$ are used in the NN weight update rule where $eye(20)$ denotes a $20X20$ identity matrix. The NN has 20 hidden layer neurons. Measurement noise is

added in the form Gaussian noise with zero mean. The noise added is one percent of the states that are inputs to the neural network. Also the simulations were carried out with different time constants for the steering dynamics and increased friction parameters. The plots shown below are the ones obtained for a time constant of 0.25 and increased friction parameters of $F_{uR} = 10, F_{uF} = 20, F_W = 30$.

From Figure 5.1, it can be seen that the follower achieves the desired position and orientation, with the position and orientation errors going to zero asymptotically as shown in Figure 5.2. In Figure 5.2 e_{F1}, e_{F2} denote the position errors in the u and w direction respectively (refer Figure 2.1) and e_{F3} denotes the error in the orientation of the follower. The torque control inputs to the drive and steering system are as shown in Figure 5.3 and Figure 5.4. This torque control input achieves the velocity profile in (66) and (68) resulting in the leader and follower trajectories as shown in Figure 5.5. It can be seen that the leader tracks a circle of 60 m radius and the follower is parallel to the leader at all times tracking a circle of radius 56 m. The velocity profile of the follower is shown in Figure 5.6 and Figure 5.7.

From Figure 5.8 it can be inferred that the velocity tracking errors defined by the error system described by (82) also go to zero asymptotically. From Figure 5.9 it can bee seen that the neural network is able to approximate $\mathbf{f}(\mathbf{x}_{Fnew})$ accurately. It is compared with the actual value of $\mathbf{f}(\mathbf{x}_{Fnew})$ which is available to us during simulation runs and not during real-time implementation. Figure 5.10 shows the relative distance and bearing angle maintained by the follower and it confirms with the desired relative distance and bearing angle calculated.

In this section simplified dynamic equations are used to obtain the torque control inputs for the drive and steering system of a car-like follower mobile robot to maintain a desired relative distance and bearing angle between the leader and the follower. Imperfect velocity tracking and uncertainties in the friction forces and the steering system modeling is taken into account.

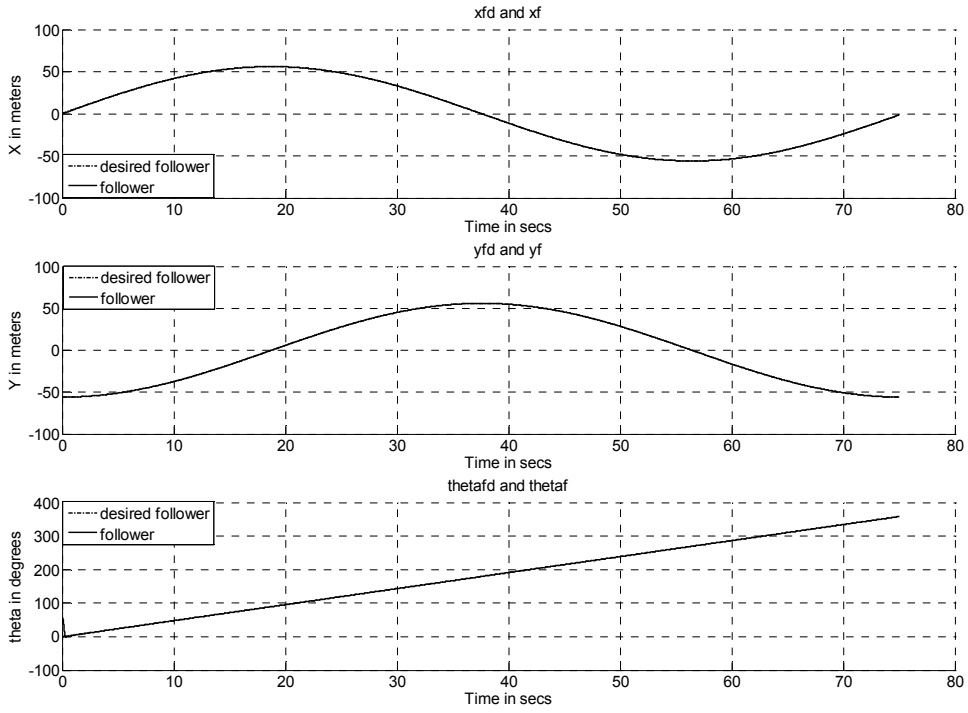

Figure 5.1 Actual and Desired Position and Orientation of the Follower

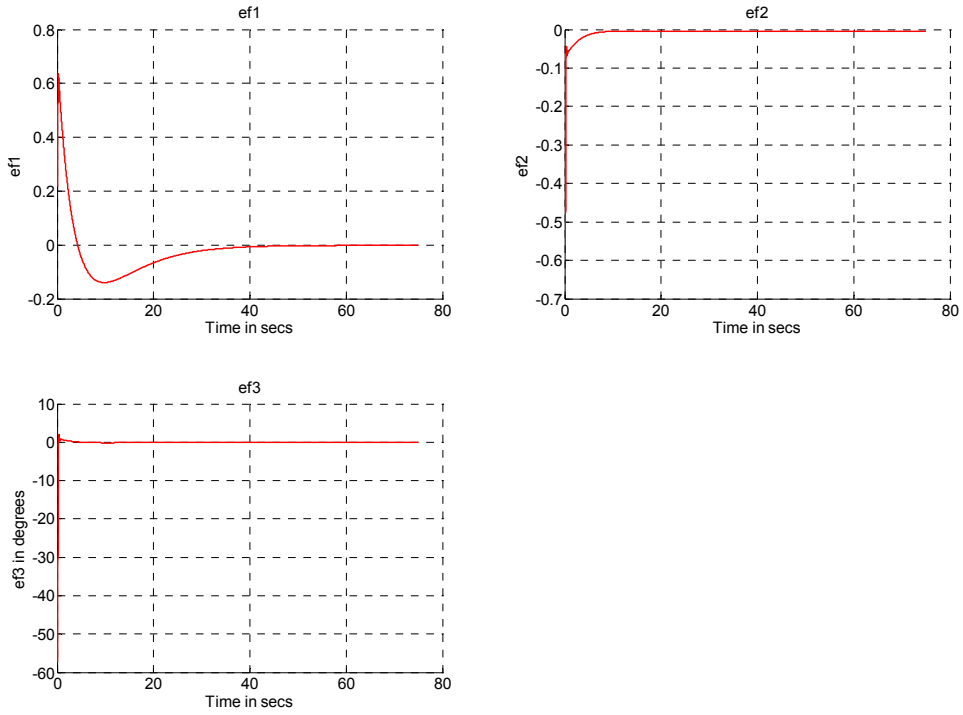

Figure 5.2 Position and Orientation Errors in Body Coordinates

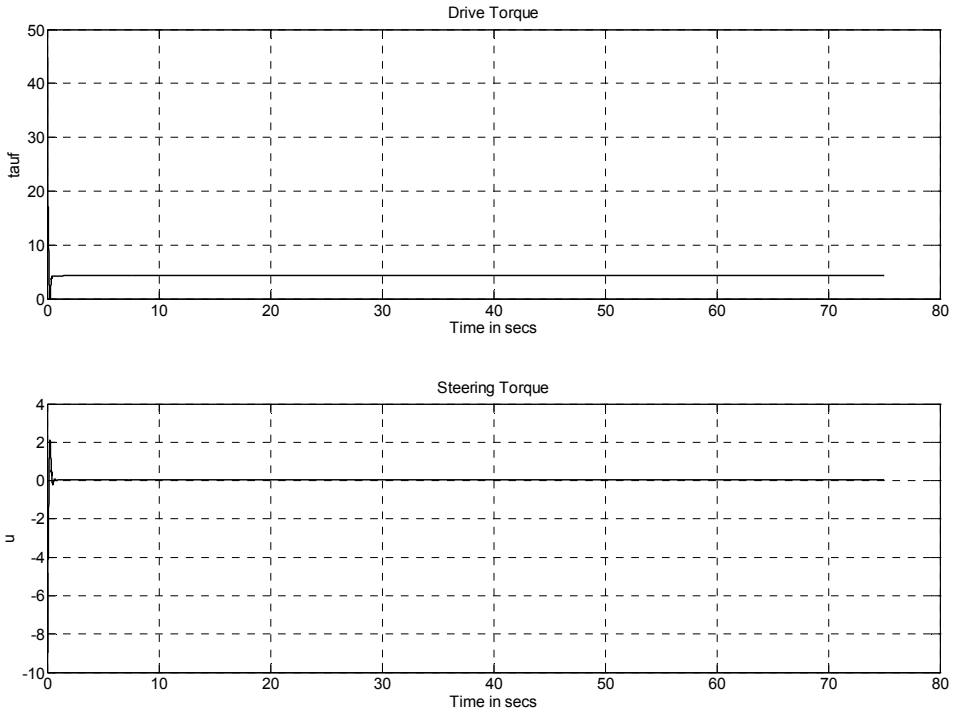

Figure 5.3 Drive and Steering Torques

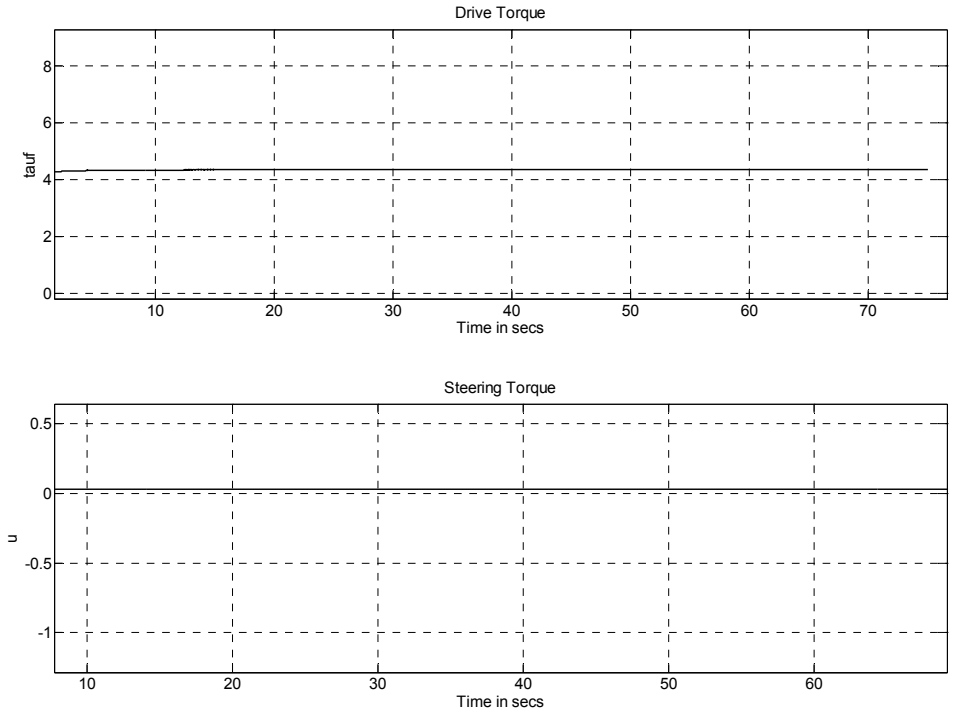

Figure 5.4 Magnified Plot of Drive and Steering Torques

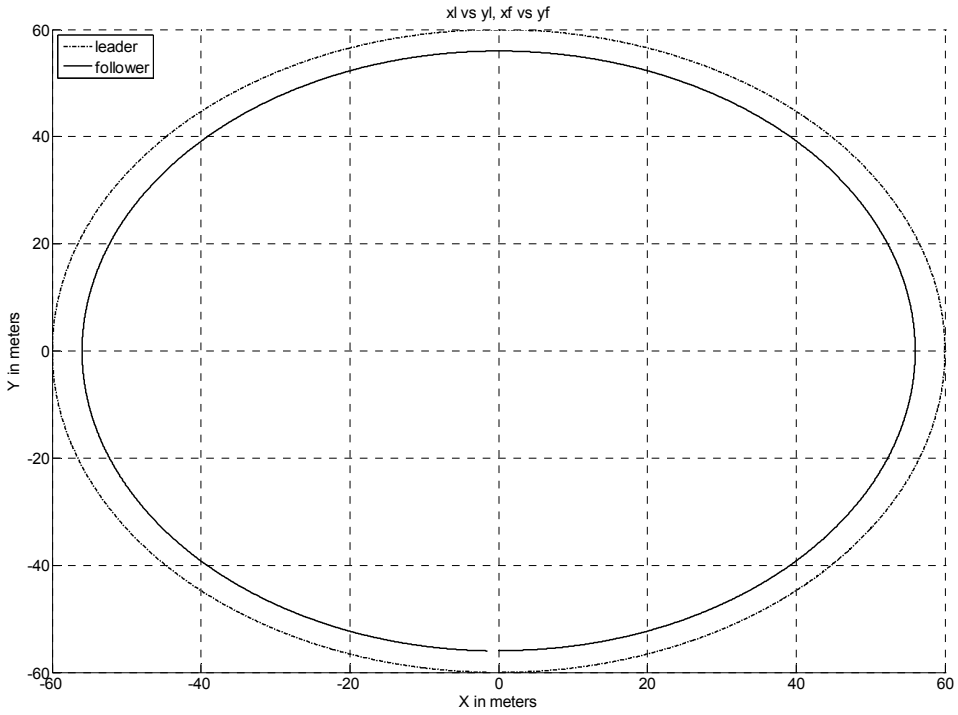

Figure 5.5 Leader and Follower Trajectories

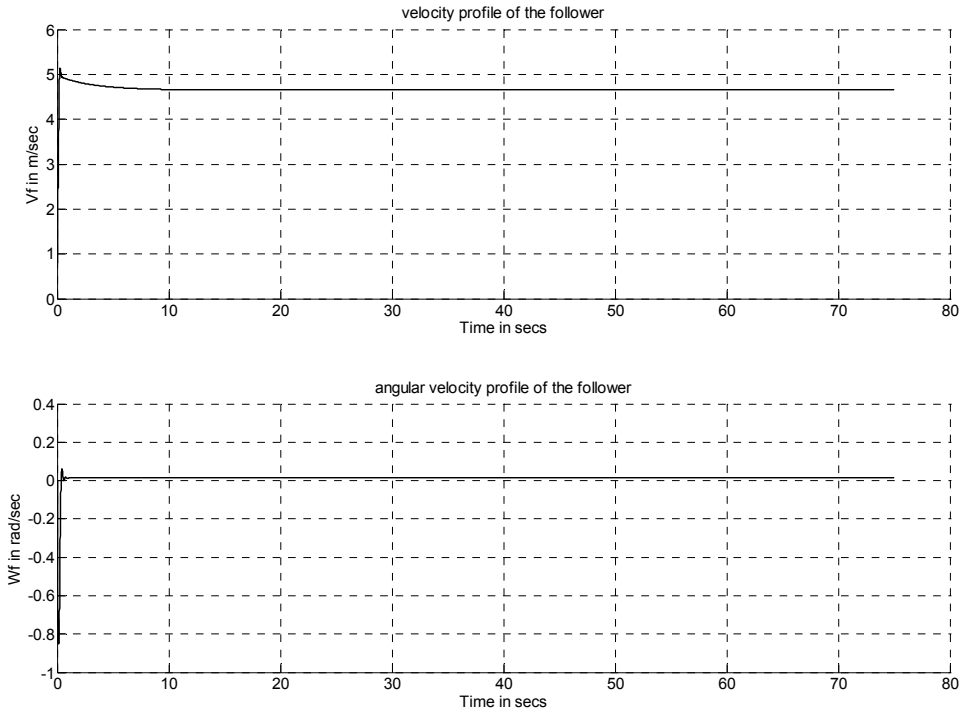

Figure 5.6 Linear and Angular Velocity Profile of the Follower

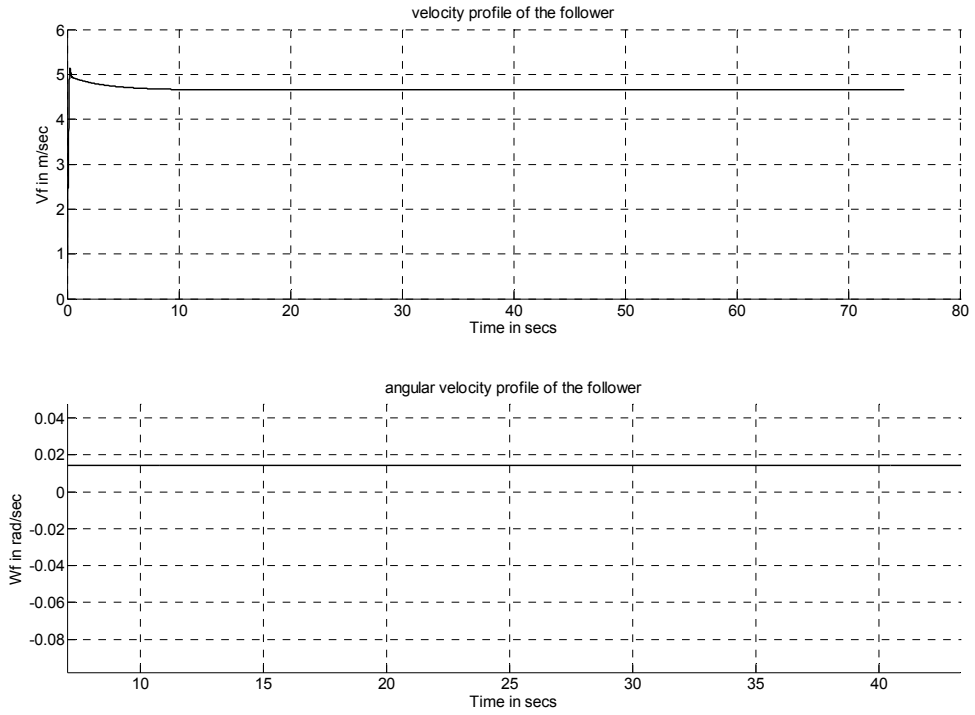

Figure 5.7 Magnified Plot of Linear and Angular Velocity Profile of the Follower

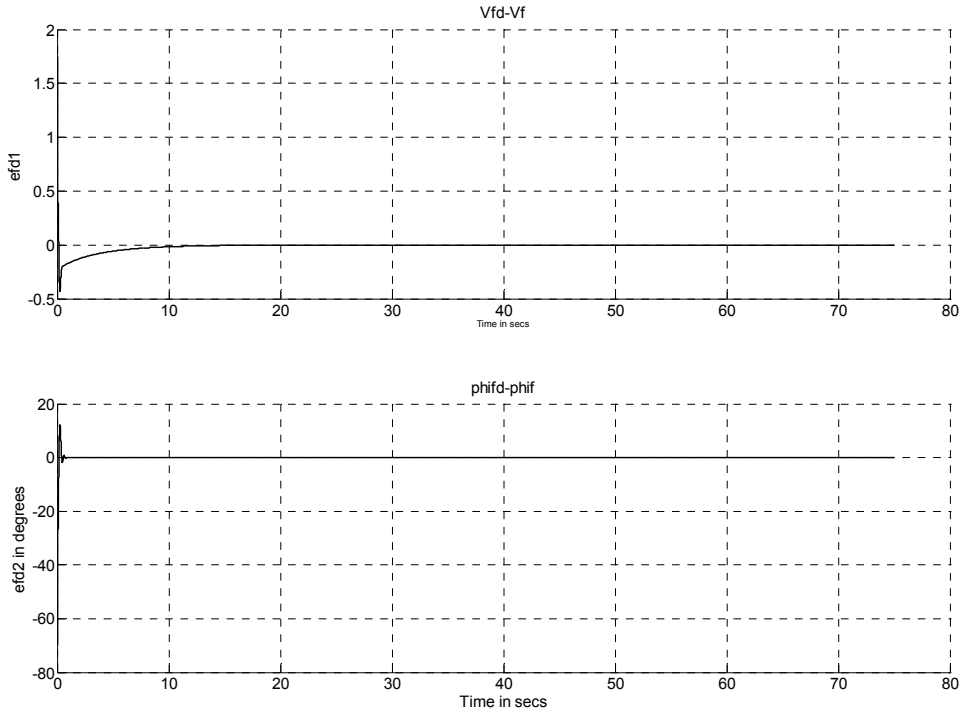

Figure 5.8 Velocity and Steering Angle Error Plots

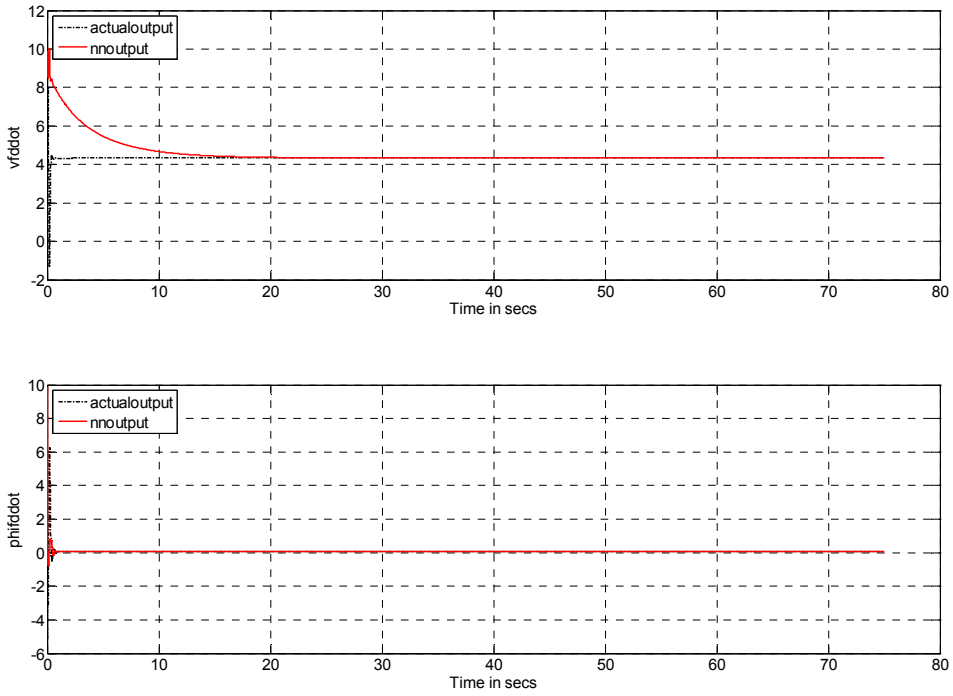

Figure 5.9 Neural Network Outputs in Comparison with Actual Outputs

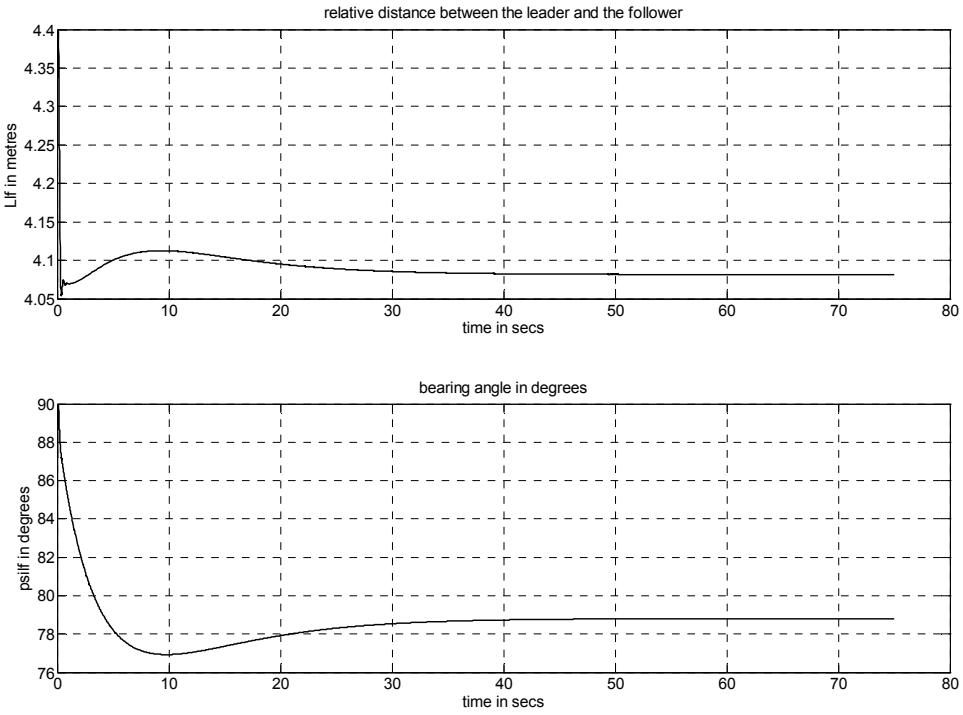

Figure 5.10 Relative Distance and Relative Bearing of the Follower w.r.t. Leader

6. ERROR SYSTEM FORMULATION FOR INTEGRATED TRACKING AND CONTROL

Control law for each follower is obtained using *integrated tracking and control scheme* [19]. Traditional tracking and control designs use a decoupled design involving two separate algorithms, one for velocity control design and another for torque control design. Weak interactions among the algorithms and separate designs make the robot performance optimization and the formation stability difficult to achieve. So a new tracking and control architecture wherein the conventional elements are replaced by a single component that performs all the functions and hence called the integrated tracking and control scheme is used. This results in achieving a level of synergism between robot control and tracking which is extremely difficult to achieve in a decoupled scheme.

The error formulation (60) obtained from the kinematic model is combined with the error formulation to be obtained from the dynamics of the robot to arrive at a combined error formulation for integrated tracking and control [19]. Once the combined framework is obtained, the state space equations thus obtained will be used to design torque control inputs for the follower drive system as well as the steering system so that the formation is maintained. From (75) the drive system dynamics is given by

$$\dot{v}_F = -\frac{F_{uf}\cos\phi_F}{m} - \frac{F_{wf}\sin\phi_F}{m} + \frac{bv_F^2\tan^2\phi_F}{L^2} - \frac{F_{ur}}{m} + \frac{\tau_F}{rm} \tag{107}$$

Define the errors for linear velocity and steering angle as given below

$$\begin{bmatrix} e_{vF} \\ e_{\phi F} \end{bmatrix} = \begin{bmatrix} v_{FD} - v_F \\ \phi_{FD} - \phi_F \end{bmatrix} \tag{108}$$

Substituting (108) in (107) , $\dot{e}_{vF}$ can be expressed as

$$\dot{e}_{vF} = F_1 - \frac{D(v_{FD})^2\tan^2\phi_F}{L^2} + \frac{2Dv_{FD}e_{vF}\tan^2\phi_F}{L^2} - \frac{D(e_{vF})^2\tan^2\phi_F}{L^2} - \frac{\tau_F}{rm} \tag{109}$$

Also from (23), the steering dynamics can be expressed as

$$\dot{e}_{\phi F} = F_2 + \frac{\phi_{FD}}{\tau_S} - \frac{e_{\phi F}}{\tau_S} - \frac{u}{\tau_S} \tag{110}$$

where

$$F_1 = \frac{F_{uR}}{m} + \frac{F_{uF}\cos\phi_F}{m} + \frac{F_w\sin\phi_F}{m} + \dot{v}_{FD} \tag{111}$$

$$F_2 = \dot{\phi}_{FD} \tag{112}$$

Therefore the combined error formulation is given by

$$\begin{bmatrix} \dot{e}_{F1} \\ \dot{e}_{F2} \\ \dot{e}_{F3} \\ \dot{e}_{vF} \\ \dot{e}_{\phi F} \end{bmatrix} = \begin{bmatrix} v_L \cos(e_{F3}) - v_F + w_L \left[-L_{LF} \sin(\gamma_F) - e_{F2} \right] + w_F e_{F2} \\ v_L \sin(e_{F3}) - L w_F + w_L \left[e_{F1} - d \right] + w_L L_{LF} \cos(\gamma_F) - w_F \left[e_{F1} - d \right] \\ w_L - w_F \\ F_1 - \dfrac{D(v_{FD})^2 \tan^2 \phi_F}{L^2} + \dfrac{2 D v_{FD} e_{vF} \tan^2 \phi_F}{L^2} - \dfrac{D(e_{vF})^2 \tan^2 \phi_F}{L^2} - \dfrac{\tau_F}{rm} \\ F_2 + \dfrac{\phi_{FD}}{\tau_S} - \dfrac{e_{\phi F}}{\tau_S} - \dfrac{u}{\tau_S} \end{bmatrix} \tag{113}$$

with F_1 and F_2 given by (111) and (112).

7. INTGERATED TRACKING AND OPTIMAL CONTROL DESIGN: APPLICATION OF SDARE

7.1. OPTIMAL CONTROL PROBLEM AND SDARE APPROACH

The common objective in many technical fields is to design control logic that commands a dynamic system to produce a desired output and augments the system stability. When the control objective is expressed as a quantitative criterion, then optimization of this criterion results in a set of equations to be solved to obtain the controller. Optimal control theory governs strategies for maximizing a performance measure or minimizing a quantitative criterion as the states of the dynamic system evolve. The fundamentals of optimal control of continuous-time dynamic linear and non-linear systems are discussed below.

The process of design of optimal control for linear systems which have quadratic performance indices is called the linear quadratic (LQ) problem. The theory for optimal control of linear systems using linear quadratic regulator (LQR) can be found in [29]. Consider a non-linear dynamic system, affine in control given by

$$\dot{\mathbf{x}} = f(\mathbf{x}) + g(\mathbf{x})\mathbf{u} \tag{114}$$

In the recent years, the SDARE method has been used to obtain the optimal control for non-linear systems. Considered below is the SDARE formulation. The problem considered here is the infinite-horizon regulation of general autonomous nonlinear systems which are affine in input [29]. Given the system equation in (114) and the performance index (PI),

$$\mathbf{J} = \frac{1}{2}\int_0^\infty (\mathbf{x}^T\mathbf{Q}(\mathbf{x})\mathbf{x} + \mathbf{u}^T\mathbf{R}(\mathbf{x})\mathbf{u})dt \tag{115}$$

which allows for trading-off state error $\mathbf{x}$ versus control input $\mathbf{u}$, via the weighting matrices $\mathbf{Q}(\mathbf{x}) \geq 0$, $\mathbf{R}(\mathbf{x}) > 0$, $\forall \mathbf{x}$, respectively. It is assumed that $f(0) = 0$ and $g(\mathbf{x}) \neq 0, \forall \mathbf{x}$. A feedback control law $\mathbf{u}(\mathbf{x})$ which regulates the system to the origin can be found by using the SDARE method [20]-[25] which approaches the problem by mimicking the LQR formulation for discussed for linear systems.

Accordingly, the system equations have to be first written in the form given by:

$$\dot{\mathbf{x}} = \mathbf{A}(\mathbf{x})\mathbf{x} + \mathbf{B}(\mathbf{x})\mathbf{u} \tag{116}$$

where the state vector $\mathbf{x} \in \Re^n$, control input $\mathbf{u} \in \Re^m$, $\mathbf{A} \in \Re^{nxn}$, $\mathbf{B} \in \Re^{mxn}$, $f(\mathbf{x}) = \mathbf{A}(\mathbf{x})\mathbf{x}$ and $g(\mathbf{x}) = \mathbf{B}(\mathbf{x})$. The cost is denoted by $\mathbf{J}$.The objective here is to find the control that minimizes the quadratic PI in(115). The control weighting matrix $\mathbf{R} \in \Re^{mxm}$ and the state weighting matrix $\mathbf{Q} \in \Re^{nxn}$ are symmetric matrices. The former parameterization is possible if and only if $f(0) = 0$ and $f(\mathbf{x})$ is continuously differentiable. Then as in the linear time-invariant case [29], a state-feedback control law of the form of

$$\mathbf{u}(\mathbf{x}) = -\mathbf{K}(\mathbf{x})\mathbf{x} = -\mathbf{R}^{-1}(\mathbf{x})\mathbf{B}^T(\mathbf{x})\mathbf{S}(\mathbf{x})\mathbf{x} \tag{117}$$

can be found. The Kalman gains given by $\mathbf{K}(\mathbf{x})$ in non-linear systems is state dependent and changes at every time step. $\mathbf{S}(\mathbf{x})$ is unique, symmetric, positive-definite solution of the state-dependent algebraic Riccati equation

$$\mathbf{A}^T(\mathbf{x})\mathbf{S}(\mathbf{x}) + \mathbf{S}(\mathbf{x})\mathbf{A}(\mathbf{x}) + \mathbf{Q}(\mathbf{x}) - \mathbf{S}(\mathbf{x})\mathbf{B}(\mathbf{x})\mathbf{R}^{-1}(\mathbf{x})\mathbf{B}^T(\mathbf{x})\mathbf{S}(\mathbf{x}) = 0 \tag{118}$$

The pair $(\mathbf{A}(\mathbf{x}), \mathbf{B}(\mathbf{x}))$ should be pointwise controllable in the linear sense so that the algebraic Riccati equation has a solution at that particular state $\mathbf{x}$ [20]-[25] [30]. Due to the nonuniqueness of $\mathbf{A}(\mathbf{x})$, different $\mathbf{A}(\mathbf{x})$ choices yield different controllability matrices and thus different pointwise controllability characteristics. From the many choices for the parameterization $(\mathbf{A}(\mathbf{x}), \mathbf{B}(\mathbf{x}))$, a pointwise stabilizable pair is chosen. The solving of the state dependent algebraic Riccati equation is very cumbersome and hence numerical tools are used.

7.2. CONTROLLER DESIGN

In order to take into account the bias terms while performing state dependent parameterization the system is augmented with a stable state [23] given by

$$\dot{z} = -\lambda z \tag{119}$$

with $\lambda > 0$.

Then the bias term $b(t)$ can be factored as $b(t) = \left(\frac{b(t)}{z} \right) z$ .Each time through the controller, the initial value $z(0)$ is used in the state dependent coefficient matrix and in calculating the control. The shifting procedure described below in equations (120) and (121) is used for factorizing any state dependent term that doesn't go through zero.

$$\cos x_1 = \left[-1 + \cos x_1 \right] + 1 \tag{120}$$

$$\left[-1 + \cos x_1 \right] = \left[\frac{-1 + \cos x_1}{x_1} \right] x_1 \tag{121}$$

Now the augmented system has 6 states given by $\left[e_{F1}, e_{F2}, e_{F3}, e_{vF}, e_{\phi F}, z \right]'$.

Therefore, the error system equations are given by

$$\dot{E} = A(E)E + B(E)u \tag{122}$$

where $A(E)$ is R^{6X6} .

From earlier derivations, the differential equations that describe the evolution of errors over time are given by

$$\dot{e}_{F1} = v_L \cos e_{F3} - v_F - w_L \left(L_{LF} \sin \gamma_F + e_{F2} \right) + w_F e_{F2} \tag{123}$$

$$\dot{e}_{F2} = v_L \sin e_{F3} + w_L \left(e_{F1} - d \right) - w_F \left(e_{F1} - d \right) - L w_F + w_L L_{LF} \cos \gamma_F \tag{124}$$

$$\dot{e}_{F3} = w_L - w_F \tag{125}$$

$$\dot{e}_{vF} = F_1 - \frac{d(v_{FD})^2 \tan^2 \phi_F}{L^2} + \frac{2 d v_{FD} e_{vF} \tan^2 \phi_F}{L^2} - \frac{d(e_{vF})^2 \tan^2 \phi_F}{L^2} - \frac{\tau_F}{rm} \tag{126}$$

$$\dot{e}_{\phi F} = F_2 + \frac{\phi_{FD}}{\tau_S} - \frac{e_{\phi F}}{\tau_S} - \frac{u}{\tau_S} \tag{127}$$

where

$$F_1 = \frac{F_{uR}}{m} + \frac{F_{uF} \cos \phi_F}{m} + \frac{F_w \sin \phi_F}{m} + \dot{v}_{FD}$$

$$F_2 = \dot{\phi}_{FD}$$

On factorization (123) becomes

$$\dot{e}_{F1}=\begin{pmatrix}\left[\frac{v_L\left[-1+\cos e_{F3}\right]}{e_{F3}}\right]e_{F3}+\frac{v_L}{z}z-w_Le_{F2}+w_Fe_{F2}-\left[\frac{w_LL_{LF}\sin\psi_{LF}\left[-1+\cos e_{F3}\right]}{e_{F3}}\right]e_{F3}\\+e_{vF}-\left[\frac{w_LL_{LF}\cos\psi_{LF}\sin e_{F3}}{e_{F3}}\right]e_{F3}-\left[\frac{w_LL_{LF}\sin\psi_{LF}}{z}\right]z-\frac{v_{FD}}{z}z\end{pmatrix} \quad (128)$$

Substituting (313) in (15) , w_F can be written as

$$w_F=\frac{(v_{FD}-e_{vF})\tan(\phi_{FD}-e_{\phi F})}{L}=\frac{v_{FD}}{L}\left(\frac{\tan\phi_{FD}-\tan e_{\phi F}}{1+\tan\phi_{FD}\tan e_{\phi F}}\right)-\frac{e_{vF}}{L}\left(\frac{\tan\phi_{FD}-\tan e_{\phi F}}{1+\tan\phi_{FD}\tan e_{\phi F}}\right) \quad (129)$$

Therefore w_Fe_{F2} can be expanded as,

$$w_Fe_{F2}=\begin{pmatrix}\frac{v_{FD}e_{F2}}{L}\left(\frac{\tan\phi_{FD}}{1+\tan\phi_{FD}\tan e_{\phi F}}\right)-\frac{v_{FD}e_{F2}}{L}\left(\frac{\tan e_{\phi F}}{1+\tan\phi_{FD}\tan e_{\phi F}}\right)\\-\frac{e_{vF}e_{F2}}{L}\left(\frac{\tan\phi_{FD}}{1+\tan\phi_{FD}\tan e_{\phi F}}\right)+\frac{e_{vF}e_{F2}}{L}\left(\frac{\tan e_{\phi F}}{1+\tan\phi_{FD}\tan e_{\phi F}}\right)\end{pmatrix} \quad (130)$$

Substituting (130) in (128) $\dot{e}_{F1}$ can be written as

$$\dot{e}_{F1}=\begin{pmatrix}\left[\frac{v_L\left[-1+\cos e_{F3}\right]}{e_{F3}}\right]e_{F3}+\frac{v_L}{z}z-w_Le_{F2}-\left[\frac{w_LL_{LF}\sin\psi_{LF}\left[-1+\cos e_{F3}\right]}{e_{F3}}\right]e_{F3}+e_{vF}\\-\left[\frac{w_LL_{LF}\cos\psi_{LF}\sin e_{F3}}{e_{F3}}\right]e_{F3}-\left[\frac{w_LL_{LF}\sin\psi_{LF}}{z}\right]z-\frac{v_{FD}}{z}z\\+\frac{v_{FD}e_{F2}}{L}\left(\frac{\tan\phi_{FD}}{1+\tan\phi_{FD}\tan e_{\phi F}}\right)-\frac{v_{FD}e_{F2}}{L}\left(\frac{\tan e_{\phi F}}{1+\tan\phi_{FD}\tan e_{\phi F}}\right)\\-\frac{e_{vF}e_{F2}}{L}\left(\frac{\tan\phi_{FD}}{1+\tan\phi_{FD}\tan e_{\phi F}}\right)+\frac{e_{vF}e_{F2}}{L}\left(\frac{\tan e_{\phi F}}{1+\tan\phi_{FD}\tan e_{\phi F}}\right)\end{pmatrix} \quad (131)$$

On further parameterization $\dot{e}_{F1}$ becomes

$$\dot{e}_{F1}=\begin{pmatrix}\left[\frac{v_L\left[-1+\cos e_{F3}\right]}{e_{F3}}\right]e_{F3}+\frac{v_L}{z}z-w_Le_{F2}-\left[\frac{w_LL_{LF}\sin\psi_{LF}\left[-1+\cos e_{F3}\right]}{e_{F3}}\right]e_{F3}+e_{vF}\\-\left[\frac{w_LL_{LF}\cos\psi_{LF}\sin e_{F3}}{e_{F3}}\right]e_{F3}-\left[\frac{w_LL_{LF}\sin\psi_{LF}}{z}\right]z-\frac{v_{FD}}{z}z\\+\frac{v_{FD}e_{F2}}{L}\left(\frac{\tan\phi_{FD}}{1+\tan\phi_{FD}\tan e_{\phi F}}\right)-\frac{\alpha v_{FD}e_{F2}}{L}\left(\frac{\tan e_{\phi F}}{1+\tan\phi_{FD}\tan e_{\phi F}}\right)\\-\frac{(1-\alpha)v_{FD}e_{F2}e_{\phi F}}{Le_{\phi F}}\left(\frac{\tan e_{\phi F}}{1+\tan\phi_{FD}\tan e_{\phi F}}\right)-\frac{\alpha e_{vF}e_{F2}}{L}\left(\frac{\tan\phi_{FD}}{1+\tan\phi_{FD}\tan e_{\phi F}}\right)\\-\frac{(1-\alpha)e_{vF}e_{F2}}{L}\left(\frac{\tan\phi_{FD}}{1+\tan\phi_{FD}\tan e_{\phi F}}\right)+\frac{\alpha e_{vF}e_{F2}}{L}\left(\frac{\tan e_{\phi F}}{1+\tan\phi_{FD}\tan e_{\phi F}}\right)\\+\frac{(1-\alpha)\alpha_1e_{vF}e_{F2}}{L}\left(\frac{\tan e_{\phi F}}{1+\tan\phi_{FD}\tan e_{\phi F}}\right)+\frac{(1-\alpha)(1-\alpha_1)e_{vF}e_{F2}e_{\phi F}}{Le_{\phi F}}\left(\frac{\tan e_{\phi F}}{1+\tan\phi_{FD}\tan e_{\phi F}}\right)\end{pmatrix} \quad (132)$$

Let $\left(\frac{\tan\phi_{FD}}{1+\tan\phi_{FD}\tan e_{\phi F}}\right)=T_1$ and $\left(\frac{\tan e_{\phi F}}{1+\tan\phi_{FD}\tan e_{\phi F}}\right)=T_2$ (133)

Substituting (133) in (132) , (132) becomes

$$\dot{e}_{F1}=\begin{pmatrix}\left[\frac{v_L\left[-1+\cos e_{F3}\right]}{e_{F3}}\right]e_{F3}+\frac{v_L}{z}z-w_Le_{F2}-\left[\frac{w_LL_{LF}\sin\psi_{LF}\left[-1+\cos e_{F3}\right]}{e_{F3}}\right]e_{F3}+e_{vF}\\-\left[\frac{w_LL_{LF}\cos\psi_{LF}\sin e_{F3}}{e_{F3}}\right]e_{F3}-\left[\frac{w_LL_{LF}\sin\psi_{LF}}{z}\right]z-\frac{v_{FD}}{z}z+\frac{v_{FD}e_{F2}T_1}{L}-\frac{\alpha v_{FD}e_{F2}T_2}{L}\\-\frac{(1-\alpha)v_{FD}e_{F2}e_{\phi F}T_2}{Le_{\phi F}}-\frac{\alpha e_{vF}e_{F2}T_1}{L}-\frac{(1-\alpha)e_{vF}e_{F2}T_1}{L}+\frac{\alpha e_{vF}e_{F2}T_2}{L}+\frac{(1-\alpha)\alpha_1e_{vF}e_{F2}T_2}{L}\\+\frac{(1-\alpha)(1-\alpha_1)e_{vF}e_{F2}e_{\phi F}T_2}{Le_{\phi F}}\end{pmatrix} \quad (134)$$

Factorizing (124) , $\dot{e}_{F2}$ can be written as

$$\dot{e}_{F2}=\begin{pmatrix} w_L e_{F1}-\frac{w_L d}{z}z+\left(\frac{v_L \sin e_{F3}}{e_{F3}}\right)e_{F3}+w_L L_{LF}\cos(\psi_{LF}+e_{F3})-\frac{de_{vF}}{L}\left(\frac{\tan e_{\phi F}}{1+\tan\phi_{FD}\tan e_{\phi F}}\right) \\ -\frac{dv_{FD}}{L}\left(\frac{\tan\phi_{FD}}{1+\tan\phi_{FD}\tan e_{\phi F}}\right)+\frac{dv_{FD}}{L}\left(\frac{\tan e_{\phi F}}{1+\tan\phi_{FD}\tan e_{\phi F}}\right)+\frac{de_{vF}}{L}\left(\frac{\tan\phi_{FD}}{1+\tan\phi_{FD}\tan e_{\phi F}}\right) \\ -\frac{v_{FD}e_{F1}}{L}\left(\frac{\tan\phi_{FD}}{1+\tan\phi_{FD}\tan e_{\phi F}}\right)+\frac{v_{FD}e_{F1}}{L}\left(\frac{\tan e_{\phi F}}{1+\tan\phi_{FD}\tan e_{\phi F}}\right) \\ +\frac{e_{vF}e_{F1}}{L}\left(\frac{\tan\phi_{FD}}{1+\tan\phi_{FD}\tan e_{\phi F}}\right)-\frac{e_{vF}e_{F1}}{L}\left(\frac{\tan e_{\phi F}}{1+\tan\phi_{FD}\tan e_{\phi F}}\right) \end{pmatrix} \quad (135)$$

Also,

$$w_L L_{LF}\cos(\psi_{LF}+e_{F3})=w_L L_{LF}\cos\psi_{LF}\cos e_{F3}-w_L L_{LF}\sin\psi_{LF}\sin e_{F3} \quad (136)$$

Parameterization of (136) results in

$$w_L L_{LF}\cos(\psi_{LF}+e_{F3})=\begin{pmatrix} \left(\frac{w_L L_{LF}\cos\psi_{LF}\left[-1+\cos e_{F3}\right]}{e_{F3}}\right)e_{F3}+\left(\frac{w_L L_{LF}\cos\psi_{LF}}{z}\right)z \\ -\left(\frac{w_L L_{LF}\sin\psi_{LF}\sin e_{F3}}{e_{F3}}\right)e_{F3} \end{pmatrix} \quad (137)$$

Substituting (133) and (137) in (135) and parameterizing $\dot{e}_{F2}$ can be written as

$$\dot{e}_{F2}=\begin{pmatrix} w_L e_{F1}-\frac{w_L d}{z}z+\left(\frac{v_L \sin e_{F3}}{e_{F3}}\right)e_{F3}+\left(\frac{w_L L_{LF}\cos\psi_{LF}\left[-1+\cos e_{F3}\right]}{e_{F3}}\right)e_{F3} \\ +\left(\frac{w_L L_{LF}\cos\psi_{LF}}{z}\right)z-\left(\frac{w_L L_{LF}\sin\psi_{LF}\sin e_{F3}}{e_{F3}}\right)e_{F3}-\frac{v_{FD}e_{F1}T_1}{L}+\frac{\alpha v_{FD}e_{F1}T_2}{L} \\ +\frac{(1-\alpha)v_{FD}e_{F1}e_{\phi F}T_2}{Le_{\phi F}}+\frac{\alpha e_{vF}e_{F1}T_1}{L}+\frac{de_{vF}T_1}{L}+\frac{(1-\alpha)e_{vF}e_{F1}T_1}{L} \\ +\frac{dv_{FD}e_{\phi F}T_2}{Le_{\phi F}}-\frac{\alpha de_{vF}T_2}{L}-\frac{(1-\alpha)de_{vF}e_{\phi F}T_2}{Le_{\phi F}} \\ -\frac{\alpha e_{vF}e_{F1}T_2}{L}-\frac{(1-\alpha)\alpha_1 e_{vF}e_{F1}T_2}{L}-\frac{(1-\alpha)(1-\alpha_1)e_{vF}e_{F1}e_{\phi F}T_2}{Le_{\phi F}}-\frac{dv_{FD}zT_1}{Lz} \end{pmatrix} \quad (138)$$

Also ,

$$\dot{e}_{F3}=\begin{pmatrix} \frac{w_L}{z}z-\frac{v_{FD}}{L}\left(\frac{\tan\phi_{FD}}{1+\tan\phi_{FD}\tan e_{\phi F}}\right)+\frac{v_{FD}}{L}\left(\frac{\tan e_{\phi F}}{1+\tan\phi_{FD}\tan e_{\phi F}}\right) \\ +\frac{e_{vF}}{L}\left(\frac{\tan\phi_{FD}}{1+\tan\phi_{FD}\tan e_{\phi F}}\right)-\frac{e_{vF}}{L}\left(\frac{\tan e_{\phi F}}{1+\tan\phi_{FD}\tan e_{\phi F}}\right) \end{pmatrix} \quad (139)$$

Parameterization of (139) results in

$$\dot{e}_{F3}=\begin{pmatrix}-\frac{v_{FD}z}{Lz}\left(\frac{\tan\phi_{FD}}{1+\tan\phi_{FD}\tan e_{\phi F}}\right)+\frac{v_{FD}e_{\phi F}}{Le_{\phi F}}\left(\frac{\tan e_{\phi F}}{1+\tan\phi_{FD}\tan e_{\phi F}}\right)+\frac{e_{vF}}{L}\left(\frac{\tan\phi_{FD}}{1+\tan\phi_{FD}\tan e_{\phi F}}\right)\\ -\frac{\alpha e_{vF}}{L}\left(\frac{\tan e_{\phi F}}{1+\tan\phi_{FD}\tan e_{\phi F}}\right)-\frac{(1-\alpha)e_{vF}e_{\phi F}}{Le_{\phi F}}\left(\frac{\tan e_{\phi F}}{1+\tan\phi_{FD}\tan e_{\phi F}}\right)+\frac{w_L}{z}z\end{pmatrix} \quad (140)$$

Substituting (133) in (140) the expression for $\dot{e}_{F3}$ becomes

$$\dot{e}_{F3}=\left(\frac{w_L}{z}z-\frac{v_{FD}T_1z}{Lz}+\frac{v_{FD}e_{\phi F}T_2}{Le_{\phi F}}+\frac{e_{vF}T_1}{L}-\frac{\alpha e_{vF}T_2}{L}-\frac{(1-\alpha)e_{vF}e_{\phi F}T_2}{Le_{\phi F}}\right) \quad (141)$$

On parameterizing $\dot{e}_{vF}$ from (126) ,

$$\dot{e}_{vF}=\begin{pmatrix}\frac{F_{uR}}{mz}z+\frac{F_{uF}\cos(\phi_{FD}-e_{\phi F})}{m}+\frac{F_w\sin(\phi_{FD}-e_{\phi F})}{m}-\frac{d(v_{FD}-e_{vF})^2\tan^2(\phi_{FD}-e_{\phi F})}{L^2}\\ +\dot{v}_{FD}-\frac{\tau_F}{rm}\end{pmatrix} \quad (142)$$

Expanding (142), $\dot{e}_{vF}$ cane be written as

$$\dot{e}_{vF}=\begin{pmatrix}\frac{F_{uR}}{mz}z+\frac{F_{uF}\cos\phi_{FD}\cos e_{\phi F}}{m}+\frac{F_{uF}\sin\phi_{FD}\sin e_{\phi F}}{m}+\frac{F_w\sin\phi_{FD}\cos e_{\phi F}}{m}\\ -\frac{F_w\cos\phi_{FD}\sin e_{\phi F}}{m}-\frac{d(v_{FD})^2\tan^2(\phi_{FD}-e_{\phi F})}{L^2}-\frac{d(e_{vF})^2\tan^2(\phi_{FD}-e_{\phi F})}{L^2}\\ +\frac{2dv_{FD}e_{vF}\tan^2(\phi_{FD}-e_{\phi F})}{L^2}+\frac{\dot{v}_{FD}}{z}z-\frac{\tau_F}{rm}\end{pmatrix} \quad (143)$$

Parameterizing (143) further

$$\dot{e}_{vF}=\begin{pmatrix}\frac{F_{uR}}{mz}z+\frac{F_{uF}\cos\phi_{FD}}{m}\left(\frac{-1+\cos e_{\phi F}}{e_{\phi F}}\right)e_{\phi F}+\left(\frac{F_{uF}\cos\phi_{FD}}{mz}\right)z+\left(\frac{F_{uF}\sin\phi_{FD}\sin e_{\phi F}}{me_{\phi F}}\right)e_{\phi F}\\ +\frac{F_w\sin\phi_{FD}}{m}\left(\frac{-1+\cos e_{\phi F}}{e_{\phi F}}\right)e_{\phi F}+\left(\frac{F_w\sin\phi_{FD}}{mz}\right)z-\left(\frac{F_w\cos\phi_{FD}\sin e_{\phi F}}{me_{\phi F}}\right)e_{\phi F}+\frac{\dot{v}_{FD}}{z}z\\ -\frac{d(v_{FD})^2\tan^2(\phi_{FD}-e_{\phi F})}{L^2}-\frac{d(e_{vF})^2\tan^2(\phi_{FD}-e_{\phi F})}{L^2}+\frac{2dv_{FD}e_{vF}\tan^2(\phi_{FD}-e_{\phi F})}{L^2}-\frac{\tau_F}{rm}\end{pmatrix} \quad (144)$$

Expanding and parameterizing a few terms in (144) is done below

$$-\frac{d(v_{FD})^2\tan^2(\phi_{FD}-e_{\phi F})}{L^2}=-\frac{d(v_{FD})^2}{L^2}\left(\frac{1-\cos\left(2\left(\phi_{FD}-e_{\phi F}\right)\right)}{1+\cos\left(2\left(\phi_{FD}-e_{\phi F}\right)\right)}\right) \quad (145)$$

$$\Rightarrow -\frac{d(v_{FD})^2 \tan^2(\phi_{FD}-e_{\phi F})}{L^2} =$$

$$\left(\begin{array}{l} -\dfrac{d(v_{FD})^2}{L^2\left(1+\cos\left(2\left(\phi_{FD}-e_{\phi F}\right)\right)\right)z}z+\dfrac{d(v_{FD})^2}{L^2}\left(\dfrac{\cos 2\phi_{FD}}{1+\cos\left(2\left(\phi_{FD}-e_{\phi F}\right)\right)}\right)\left(\dfrac{-1+\cos 2e_{\phi F}}{e_{\phi F}}\right)e_{\phi F} \\ +\dfrac{d(v_{FD})^2 z}{L^2 z}\left(\dfrac{\cos 2\phi_{FD}}{1+\cos\left(2\left(\phi_{FD}-e_{\phi F}\right)\right)}\right)+\dfrac{d(v_{FD})^2}{L^2 e_{\phi F}}\left(\dfrac{\sin 2\phi_{FD}\sin 2e_{\phi F}}{1+\cos\left(2\left(\phi_{FD}-e_{\phi F}\right)\right)}\right)e_{\phi F} \end{array}\right) \quad (146)$$

Similarly

$$\frac{2dv_{FD}e_{vF}\tan^2(\phi_{FD}-e_{\phi F})}{L^2}$$

$$=\left(\begin{array}{l} \dfrac{2dv_{FD}}{L^2\left(1+\cos\left(2\left(\phi_{FD}-e_{\phi F}\right)\right)\right)}e_{vF}-\dfrac{2dv_{FD}e_{vF}\cos 2\phi_{FD}\cos 2e_{\phi F}}{L^2\left(1+\cos\left(2\left(\phi_{FD}-e_{\phi F}\right)\right)\right)} \\ -\dfrac{2dv_{FD}e_{vF}\sin 2\phi_{FD}\sin 2e_{\phi F}}{L^2\left(1+\cos\left(2\left(\phi_{FD}-e_{\phi F}\right)\right)\right)} \end{array}\right) \quad (147)$$

Further expanding and parameterizing (147) the expression becomes

$$\Rightarrow \frac{2dv_{FD}e_{vF}\tan^2(\phi_{FD}-e_{\phi F})}{L^2} =$$

$$\left(\begin{array}{l} \dfrac{2dv_{FD}}{L^2\left(1+\cos\left(2\left(\phi_{FD}-e_{\phi F}\right)\right)\right)}e_{vF}-\dfrac{\alpha 2dv_{FD}e_{vF}}{L^2}\left(\dfrac{\cos 2\phi_{FD}\cos 2e_{\phi F}}{1+\cos\left(2\left(\phi_{FD}-e_{\phi F}\right)\right)}\right) \\ -\dfrac{(1-\alpha)2dv_{FD}e_{vF}}{L^2}\left(\dfrac{\cos 2\phi_{FD}}{1+\cos\left(2\left(\phi_{FD}-e_{\phi F}\right)\right)}\right) \\ -\dfrac{(1-\alpha)2dv_{FD}e_{vF}}{L^2}\left(\dfrac{\cos 2\phi_{FD}}{1+\cos\left(2\left(\phi_{FD}-e_{\phi F}\right)\right)}\right)\left(\dfrac{-1+\cos 2e_{\phi F}}{e_{\phi F}}\right)e_{\phi F} \\ -\dfrac{\alpha 2dv_{FD}e_{vF}}{L^2}\left(\dfrac{\sin 2\phi_{FD}\sin 2e_{\phi F}}{1+\cos\left(2\left(\phi_{FD}-e_{\phi F}\right)\right)}\right)-\dfrac{(1-\alpha)2dv_{FD}e_{vF}}{L^2 e_{\phi F}}\left(\dfrac{\sin 2\phi_{FD}\sin 2e_{\phi F}}{1+\cos\left(2\left(\phi_{FD}-e_{\phi F}\right)\right)}\right)e_{\phi F} \end{array}\right) \quad (148)$$

Also,

$$-\frac{d(e_{vF})^2\tan^2(\phi_{FD}-e_{\phi F})}{L^2} = -\frac{d(e_{vF})^2}{L^2}\left(\frac{1-\cos\left(2\left(\phi_{FD}-e_{\phi F}\right)\right)}{1+\cos\left(2\left(\phi_{FD}-e_{\phi F}\right)\right)}\right) \quad (149)$$

$$\Rightarrow -\frac{d(e_{vF})^2\tan^2(\phi_{FD}-e_{\phi F})}{L^2}=+\frac{\alpha d(e_{vF})^2}{L^2}\left(\frac{\cos 2\phi_{FD}\cos 2e_{\phi F}}{1+\cos\left(2\left(\phi_{FD}-e_{\phi F}\right)\right)}\right)$$
$$+\frac{(1-\alpha)d(e_{vF})^2}{L^2}\left(\frac{\cos 2\phi_{FD}}{1+\cos\left(2\left(\phi_{FD}-e_{\phi F}\right)\right)}\right)+\frac{\alpha d(e_{vF})^2}{L^2}\left(\frac{\sin 2\phi_{FD}\sin 2e_{\phi F}}{1+\cos\left(2\left(\phi_{FD}-e_{\phi F}\right)\right)}\right)$$
$$+\frac{(1-\alpha)d(e_{vF})^2}{L^2}\left(\frac{\cos 2\phi_{FD}}{1+\cos\left(2\left(\phi_{FD}-e_{\phi F}\right)\right)}\right)\left(\frac{-1+\cos 2e_{\phi F}}{e_{\phi F}}\right)e_{\phi F}-\frac{d(e_{vF})^2}{L^2\left(1+\cos\left(2\left(\phi_{FD}-e_{\phi F}\right)\right)\right)}$$
$$+\frac{(1-\alpha)d(e_{vF})^2}{L^2e_{\phi F}}\left(\frac{\sin 2\phi_{FD}\sin 2e_{\phi F}}{1+\cos\left(2\left(\phi_{FD}-e_{\phi F}\right)\right)}\right)e_{\phi F} \tag{150}$$

Defining $L^2\left(1+\cos\left(2\left(\phi_{FD}-e_{\phi F}\right)\right)\right)=T_3$ (151)

and substituting all the above equations (146) through (151) in (144) the parameterized expression for $\dot{e}_{vF}$ is given as

$$\dot{e}_{vF}=\left(\begin{array}{l}
\frac{F_{uR}}{mz}z+\frac{F_{uF}\cos\phi_{FD}}{m}\left(\frac{-1+\cos e_{\phi F}}{e_{\phi F}}\right)e_{\phi F}+\left(\frac{F_{uF}\cos\phi_{FD}}{mz}\right)z+\left(\frac{F_{uF}\sin\phi_{FD}\sin e_{\phi F}}{me_{\phi F}}\right)e_{\phi F}\\
+\frac{F_w\sin\phi_{FD}}{m}\left(\frac{-1+\cos e_{\phi F}}{e_{\phi F}}\right)e_{\phi F}+\left(\frac{F_w\sin\phi_{FD}}{mz}\right)z-\left(\frac{F_w\cos\phi_{FD}\sin e_{\phi F}}{me_{\phi F}}\right)e_{\phi F}+\frac{\dot{v}_{FD}}{z}z\\
-\frac{d(v_{FD})^2}{T_3z}z+\frac{d(v_{FD})^2\cos 2\phi_{FD}}{T_3}\left(\frac{-1+\cos 2e_{\phi F}}{e_{\phi F}}\right)e_{\phi F}+\frac{d(v_{FD})^2\cos 2\phi_{FD}}{T_3z}z\\
-\left(\frac{(1-\alpha)2dv_{FD}e_{vF}\sin 2\phi_{FD}\sin 2e_{\phi F}}{T_3e_{\phi F}}\right)e_{\phi F}+\frac{(1-\alpha)d(e_{vF})^2\cos 2\phi_{FD}}{T_3}\\
+\left(\frac{d(v_{FD})^2\sin 2\phi_{FD}\sin 2e_{\phi F}}{T_3e_{\phi F}}\right)e_{\phi F}+\frac{2dv_{FD}}{T_3}e_{vF}-\frac{(1-\alpha)2dv_{FD}e_{vF}\cos 2\phi_{FD}}{T_3}\\
-\frac{\alpha 2dv_{FD}e_{vF}\cos 2\phi_{FD}\cos 2e_{\phi F}}{T_3}-\frac{(1-\alpha)2dv_{FD}e_{vF}\cos 2\phi_{FD}}{T_3}\left(\frac{-1+\cos 2e_{\phi F}}{e_{\phi F}}\right)e_{\phi F}\\
-\frac{\alpha 2dv_{FD}e_{vF}\sin 2\phi_{FD}\sin 2e_{\phi F}}{T_3}-\frac{d(e_{vF})^2}{T_3}+\frac{\alpha d(e_{vF})^2\cos 2\phi_{FD}\cos 2e_{\phi F}}{T_3}\\
+\frac{(1-\alpha)d(e_{vF})^2\cos 2\phi_{FD}}{T_3}\left(\frac{-1+\cos 2e_{\phi F}}{e_{\phi F}}\right)e_{\phi F}+\frac{\alpha d(e_{vF})^2\sin 2\phi_{FD}\sin 2e_{\phi F}}{T_3}\\
+\left(\frac{(1-\alpha)d(e_{vF})^2\sin 2\phi_{FD}\sin 2e_{\phi F}}{T_3e_{\phi F}}\right)e_{\phi F}-\frac{\tau_F}{rm}
\end{array}\right) \tag{152}$$

Parameterization (127) results in

$$\dot{e}_{\phi F} = \frac{\dot{\phi}_{FD}}{z} z + \frac{\phi_{FD}}{\tau_S z} z - \frac{e_{\phi F}}{\tau_S} - \frac{u}{\tau_S} \tag{153}$$

And the augmented stable state is given by

$$\dot{z} = -\lambda z \tag{154}$$

From (122) the error system can be written as

$$\dot{E} = A(E)E + B(E)U \tag{155}$$

where

$$A(E) = \begin{pmatrix} a_{11} & a_{12} & a_{13} & a_{14} & a_{15} & a_{16} \\ a_{21} & a_{22} & a_{23} & a_{24} & a_{25} & a_{26} \\ a_{31} & a_{32} & a_{33} & a_{34} & a_{35} & a_{36} \\ a_{41} & a_{42} & a_{43} & a_{44} & a_{45} & a_{46} \\ a_{51} & a_{52} & a_{53} & a_{54} & a_{55} & a_{56} \\ a_{61} & a_{62} & a_{63} & a_{64} & a_{65} & a_{66} \end{pmatrix} \text{ and } B(E) = \begin{pmatrix} b_{11} & b_{12} \\ b_{21} & b_{22} \\ b_{31} & b_{32} \\ b_{41} & b_{42} \\ b_{51} & b_{52} \\ b_{61} & b_{62} \end{pmatrix}$$

From the equations(134), (138) and (140) the expressions for the elements of matrices $A(E)$ and $B(E)$ are as given below

$$a_{11} = 0 \tag{156}$$

$$a_{12} = -w_L + \frac{v_{FD}T_1}{L} - \frac{\alpha v_{FD}T_2}{L} + \frac{\alpha e_{vF}T_2}{L} - \frac{\alpha e_{vF}T_1}{L} \tag{157}$$

$$a_{13} = \left[\frac{v_L\left[-1+\cos e_{F3}\right]}{e_{F3}}\right] - \left[\frac{w_L L_{LF}\sin\psi_{LF}\left[-1+\cos e_{F3}\right]}{e_{F3}}\right] - \left[\frac{w_L L_{LF}\cos\psi_{LF}\sin e_{F3}}{e_{F3}}\right] \tag{158}$$

$$a_{14} = 1 + \frac{(1-\alpha)\alpha_1 e_{F2}T_2}{L} - \frac{(1-\alpha)e_{F2}T_1}{L} \tag{159}$$

$$a_{15} = \frac{(1-\alpha)(1-\alpha_1)e_{vF}e_{F2}T_2}{Le_{\phi F}} - \frac{(1-\alpha)v_{FD}e_{F2}T_2}{Le_{\phi F}} \tag{160}$$

$$a_{16} = \frac{v_L}{z} - \frac{v_{FD}}{z} - \left[\frac{w_L L_{LF}\sin\psi_{LF}}{z}\right] \tag{161}$$

$$a_{21} = w_L - \frac{v_{FD}T_1}{L} + \frac{\alpha v_{FD}T_2}{L} - \frac{\alpha e_{vF}T_2}{L} + \frac{\alpha e_{vF}T_1}{L} \tag{162}$$

$$a_{22} = 0 \tag{163}$$

$$a_{23} = \left[\frac{v_L \sin e_{F3}}{e_{F3}}\right] + \left[\frac{w_L L_{LF} \cos\psi_{LF}\left[-1+\cos e_{F3}\right]}{e_{F3}}\right] - \left[\frac{w_L L_{LF} \sin\psi_{LF} \sin e_{F3}}{e_{F3}}\right] \tag{164}$$

$$a_{24} = \frac{(1-\alpha)e_{F1}T_1}{L} - \frac{(1-\alpha)\alpha_1 e_{F1}T_2}{L} + \frac{dT_1}{L} - \frac{\alpha dT_2}{L} \tag{165}$$

$$a_{25} = -\frac{(1-\alpha)(1-\alpha_1)e_{vF}e_{F1}T_2}{Le_{\phi F}} + \frac{(1-\alpha)v_{FD}e_{F1}T_2}{Le_{\phi F}} + \frac{dv_{FD}T_2}{Le_{\phi F}} - \frac{(1-\alpha)de_{vF}T_2}{Le_{\phi F}} \tag{166}$$

$$a_{26} = -\frac{w_L d}{z} - \frac{dv_{FD}T_1}{Lz} + \left[\frac{w_L L_{LF} \cos\psi_{LF}}{z}\right] \tag{167}$$

$$a_{31} = 0 \tag{168}$$

$$a_{32} = 0 \tag{169}$$

$$a_{33} = 0 \tag{170}$$

$$a_{34} = \frac{T_1}{L} - \frac{\alpha T_2}{L} \tag{171}$$

$$a_{35} = \frac{v_{FD}T_2}{Le_{\phi F}} - \frac{(1-\alpha)e_{vF}T_2}{Le_{\phi F}} \tag{172}$$

$$a_{36} = \frac{w_L}{z} - \frac{v_{FD}T_1}{Lz} \tag{173}$$

Let

$$\frac{\left[-1+\cos(2e_{\phi F})\right]}{e_{\phi F}} = T_4 \tag{174}$$

$$\cos(2e_{\phi F})\cos(2\phi_{FD}) = T_5 \tag{175}$$

$$\sin(2e_{\phi F})\sin(2\phi_{FD}) = T_6 \tag{176}$$

$$\frac{\left[-1+\cos e_{\phi F}\right]}{e_{\phi F}} = T_7 \tag{177}$$

$$\sin e_{\phi F} \sin\phi_{FD} = T_8 \tag{178}$$

Using (174) through (178) in (152) through (154) results in

$$a_{41} = 0 \tag{179}$$

$$a_{42} = 0 \tag{180}$$

$$a_{43} = 0 \tag{181}$$

$$a_{44}=\left(\begin{array}{l}\frac{2dv_{FD}}{T_3}-\frac{\alpha 2dv_{FD}T_5}{T_3}-\frac{\alpha 2dv_{FD}T_6}{T_3}-\frac{de_{vF}}{T_3}-\frac{(1-\alpha)2dv_{FD}\cos(2\phi_{FD})}{T_3}+\frac{\alpha de_{vF}T_5}{T_3}\\+\frac{(1-\alpha)de_{vF}\cos(2\phi_{FD})}{T_3}+\frac{\alpha de_{vF}T_6}{T_3}\end{array}\right) \tag{182}$$

$$a_{45}=\left(\begin{array}{l}\frac{F_{uF}\cos\phi_{FD}T_7}{m}+\frac{F_{uF}T_8}{me_{\phi F}}+\frac{F_w\sin\phi_{FD}T_7}{m}-\frac{F_w\cos\phi_{FD}\sin e_{\phi F}}{me_{\phi F}}+\frac{dv_{FD}^2\cos(2\phi_{FD})T_4}{T_3}\\+\frac{dv_{FD}^2T_6}{T_3e_{\phi F}}-\frac{(1-\alpha)2dv_{FD}\cos(2\phi_{FD})T_4e_{vF}}{T_3}-\frac{(1-\alpha)2dv_{FD}T_6e_{vF}}{T_3e_{\phi F}}+\frac{(1-\alpha)de_{vF}^2T_6}{T_3e_{\phi F}}\\+\frac{(1-\alpha)d\cos(2\phi_{FD})T_4e_{vF}^2}{T_3}\end{array}\right) \tag{183}$$

$$a_{46}=\left(\frac{F_{uR}}{mz}+\frac{F_w\sin\phi_{FD}}{mz}+\frac{F_{uF}\sin\phi_{FD}}{mz}+\frac{\dot{v}_{FD}}{z}+\frac{dv_{FD}^2\cos(2\phi_{FD})}{T_3z}-\frac{dv_{FD}^2}{T_3z}\right) \tag{184}$$

$$a_{51}=0 \tag{185}$$

$$a_{52}=0 \tag{186}$$

$$a_{53}=0 \tag{187}$$

$$a_{54}=0 \tag{188}$$

$$a_{55}=\frac{-1}{\tau_S} \tag{189}$$

$$a_{56}=\frac{\dot{\phi}_{FD}}{z}+\frac{\phi_{FD}}{\tau_S z} \tag{190}$$

$$a_{61}=0 \tag{191}$$

$$a_{62}=0 \tag{192}$$

$$a_{63}=0 \tag{193}$$

$$a_{64}=0 \tag{194}$$

$$a_{65}=0 \tag{195}$$

$$a_{66}=-\lambda \tag{196}$$

$$b_{11}=0\,;b_{12}=0 \tag{197}$$

$$b_{21}=0\,;b_{22}=0 \tag{198}$$

$$b_{31} = 0 ; b_{32} = 0 \tag{199}$$

$$b_{41} = -\frac{1}{rm} ; b_{42} = 0 \tag{200}$$

$$b_{51} = 0 ; b_{52} = -\frac{1}{\tau_S} \tag{201}$$

$$b_{61} = 0 ; b_{62} = 0 \tag{202}$$

The state dependent algebraic Riccati equation in (118) is solved using MATLAB and the gains are obtained for the controller. The torque control inputs to the follower are given by

$$U = -K(E)E \tag{203}$$

where

$U = \begin{bmatrix} \tau_F \\ u \end{bmatrix}$, E is the augmented error vector and $K(E)$ is the gain matrix obtained by solving the SDARE.

7.3. FORMATION STABILITY

Consider a formation of $N+1$ robots consisting of a leader "l_i" and N followers. Let the torque control inputs $\begin{bmatrix} \tau_L & u_L \end{bmatrix}^T$ be applied to the leader such that the leader tracks a virtual reference robot. The torque control inputs for the leader can be derived in a similar way as the torque control inputs for the follower. It is assumed that the leader's motion is known i.e. there exists a control law that drives the leader independently to its desired trajectory. The torque control inputs are given by(203). Then the origin given by $E = \begin{bmatrix} e_{l_1} & e_{l_2} & e_{l_3} & e_{vl} & e_{\phi l} & e_{F1i}^T & e_{F2i}^T & e_{F3i}^T & e_{vFi}^T & e_{\phi Fi}^T \end{bmatrix}^T$ where $E \in \mathbb{R}^{(5(N+1))X1}$, which represents the augmented position, orientation and velocity tracking error systems for the leader "l_i" and N followers, respectively, is asymptotically stable in the presence of uncertainties and noise is proved below.

Consider the following Lyapunov candidate function

$$V_W = \frac{1}{2} E^T E \tag{204}$$

On taking the derivative of (204) yields

$$\dot{V}_W = \dot{E}E \tag{205}$$

Substituting (203) in (155) and substituting the resultant equation in (205) results in

$$\dot{V}_W = (A(E) - BK(E))E \tag{206}$$

where $A_{CL} = A(E) - BK(E)$ is negative definite as $K(E)$ is chosen to make A_{CL} negative definite. Therefore, $\dot{V}_W < 0$. Consider a new Lyapunov function candidate given by

$$V_{Formation} = \sum_{1}^{N} V_{Wi} + V_{l_1} \tag{207}$$

where V_{Wi} is given by (204) and

$$V_{l_1} = e_{l_1}^2 + e_{l_2}^2 + e_{l_3}^2 + e_{vl}^2 + e_{\phi l}^2 \tag{208}$$

Also (207) is positive for $E = \begin{bmatrix} e_{l_1} & e_{l_2} & e_{l_3} & e_{vl} & e_{\phi l} & e_{F1i}^T & e_{F2i}^T & e_{F3i}^T & e_{vFi}^T & e_{\phi Fi}^T \end{bmatrix}^T \neq 0$. Differentiating (207) yields

$$\dot{V}_{Formation} = \sum_{1}^{N} \dot{V}_{Wi} + \dot{V}_{l_1} \tag{209}$$

Since when $\dot{V}_{Wi} < 0$ for all $i = 1 to N$, so it automatically follows that $\sum_{1}^{N} \dot{V}_{Wi} < 0$. Also, the leader torque control inputs are designed such that the errors go to zero asymptotically and hence $\dot{V}_{l_1}$ is negative. Therefore, $\dot{V}_{Formation} < 0$, and the entire formation is asymptotically stable.

7.4. RESULTS AND DISCUSSION

A single leader single follower scenario is considered and the simulations are carried out using MATLAB for the same. The leader executes a circular trajectory with radius = 60 m, linear velocity of 5 m/sec and an angular velocity ~ 0.08 rad/sec. It is desired for the follower to execute a circle of radius = 56 m being parallel to the leader at all times. So the desired relative distance to be maintained is 4.0774 m and a relative bearing angle of 78.8199 degrees. The state weighting and control weighting matrices used for the simulation are Q = diag ([1400,900,900,900,1,1]); and R = diag ([1,1]).Also

the simulations were carried out with different time constants for the steering dynamics and increased friction parameters. The plots shown below are the ones obtained for a time constant of 0.25 and increased friction parameters of $F_{uR} = 10, F_{uF} = 20, F_W = 30$.

From Figure 7.1 it can be seen that the follower achieves the desired position and orientation, with the position and orientation errors going to zero asymptotically as shown in Figure 7.2. In Figure 7.2 e_{F1}, e_{F2} denote the position errors in the u and w direction respectively (refer Figure 2.1) and e_{F3} denotes the error in the orientation of the follower. The torque control inputs to the drive and steering system are as shown in Figure 7.3. This torque control input drives the errors in (113) to zero asymptotically resulting in the leader and follower trajectories as shown in Figure 7.4. It can be seen that the leader tracks a circle of 60 m radius and the follower is parallel to the leader at all times tracking a circle of radius 56 m. Figure 7.5 shows the velocity profile of the follower. From Figure 7.6 it can be inferred that the velocity tracking errors defined by the error system described by (113) also go to zero asymptotically. Figure 7.7 shows the relative distance and bearing angle maintained by the follower and it confirms with the desired relative distance and bearing angle calculated. In Figure 7.8 the position and orientation errors in inertial coordinates are shown.

In this section, an error system formulation (113) derived for integrated tracking and control is used to obtain the optimal torque control inputs. The input torque is obtained for the drive and steering system of a car-like follower mobile robot using SDARE approach to maintain a desired relative distance and bearing angle between the leader and the follower.

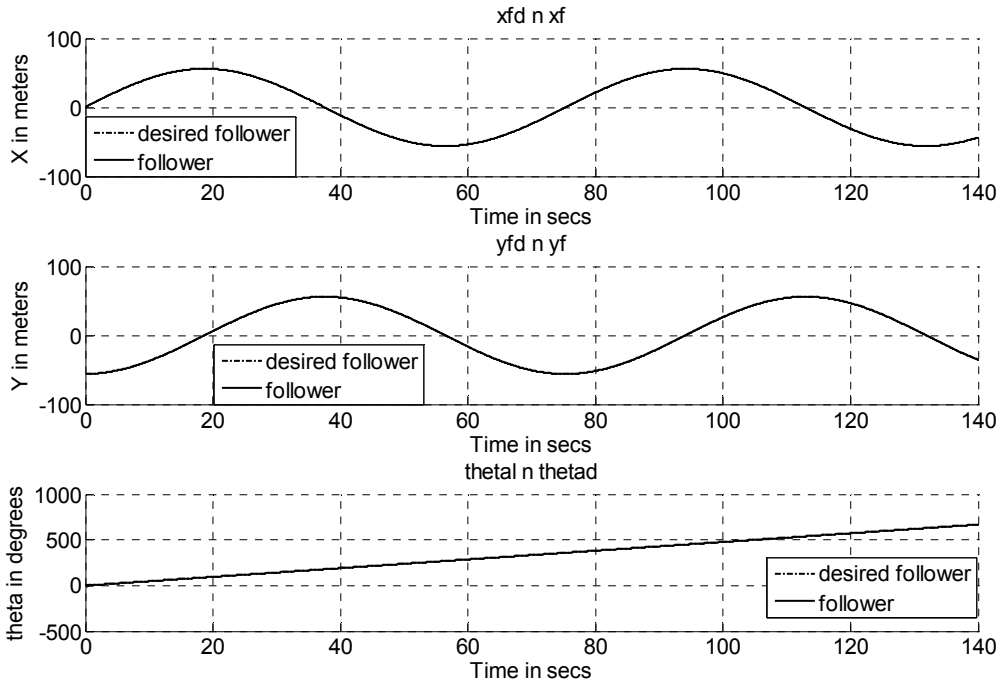

Figure 7.1 Actual and Desired Position and Orientation of the Follower

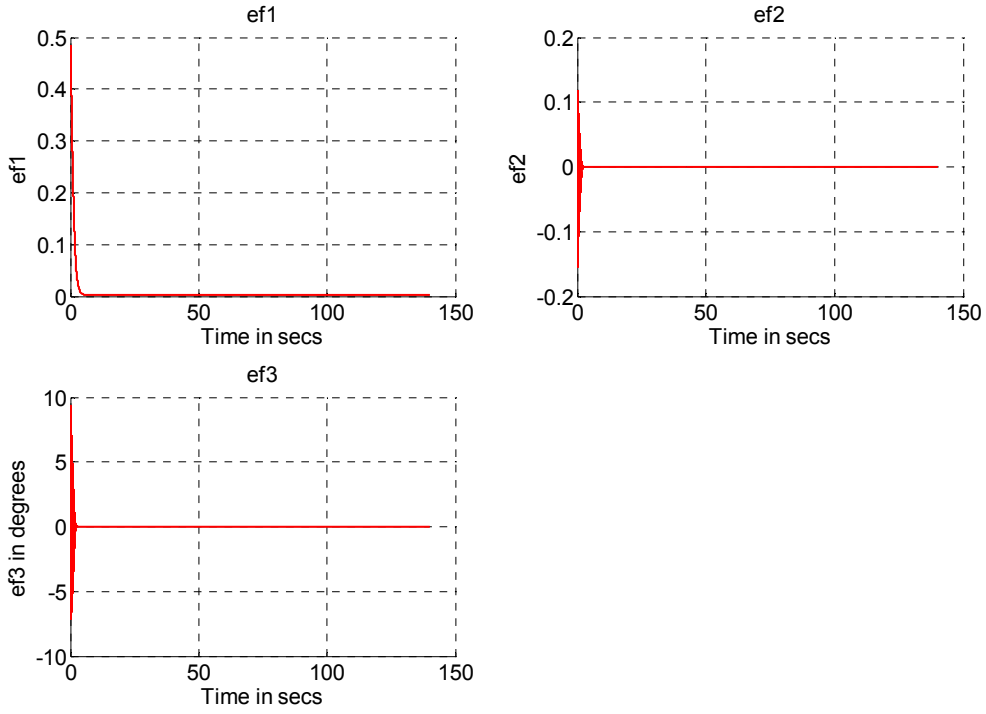

Figure 7.2 Position and Orientation Errors in Body Coordinates

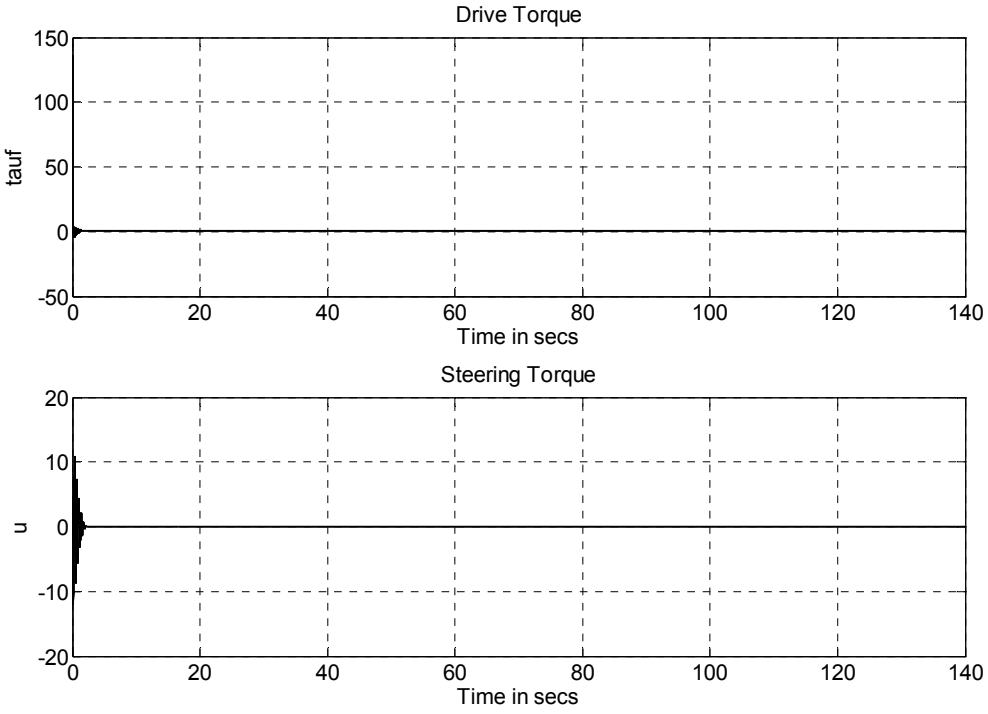

Figure 7.3 Drive and Steering Torques

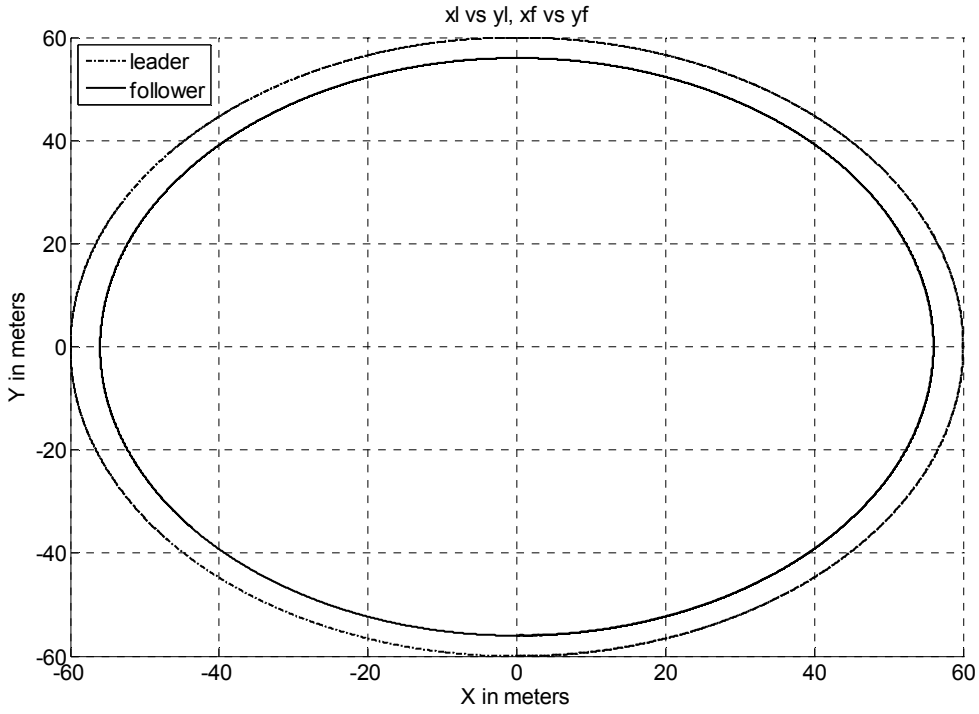

Figure 7.4 Leader and Follower Trajectories

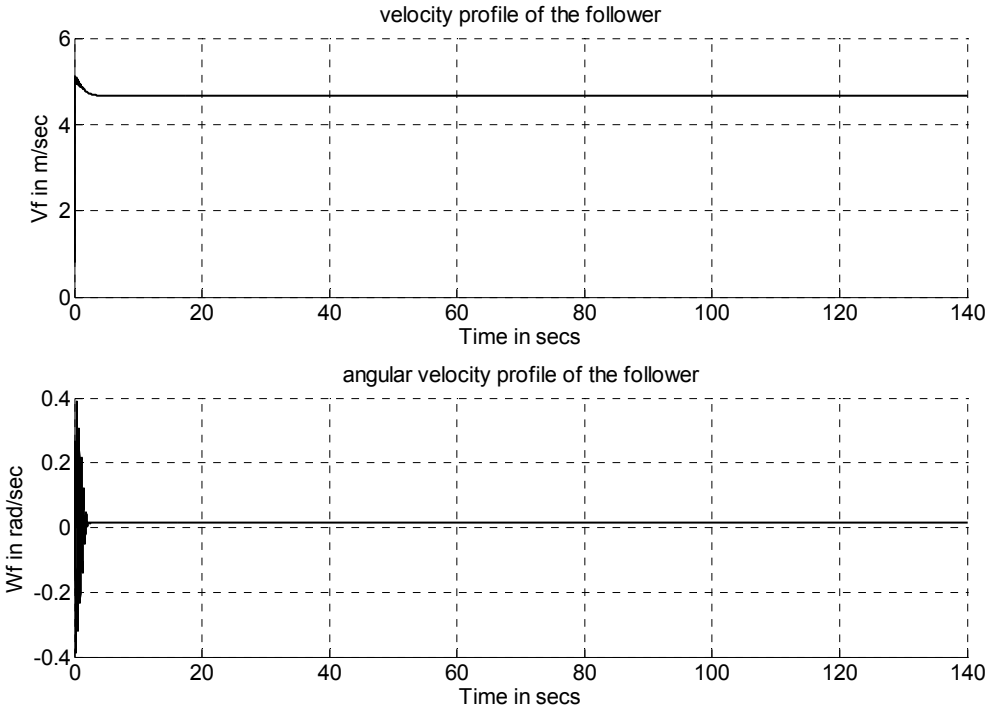

Figure 7.5 Linear Velocity and Angular Velocity Profile of the Follower

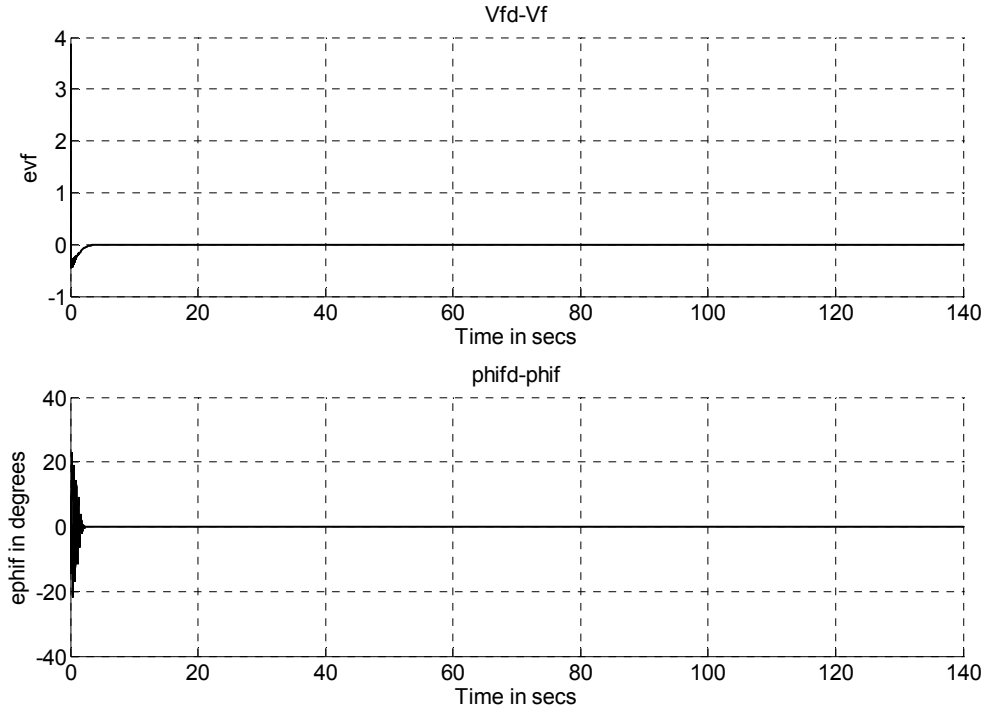

Figure 7.6 Velocity Error and Steering Angle Error Plots

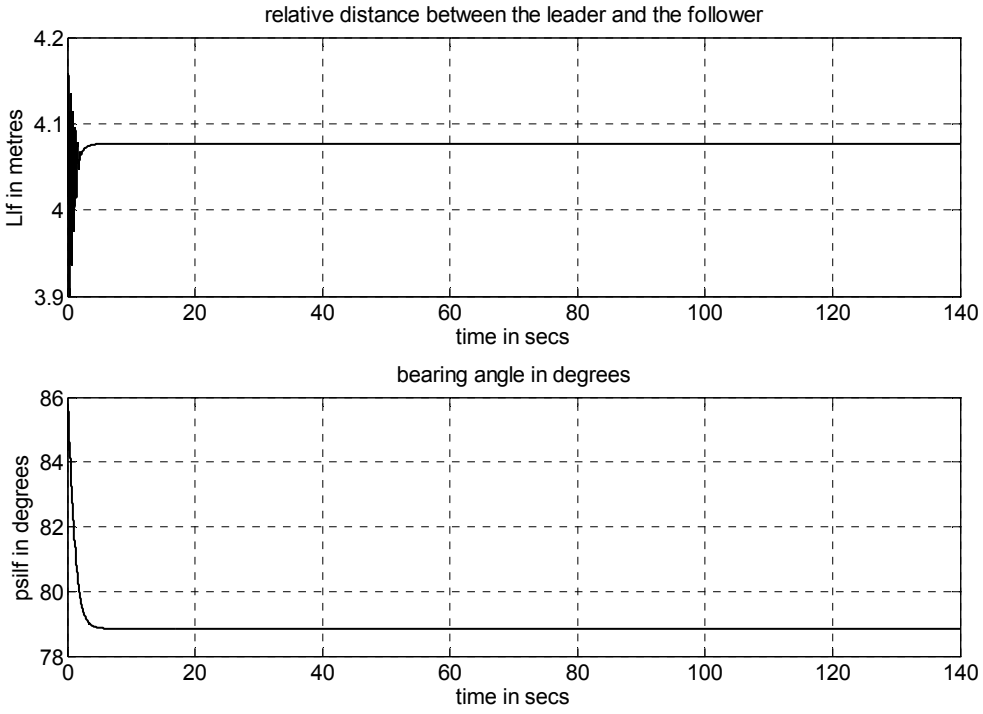

Figure 7.7 Relative Distance and Relative Bearing Angle of the Follower w.r.t. Leader

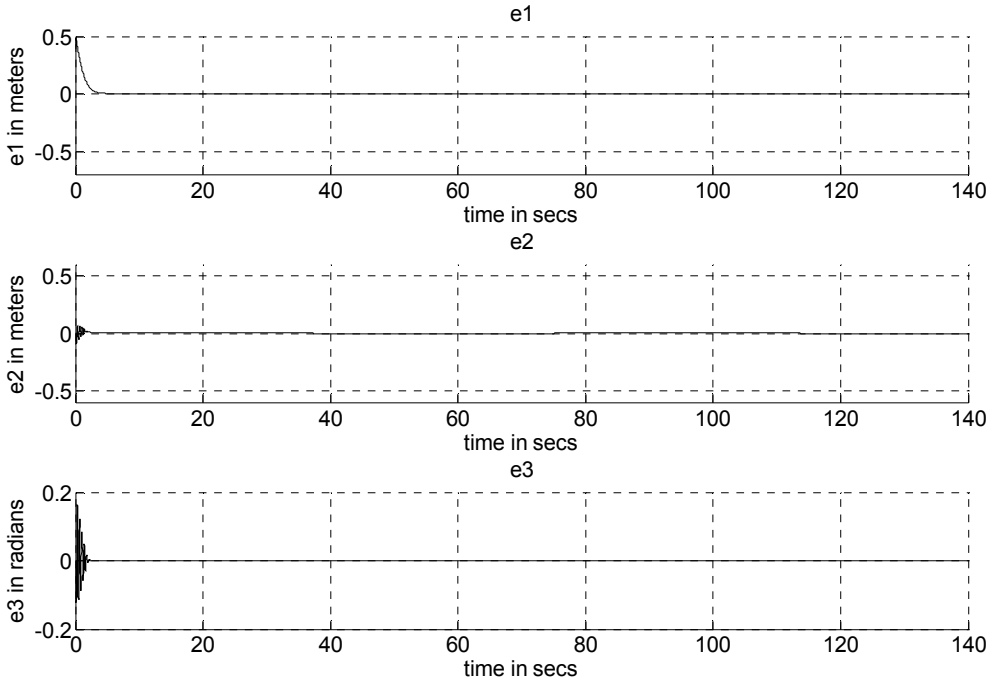

Figure 7.8 Position and Orientation Errors in Inertial Coordinates

8. INTEGRATED TRACKING AND ROBUST OPTIMAL CONTROL DESIGN USING ONLINE NEURAL NETWORK AND SDARE APPROACH

8.1. PROBLEM DESCRIPTION

The error system dynamics for the integrated tracking and control formulation is given by(113). Consider a subsystem of (113) given by

$$\begin{bmatrix} \dot{e}_{vF} \\ \dot{e}_{\phi F} \end{bmatrix} = \begin{bmatrix} F_1 - \frac{D(v_{FD})^2 \tan^2 \phi_F}{L^2} + \frac{2Dv_{FD}e_{vF} \tan^2 \phi_F}{L^2} - \frac{D(e_{vF})^2 \tan^2 \phi_F}{L^2} - \frac{\tau_F}{rm} \\ F_2 + \frac{\phi_{FD}}{\tau_S} - \frac{e_{\phi F}}{\tau_S} - \frac{u}{\tau_S} \end{bmatrix} \tag{210}$$

where

$$F_1 = \frac{F_{uR}}{m} + \frac{F_{uF} \cos \phi_F}{m} + \frac{F_w \sin \phi_F}{m} + \dot{v}_{FD}$$

$$F_2 = \dot{\phi}_{FD}$$

Grouping the error subsystem in (210) results in

$$\dot{E}_{SUB} = D\left(E_{SUB}\right) + F_{SUB} + B_{SUB}U \tag{211}$$

where

$$D\left(E_{SUB}\right) = \begin{bmatrix} F_1 \\ F_2 \end{bmatrix} \tag{212}$$

$$F_{SUB} = \begin{bmatrix} -\frac{D(v_{FD})^2 \tan^2 \phi_F}{L^2} + \frac{2Dv_{FD}e_{vF} \tan^2 \phi_F}{L^2} - \frac{D(e_{vF})^2 \tan^2 \phi_F}{L^2} \\ \frac{\phi_{FD}}{\tau_S} - \frac{e_{\phi F}}{\tau_S} \end{bmatrix} \tag{213}$$

$$B_{SUB} = \begin{bmatrix} -\frac{1}{rm} & 0 \\ 0 & -\frac{1}{\tau_S} \end{bmatrix} \tag{214}$$

$$U = \begin{bmatrix} \tau_F \\ u \end{bmatrix} \tag{215}$$

The expression in (212) represents the uncertainties in the system. The goal is to find an extra control that can make up for the effects of these uncertainties and one that

makes the controller robust to uncertainties due to modeling error or parameter variations.

8.2. OPTIMAL CONTROL DERIVATION FOR THE NOMINAL SYSTEM

The optimal control for the nominal system is obtained by using the SDARE approach. The nominal system is one without uncertainties. The expression for the nominal system is given by

$$\dot{E} = F(E) + B(E)U_{OPT} = A(E)E + B(E)U_{OPT} \tag{216}$$

where $A(E)$ is R^{6X6} and $U_{OPT} = \begin{bmatrix} u_1 \\ u_2 \end{bmatrix}$.

From earlier derivations, the differential equations that describe the evolution of errors over time are given by

$$\dot{e}_{F1} = v_L \cos e_{F3} - v_F - w_L \left(L_{LF} \sin \gamma_F + e_{F2} \right) + w_F e_{F2} \tag{217}$$

$$\dot{e}_{F2} = v_L \sin e_{F3} + w_L \left(e_{F1} - d \right) - w_F \left(e_{F1} - d \right) - L w_F + w_L L_{LF} \cos \gamma_F \tag{218}$$

$$\dot{e}_{F3} = w_L - w_F \tag{219}$$

$$\dot{e}_{vF} = F_1 - \frac{d(v_{FD})^2 \tan^2 \phi_F}{L^2} + \frac{2 d v_{FD} e_{vF} \tan^2 \phi_F}{L^2} - \frac{d(e_{vF})^2 \tan^2 \phi_F}{L^2} - \frac{\tau_F}{rm} \tag{220}$$

$$\dot{e}_{\phi F} = F_2 + \frac{\phi_{FD}}{\tau_S} - \frac{e_{\phi F}}{\tau_S} - \frac{u}{\tau_S} \tag{221}$$

The uncertainties F_1 and F_2 are not present in the nominal system. Therefore, the expression for $\dot{e}_{vFNOM}$ and $\dot{e}_{\phi FNOM}$ are given by

$$\dot{e}_{vFNOM} = \frac{-d(v_{FD})^2 \tan^2 \phi_F}{L^2} + \frac{2 d e_{vF} v_{FD} \tan^2 \phi_F}{L^2} - \frac{d(e_{vF})^2 \tan^2 \phi_F}{L^2} - \frac{u_1}{rm} \tag{222}$$

$$\dot{e}_{\phi FNOM} = \frac{\phi_{FD}}{\tau_S} - \frac{e_{\phi F}}{\tau_S} - \frac{u_2}{\tau_S} \tag{223}$$

The parameterization of $\dot{e}_{F1}, \dot{e}_{F2}$ and $\dot{e}_{F3}$ is similar to the what was done earlier and the parameterized equations are given by (134), (138) and (141).

On parameterizing $\dot{e}_{vFNOM}$ from (222) the parameterized expression for $\dot{e}_{vFNOM}$ is given by

$$\dot{e}_{vF} = \left(\begin{array}{l} -\frac{d(v_{FD})^2}{T_3 z} z + \frac{d(v_{FD})^2 \cos 2\phi_{FD}}{T_3} \left(\frac{-1+\cos 2e_{\phi F}}{e_{\phi F}} \right) e_{\phi F} + \frac{d(v_{FD})^2 \cos 2\phi_{FD}}{T_3 z} z \\ -\left(\frac{(1-\alpha)2dv_{FD}e_{vF} \sin 2\phi_{FD} \sin 2e_{\phi F}}{T_3 e_{\phi F}} \right) e_{\phi F} + \frac{(1-\alpha)d(e_{vF})^2 \cos 2\phi_{FD}}{T_3} \\ +\left(\frac{d(v_{FD})^2 \sin 2\phi_{FD} \sin 2e_{\phi F}}{T_3 e_{\phi F}} \right) e_{\phi F} + \frac{2dv_{FD}}{T_3} e_{vF} - \frac{(1-\alpha)2dv_{FD}e_{vF} \cos 2\phi_{FD}}{T_3} \\ -\frac{\alpha 2dv_{FD}e_{vF} \cos 2\phi_{FD} \cos 2e_{\phi F}}{T_3} - \frac{(1-\alpha)2dv_{FD}e_{vF} \cos 2\phi_{FD}}{T_3} \left(\frac{-1+\cos 2e_{\phi F}}{e_{\phi F}} \right) e_{\phi F} \\ -\frac{\alpha 2dv_{FD}e_{vF} \sin 2\phi_{FD} \sin 2e_{\phi F}}{T_3} - \frac{d(e_{vF})^2}{T_3} + \frac{\alpha d(e_{vF})^2 \cos 2\phi_{FD} \cos 2e_{\phi F}}{T_3} \\ +\frac{(1-\alpha)d(e_{vF})^2 \cos 2\phi_{FD}}{T_3} \left(\frac{-1+\cos 2e_{\phi F}}{e_{\phi F}} \right) e_{\phi F} + \frac{\alpha d(e_{vF})^2 \sin 2\phi_{FD} \sin 2e_{\phi F}}{T_3} \\ +\left(\frac{(1-\alpha)d(e_{vF})^2 \sin 2\phi_{FD} \sin 2e_{\phi F}}{T_3 e_{\phi F}} \right) e_{\phi F} - \frac{u_1}{rm} \end{array} \right) \quad (224)$$

On parameterizing $\dot{e}_{\phi FNOM}$ from (223) the parameterized expression for $\dot{e}_{\phi FNOM}$ is given by

$$\dot{e}_{\phi F} = \frac{\phi_{FD}}{\tau_S z} z - \frac{e_{\phi F}}{\tau_S} - \frac{u_2}{\tau_S} \quad (225)$$

From the equations(134), (138) , (141), (224) and (225) the expressions for the elements of matrices $A(E)$ and $B(E)$ are as given below

$$a_{11} = 0 \quad (226)$$

$$a_{12} = -w_L + \frac{v_{FD}T_1}{L} - \frac{\alpha v_{FD}T_2}{L} + \frac{\alpha e_{vF}T_2}{L} - \frac{\alpha e_{vF}T_1}{L} \quad (227)$$

$$a_{13} = \left[\frac{v_L[-1+\cos e_{F3}]}{e_{F3}} \right] - \left[\frac{w_L L_{LF} \sin \psi_{LF}[-1+\cos e_{F3}]}{e_{F3}} \right] - \left[\frac{w_L L_{LF} \cos \psi_{LF} \sin e_{F3}}{e_{F3}} \right] \quad (228)$$

$$a_{14} = 1 + \frac{(1-\alpha)\alpha_1 e_{F2}T_2}{L} - \frac{(1-\alpha)e_{F2}T_1}{L} \quad (229)$$

$$a_{15} = \frac{(1-\alpha)(1-\alpha_1)e_{vF}e_{F2}T_2}{Le_{\phi F}} - \frac{(1-\alpha)v_{FD}e_{F2}T_2}{Le_{\phi F}} \quad (230)$$

$$a_{16} = \frac{v_L}{z} - \frac{v_{FD}}{z} - \left[\frac{w_L L_{LF} \sin\psi_{LF}}{z}\right] \tag{231}$$

$$a_{21} = w_L - \frac{v_{FD}T_1}{L} + \frac{\alpha v_{FD}T_2}{L} - \frac{\alpha e_{vF}T_2}{L} + \frac{\alpha e_{vF}T_1}{L} \tag{232}$$

$$a_{22} = 0 \tag{233}$$

$$a_{23} = \left[\frac{v_L \sin e_{F3}}{e_{F3}}\right] + \left[\frac{w_L L_{LF} \cos\psi_{LF}\left[-1+\cos e_{F3}\right]}{e_{F3}}\right] - \left[\frac{w_L L_{LF} \sin\psi_{LF} \sin e_{F3}}{e_{F3}}\right] \tag{234}$$

$$a_{24} = \frac{(1-\alpha)e_{F1}T_1}{L} - \frac{(1-\alpha)\alpha_1 e_{F1}T_2}{L} + \frac{dT_1}{L} - \frac{\alpha dT_2}{L} \tag{235}$$

$$a_{25} = -\frac{(1-\alpha)(1-\alpha_1)e_{vF}e_{F1}T_2}{Le_{\phi F}} + \frac{(1-\alpha)v_{FD}e_{F1}T_2}{Le_{\phi F}} + \frac{dv_{FD}T_2}{Le_{\phi F}} - \frac{(1-\alpha)de_{vF}T_2}{Le_{\phi F}} \tag{236}$$

$$a_{26} = -\frac{w_L d}{z} - \frac{dv_{FD}T_1}{Lz} + \left[\frac{w_L L_{LF} \cos\psi_{LF}}{z}\right] \tag{237}$$

$$a_{31} = 0 \tag{238}$$

$$a_{32} = 0 \tag{239}$$

$$a_{33} = 0 \tag{240}$$

$$a_{34} = \frac{T_1}{L} - \frac{\alpha T_2}{L} \tag{241}$$

$$a_{35} = \frac{v_{FD}T_2}{Le_{\phi F}} - \frac{(1-\alpha)e_{vF}T_2}{Le_{\phi F}} \tag{242}$$

$$a_{36} = \frac{w_L}{z} - \frac{v_{FD}T_1}{Lz} \tag{243}$$

Let

$$\frac{\left[-1+\cos(2e_{\phi F})\right]}{e_{\phi F}} = T_4 \tag{244}$$

$$\cos(2e_{\phi F})\cos(2\phi_{FD}) = T_5 \tag{245}$$

$$\sin(2e_{\phi F})\sin(2\phi_{FD}) = T_6 \tag{246}$$

$$\frac{\left[-1+\cos e_{\phi F}\right]}{e_{\phi F}} = T_7 \tag{247}$$

$$\sin e_{\phi F} \sin\phi_{FD} = T_8 \tag{248}$$

Using (174) through (178) in (152) through (154) results in

$$a_{41} = 0 \tag{249}$$

$$a_{42} = 0 \tag{250}$$

$$a_{43} = 0 \tag{251}$$

$$a_{44} = \left(\begin{array}{l} \frac{2dv_{FD}}{T_3} - \frac{\alpha 2dv_{FD}T_5}{T_3} - \frac{\alpha 2dv_{FD}T_6}{T_3} - \frac{de_{vF}}{T_3} - \frac{(1-\alpha)2dv_{FD}\cos(2\phi_{FD})}{T_3} + \frac{\alpha de_{vF}T_5}{T_3} \\ + \frac{(1-\alpha)de_{vF}\cos(2\phi_{FD})}{T_3} + \frac{\alpha de_{vF}T_6}{T_3} \end{array} \right) \tag{252}$$

$$a_{45} = \left(\begin{array}{l} + \frac{dv_{FD}^2\cos(2\phi_{FD})T_4}{T_3} + \frac{dv_{FD}^2T_6}{T_3e_{\phi F}} - \frac{(1-\alpha)2dv_{FD}\cos(2\phi_{FD})T_4e_{vF}}{T_3} \\ - \frac{(1-\alpha)2dv_{FD}T_6e_{vF}}{T_3e_{\phi F}} + \frac{(1-\alpha)de_{vF}^2T_6}{T_3e_{\phi F}} + \frac{(1-\alpha)d\cos(2\phi_{FD})T_4e_{vF}^2}{T_3} \end{array} \right) \tag{253}$$

$$a_{46} = \left(+ \frac{dv_{FD}^2\cos(2\phi_{FD})}{T_3z} - \frac{dv_{FD}^2}{T_3z} \right) \tag{254}$$

$$a_{51} = 0 \tag{255}$$

$$a_{52} = 0 \tag{256}$$

$$a_{53} = 0 \tag{257}$$

$$a_{54} = 0 \tag{258}$$

$$a_{55} = \frac{-1}{\tau_S} \tag{259}$$

$$a_{56} = \frac{\phi_{FD}}{\tau_S z} \tag{260}$$

$$a_{61} = 0 \tag{261}$$

$$a_{62} = 0 \tag{262}$$

$$a_{63} = 0 \tag{263}$$

$$a_{64} = 0 \tag{264}$$

$$a_{65} = 0 \tag{265}$$

$$a_{66} = -\lambda \tag{266}$$

$$b_{11} = 0 \; ; b_{12} = 0 \tag{267}$$

$$b_{21} = 0 ; b_{22} = 0 \tag{268}$$

$$b_{31} = 0 ; b_{32} = 0 \tag{269}$$

$$b_{41} = -\frac{1}{rm} ; b_{42} = 0 \tag{270}$$

$$b_{51} = 0 ; b_{52} = -\frac{1}{\tau_S} \tag{271}$$

$$b_{61} = 0 ; b_{62} = 0 \tag{272}$$

The state dependent algebraic Riccati equation in (118) is solved using MATLAB and the gains K are obtained for the controller. The optimal control input to the system is given by

$$U_{OPT} = -K(E)E \tag{273}$$

and the system is pointwise stable.

8.3. UNCERTAINITY MODELING, WEIGHT UPDATES AND EXTRA CONTROL DERIVATION

Two single layer functional link neural networks (FLNN) are used for the approximation of F_1 and F_2, the elements of $D\left(E_{SUB}\right)$. These terms involve the friction terms and desired accelerations terms that cannot be computed in real life accurately. Hence, online neural networks will be used to estimate F_1 and F_2, and they are defined as

$$D(E_{SUB}) = \begin{bmatrix} \mathbf{f}(\mathbf{x}_{Fnew1}) \\ \mathbf{f}(\mathbf{x}_{Fnew2}) \end{bmatrix} \tag{274}$$

The activation functions $\phi(\mathbf{x}_{Fnew1}), \phi(\mathbf{x}_{Fnew2})$ can be chosen as a basis set for the universal approximation property to hold for single layer FLNN. Then there exists weights W_1 and W_2 such that

$$\mathbf{f}(\mathbf{x}_{Fnew1}) = W_1^T \phi(\mathbf{x}_{Fnew1}) + \varepsilon_1 \tag{275}$$

$$\mathbf{f}(\mathbf{x}_{Fnew2}) = W_2^T \phi(\mathbf{x}_{Fnew2}) + \varepsilon_2 \tag{276}$$

with the estimation errors ε_1 and ε_2 bounded. The bounds are given by $\|\varepsilon_1\| < \varepsilon_{1N}$ and $\|\varepsilon_2\| < \varepsilon_{2N}$. The ideal approximating weights are unknown and nonunique. So an

assumption is made that $\|W_1\|_F < W_{1B}$ and $\|W_2\|_F < W_{2B}$ with the bounds W_{1B} and W_{2B} known. The Forbenius norm is denoted by $\| \ \|_F$. Then estimates of $\mathbf{f}(\mathbf{x}_{Fnew1})$ and $\mathbf{f}(\mathbf{x}_{Fnew2})$ are given by

$$\hat{F}_1 = \hat{\mathbf{f}}(\mathbf{x}_{Fnew1}) = \hat{W}_1^T \phi(\mathbf{x}_{Fnew1}) \tag{277}$$

$$\hat{F}_2 = \hat{\mathbf{f}}(\mathbf{x}_{Fnew2}) = \hat{W}_2^T \phi(\mathbf{x}_{Fnew2}) \tag{278}$$

with $\hat{W}_1$ and $\hat{W}_2$ being the weights of the two neural networks.

Let U_{OPT} denote the control generated by the optimal controller using SDARE approach for the nominal system and let U_{EX} denote the extra control [22] applied to compensate for the uncertainties. Hence the total control applied to the system is

$$U = U_{OPT} + U_{EX} \tag{279}$$

Substituting (279) in (211) the expression for $\dot{E}_{SUB}$ becomes,

$$\dot{E}_{SUB} = D_{SUB} + F_{SUB} + B_{SUB}U_{OPT} + B_{SUB}U_{EX} \tag{280}$$

The uncertainty is compensated for by choosing the extra control U_{EX} as

$$U_{EX} = -B_{SUB}^{-1}\hat{D}_{SUB} \tag{281}$$

where

$$\hat{D}_{SUB} = \begin{bmatrix} \hat{W}_1^T \phi(\mathbf{x}_{FNEW1}) \\ \hat{W}_2^T \phi(\mathbf{x}_{FNEW2}) \end{bmatrix} \tag{282}$$

Substituting (281) in (280) , the expression for $\dot{E}_{SUB}$ becomes

$$\dot{E}_{SUB} = \tilde{D}_{SUB} + F_{SUB} + B_{SUB}U_{OPT} \tag{283}$$

When there is function estimation error present, then the system equation after substituting $U_{OPT} = -K(E)E$ becomes

$$\dot{E} = A(E)E - BK(E)E + \tilde{D} \tag{284}$$

where

$$\tilde{D} = \begin{bmatrix} 0 & 0 & 0 & \tilde{W}_1^T \phi(\mathbf{x}_{FNEW1}) & \tilde{W}_2^T \phi(\mathbf{x}_{FNEW2}) \end{bmatrix}^T$$

An online weight update rule is now developed to guarantee stable tracking and yet guarantee bounded-ness of weights. The weight estimation error is defined as

$$\tilde{W}_1 = W_1 - \hat{W}_1 \tag{285}$$

$$\tilde{W}_2 = W_2 - \hat{W}_2 \tag{286}$$

To derive the weight tuning law consider the Lyapunov candidate function given by

$$V_W = \frac{1}{2}E^T E + \frac{1}{2}tr\left\{\tilde{W}_1^T L_1^{-1}\tilde{W}_1\right\} + \frac{1}{2}tr\left\{\tilde{W}_2^T L_2^{-1}\tilde{W}_2\right\} \tag{287}$$

On differentiating (287) and substituting (284) , the expression for $\dot{V}_W$ is given by

$$\dot{V}_W = \begin{pmatrix} E^T(A(E) - BK(E))E + e_{vF}\tilde{W}_1^T\phi(\mathbf{x}_{FNEW1}) + e_{\phi F}\tilde{W}_2^T\phi(\mathbf{x}_{FNEW2}) \\ +tr\left\{\tilde{W}_1^T L_1^{-1}\dot{\tilde{W}}_1\right\} + tr\left\{\tilde{W}_2^T L_2^{-1}\dot{\tilde{W}}_2\right\} \end{pmatrix} \tag{288}$$

where L_1, L_2 are user defined tuning matrices.

Further grouping the terms in (288), $\dot{V}_W$ becomes

$$\dot{V}_W = \begin{pmatrix} E^T(A(E) - BK(E))E + tr\left\{\tilde{W}_1^T\left(L_1^{-1}\dot{\tilde{W}}_1 + \phi(\mathbf{x}_{Fnew1})e_{vF}\right)\right\} \\ +tr\left\{\tilde{W}_2^T\left(L_2^{-1}\dot{\tilde{W}}_2 + \phi(\mathbf{x}_{Fnew2})e_{\phi F}\right)\right\} \end{pmatrix} \tag{289}$$

Selecting the weight tuning laws as

$$\dot{\hat{W}}_1 = L_1\phi(\mathbf{x}_{Fnew1})e_{vF} - k_{NEW1}L_1\left\|\mathbf{e}_{vF}\right\|\hat{W}_1 \tag{290}$$

$$\dot{\hat{W}}_2 = L_2\phi(\mathbf{x}_{Fnew2})e_{\phi F} - k_{NEW2}L_2\left\|e_{\phi F}\right\|\hat{W}_2 \tag{291}$$

Substituting (290) and (291) in (289) $\dot{V}_W$ can be written as

$$\dot{V}_W = \begin{pmatrix} E^T(A(E) - BK(E))E + k_{NEW1}\left\|e_{vF}\right\|tr\left\{\tilde{W}_1^T\left(W_1 - \hat{W}_1\right)\right\} \\ +k_{NEW2}\left\|e_{\phi F}\right\|tr\left\{\tilde{W}_2^T\left(W_2 - \hat{W}_2\right)\right\} \end{pmatrix} \tag{292}$$

Also from [20]

$$tr\left\{\tilde{W}^T(W - \hat{W})\right\} = \left\langle\tilde{W}, W\right\rangle_F - \left\|\tilde{W}\right\|_F^2 \le \left\|\tilde{W}\right\|_F\left\|W\right\|_F - \left\|\tilde{W}\right\|_F^2 \tag{293}$$

Using (293) and further simplifying (292)

$$\dot{V}_W \le \begin{pmatrix} (BK - A)_{\min}\left(\sqrt{e_{F1}^2 + e_{F2}^2 + e_{F3}^2}\right)^2 \\ -\left\|e_{vF}\right\|\left\{(BK - A)_{\min}\left\|e_{vF}\right\| + k_{NEW1}\left\|\tilde{W}_1\right\|_F\left(\left\|\tilde{W}_1\right\|_F - W_{1B}\right)\right\} \\ -\left\|e_{\phi F}\right\|\left\{(BK - A)_{\min}\left\|e_{\phi F}\right\| + k_{NEW2}\left\|\tilde{W}_2\right\|_F\left(\left\|\tilde{W}_2\right\|_F - W_{2B}\right)\right\} \end{pmatrix} \tag{294}$$

The term given by

$$(BK-A)_{\min}\left\|e_{vF}\right\|+k_{NEW1}\left\|\tilde{W}_1\right\|_F\left(\left\|\tilde{W}_1\right\|_F-W_{1B}\right)=\begin{pmatrix}k_{NEW1}\left(\left\|\tilde{W}_1\right\|_F-\dfrac{W_{1B}}{2}\right)^2-\dfrac{k_{NEW1}W_{1B}^2}{4}\\+(BK-A)_{\min}\left\|e_{vF}\right\|\end{pmatrix} \tag{295}$$

is guaranteed positive as long as

$$\left\|e_{vF}\right\|\geq\frac{k_{NEW1}W_{1B}^2}{4(BK-A)_{\min}}\equiv b_{e_{FD1}}\,or\,\left\|\tilde{W}_1\right\|_F>\frac{W_{1B}}{2}+\sqrt{\frac{W_{1B}^2}{4}}\equiv b_{W1} \tag{296}$$

The term given by

$$(BK-A)_{\min}\left\|e_{\phi F}\right\|+k_{NEW2}\left\|\tilde{W}_2\right\|_F\left(\left\|\tilde{W}_2\right\|_F-W_{2B}\right)=\begin{pmatrix}k_{NEW2}\left(\left\|\tilde{W}_2\right\|_F-\dfrac{W_{2B}}{2}\right)^2-\dfrac{k_{NEW2}W_{2B}^2}{4}\\+(BK-A)_{\min}\left\|e_{\phi F}\right\|\end{pmatrix} \tag{297}$$

is guaranteed positive as long as

$$\left\|e_{\phi F}\right\|\geq\frac{k_{NEW2}W_{2B}^2}{4(BK-A)_{\min}}\equiv b_{e_{FD2}}\,or\,\left\|\tilde{W}_2\right\|_F>\frac{W_{2B}}{2}+\sqrt{\frac{W_{2B}^2}{4}}\equiv b_{W2} \tag{298}$$

So, $\dot{V}_W$ is negative outside a compact set. Let the NN function approximation property holds for $\mathbf{f}(\mathbf{x}_{Fnew1})$ and $\mathbf{f}(\mathbf{x}_{Fnew2})$ with an accuracy of ε_{N1} and ε_{N2} respectively for all $\mathbf{x}_{Fnew1}$ and $\mathbf{x}_{Fnew2}$ in the compact sets $S_{Fnew1}\equiv\{x_{Fnew1}\,|\,\left\|x_{Fnew1}\right\|<b_{x_{Fnew1}}\}$ and $S_{Fnew2}\equiv\{x_{Fnew2}\,|\,\left\|x_{Fnew2}\right\|<b_{x_{Fnew2}}\}$ with $b_{x_{Fnew1}}>e_{vFB}$ and $b_{x_{Fnew2}}>e_{\phi FB}$ where e_{vFB} and $\sin e_{\phi FB}$ are the bounds on the desired trajectory e_{vFD} and $\sin e_{\phi FD}$.

Define $S_{e_{VF}}\equiv\{e_{vF}\,|\,\left\|e_{VF}\right\|<(b_{x_{Fnew1}}-e_{vFB})/(c_0+c_1)\}$ (299)

$$S_{e_{\phi F}}\equiv\{e_{\phi F}\,|\,\left\|e_{\phi F}\right\|<(b_{x_{Fnew2}}-e_{\phi FB})/(c_2+c_3)\} \tag{300}$$

Now selecting the gains

$$(BK-A)_{\min}>\frac{k_{NEW1}W_{1B}^2(c_0+c_1)}{4(b_{x_{Fnew1}}-e_{vFB})} \tag{301}$$

$$(BK-A)_{\min}>\frac{k_{NEW2}W_{2B}^2(c_2+c_3)}{4(b_{x_{Fnew2}}-e_{\phi FB})} \tag{302}$$

ensures that the compact sets defined by $\|e_{vF}\| < b_{e_{FD1}}$ and $\|e_{\phi F}\| < b_{e_{FD2}}$ are contained in S_{evF} and $S_{e\phi F}$. This guarantees that the error $e_{vF}, e_{\phi F}$ and the NN weight estimates $\hat{W}_1$ and $\hat{W}_2$ are uniformly ultimately bounded (UUB) [20] with bounds given by (296) and (298).

8.4. FORMATION STABILITY

Consider a formation of $N+1$ robots consisting of a leader "l_i" and N followers. Let the torque control inputs $\begin{bmatrix} \tau_L & u_L \end{bmatrix}^T$ be applied to the leader such that the leader tracks a virtual reference robot. The torque control inputs for the leader can be derived in a similar way as the torque control inputs for the follower. It is assumed that the leader's motion is known i.e. there exists a control law that drives the leader independently to its desired trajectory. The torque control inputs are given by $U = U_{OPT} + U_{EX}$ with U_{OPT} and U_{EX} given by (273) and (281) respectively. Then the origin given by $E = \begin{bmatrix} e_{l_1} & e_{l_2} & e_{l_3} & e_{vl} & e_{\phi l} & e_{F1i}^T & e_{F2i}^T & e_{F3i}^T & e_{vFi}^T & e_{\phi Fi}^T \end{bmatrix}^T$ where $E \in \square^{(5(N+1))X1}$, which represents the augmented position, orientation and velocity tracking error systems for the leader "l_i" and N followers, respectively, is asymptotically stable in the presence of uncertainties and noise is proved below.

Consider the following Lyapunov candidate function

$$V_{Formation} = \sum_{1}^{N} V_{Wi} + V_{l_1} \tag{303}$$

where V_{Wi} is given by (287) and

$$V_{l_1} = e_{l_1}^2 + e_{l_2}^2 + e_{l_3}^2 + e_{vl}^2 + e_{\phi l}^2 \tag{304}$$

Also (303) is positive for $E = \begin{bmatrix} e_{l_1} & e_{l_2} & e_{l_3} & e_{vl} & e_{\phi l} & e_{F1i}^T & e_{F2i}^T & e_{F3i}^T & e_{vFi}^T & e_{\phi Fi}^T \end{bmatrix}^T \neq 0$. Differentiating (303) yields

$$\dot{V}_{Formation} = \sum_{1}^{N} \dot{V}_{Wi} + \dot{V}_{l_1} \tag{305}$$

In the previous subsection it has been proved that V_{Wi} for all $i = 1 to N$ individually is negative outside a compact set and that the errors and the NN weight estimates $\hat{W}_1$ and $\hat{W}_2$ are uniformly ultimately bounded (UUB). Hence when $\dot{V}_{Wi} < 0$ for all $i = 1 to N$, so it automatically follows that $\sum_{1}^{N} \dot{V}_{Wi} < 0$. Also the leader torque control inputs are designed such that the errors go to zero asymptotically and hence $\dot{V}_{l_1}$ is negative. Therefore $\dot{V}_{Formation} < 0$, and the entire formation is asymptotically stable

8.5. RESULTS AND DISCUSSION

A single leader single follower scenario is considered and the simulations are carried out using MATLAB for the same. The leader executes a circular trajectory with radius = 60 m, linear velocity of 5 m/sec and an angular velocity ~ 0.08 rad/sec. It is desired for the follower to execute a circle of radius = 56 m being parallel to the leader at all times. So the desired relative distance to be maintained is 4.0774 m and a relative bearing angle of 78.8199 degrees. The state weighting and control weighting matrices used for the simulation are Q= diag([900,900,900,900,400,1]) and R=diag([1,1]).

The constants $k_{NEW1} = 100$, $k_{NEW2} = 100$, $L_1 = .044 * eye(20)$ and $L_2 = 1 * eye(20)$ are used in the NN weight update rule where $eye(20)$ denotes a $20 X 20$ identity matrix. The NN's have 20 hidden layer neurons each. Measurement noise is added in the form Gaussian noise with zero mean. The noise added is one percent of the states that are inputs to the neural network. Also the simulations were carried out with different time constants for the steering dynamics and increased friction parameters. The plots shown below are the ones obtained for a time constant of 0.25 and increased friction parameters of $F_{uR} = 10, F_{uF} = 20, F_W = 30$.

From Figure 8.1 it can be seen that the follower achieves the desired position and orientation, with the position and orientation errors going to zero asymptotically as shown in Figure 8.2. In Figure 8.2 e_{F1}, e_{F2} denote the position errors in the u and w direction respectively (refer Figure 2.1) and e_{F3} denotes the error in the orientation of the

follower. Figure 8.3 shows the position and orientation errors in inertial coordinates. The optimal torque control inputs to the drive and steering system are as shown in Figure 8.4 and Figure 8.5. The extra control inputs to the follower that compensate for the uncertainties are shown in Figure 8.6 and Figure 8.7. The drive and steering torque inputs shown in Figure 8.8 drive the errors in (113) to zero asymptotically resulting in the leader and follower trajectories are as shown in Figure 8.9. The drive and steering torque are a combination of the optimal and extra control drive and steering inputs. It can be seen that the leader tracks a circle of 60 m radius and the follower is parallel to the leader at all times tracking a circle of radius 56 m. The velocity profile is shown in Figure 8.10.

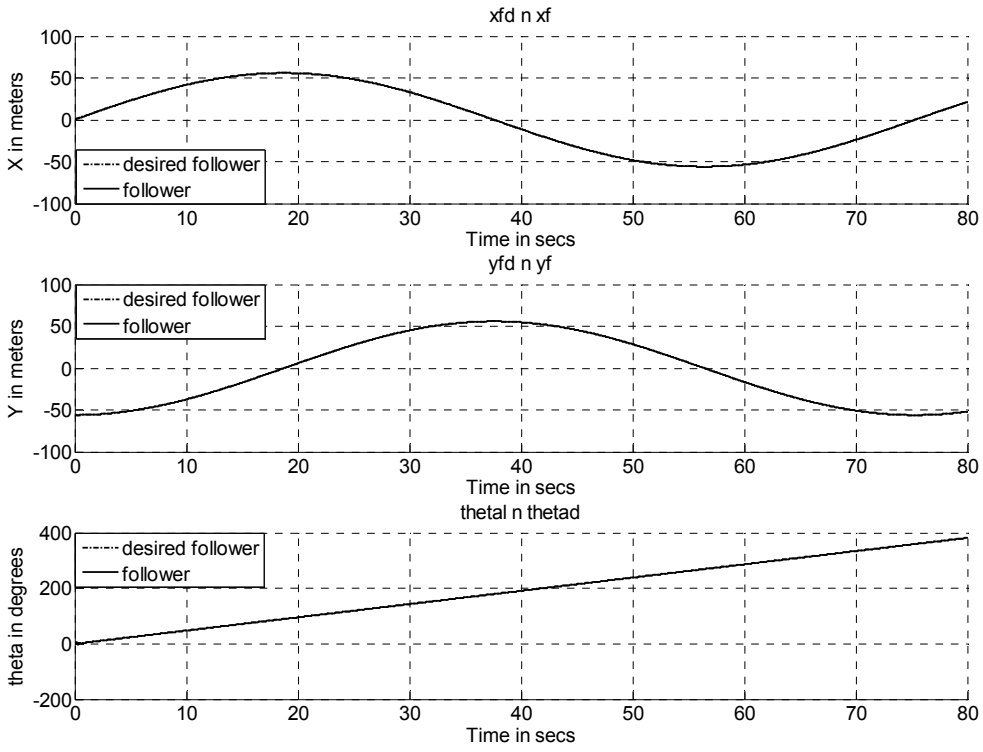

Figure 8.1 Actual and Desired Position and Orientation of the Follower

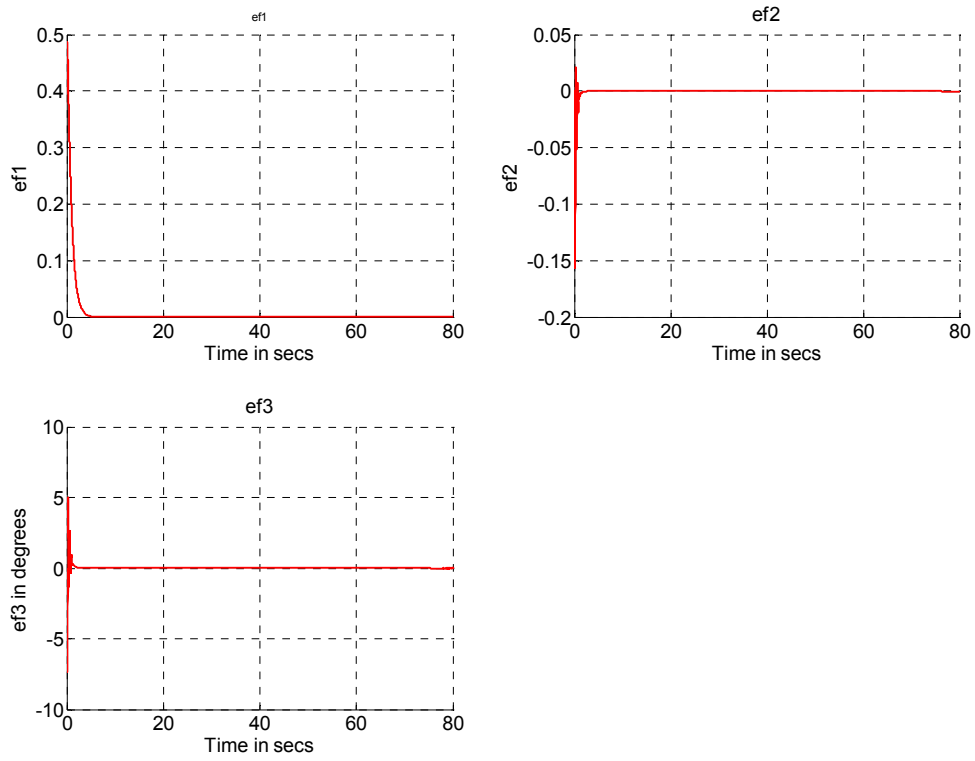

Figure 8.2 Position and Orientation Errors of the Follower in Body Coordinates

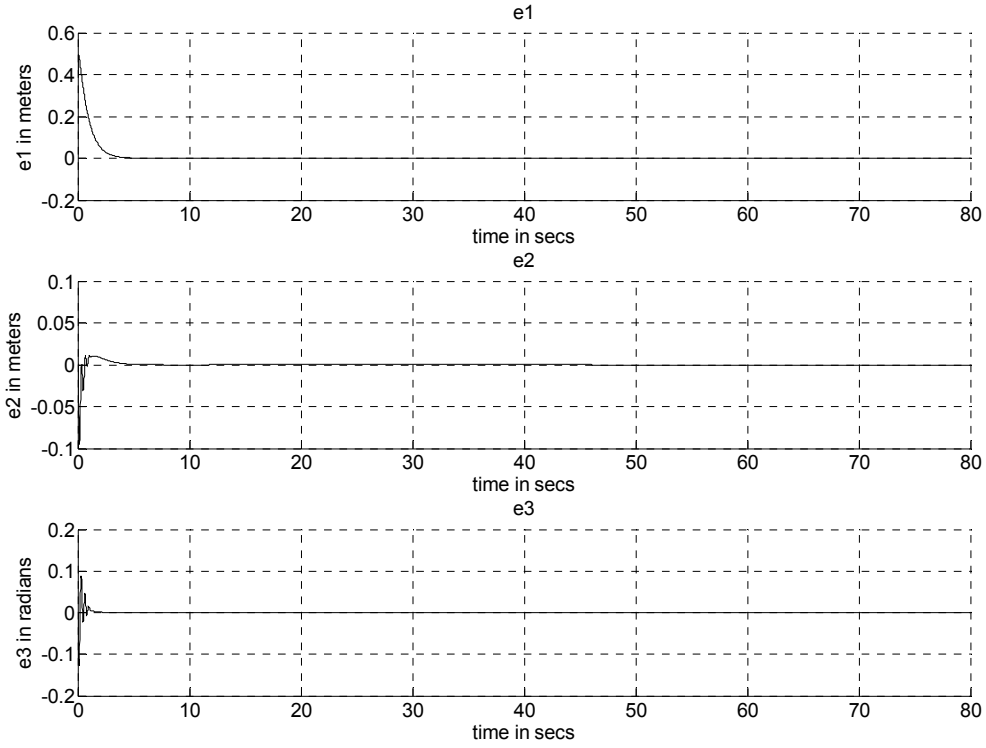

Figure 8.3 Position and Orientation Errors of the Follower in Inertial Coordinates

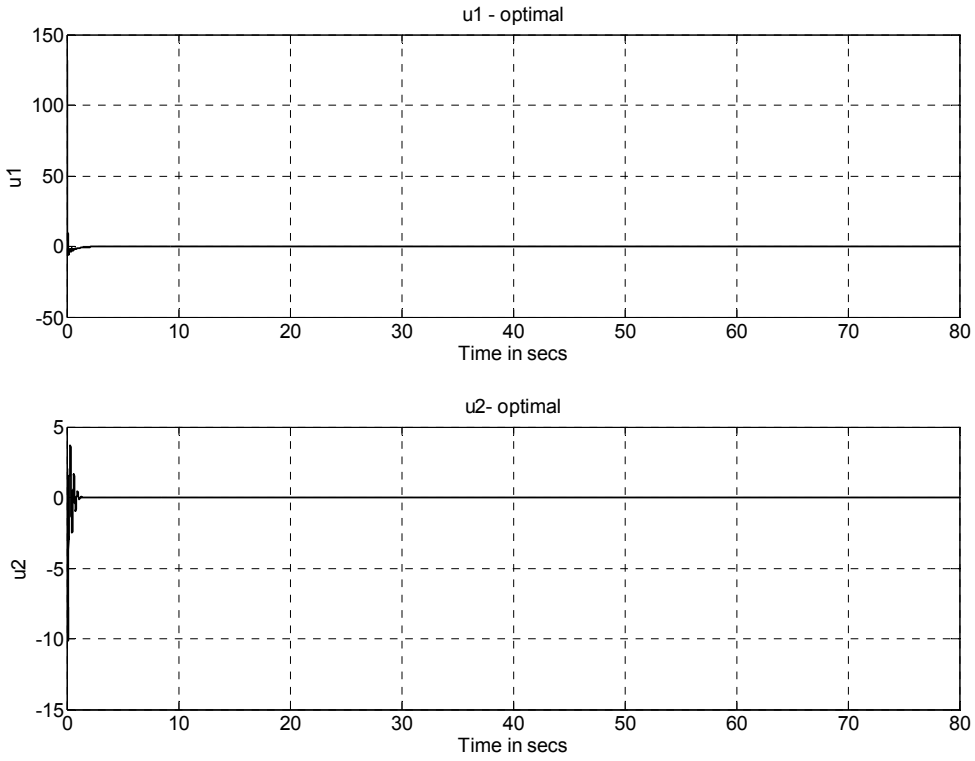

Figure 8.4 Optimal Control Inputs to the Follower Linear and Angular

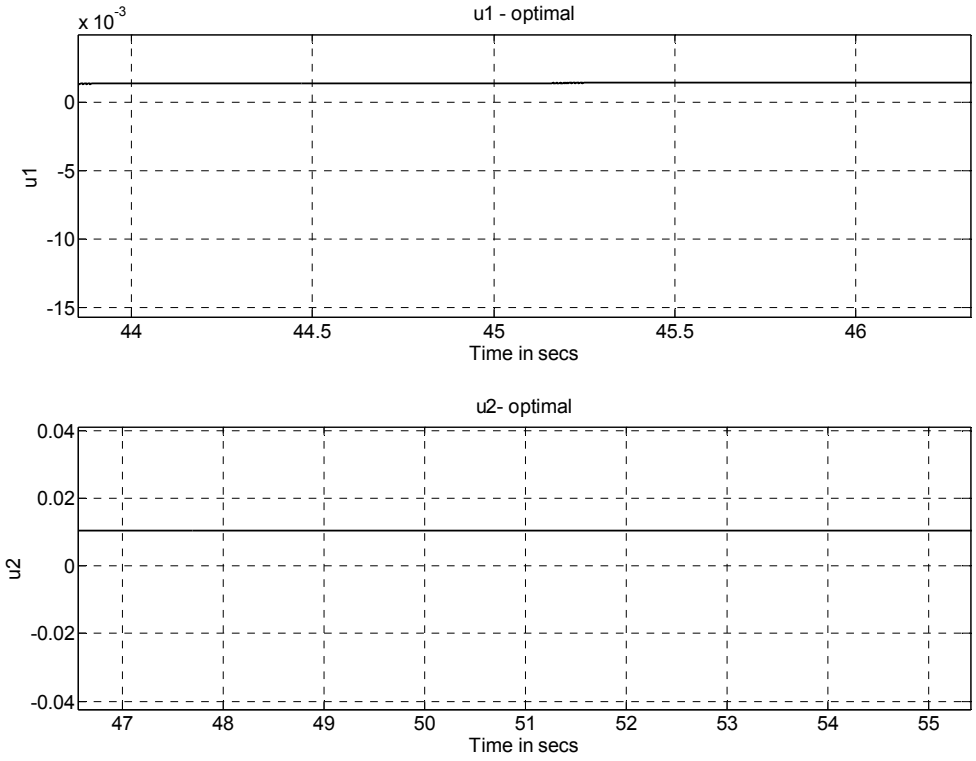

Figure 8.5 Magnified Plot of Optimal Control Inputs to the Follower

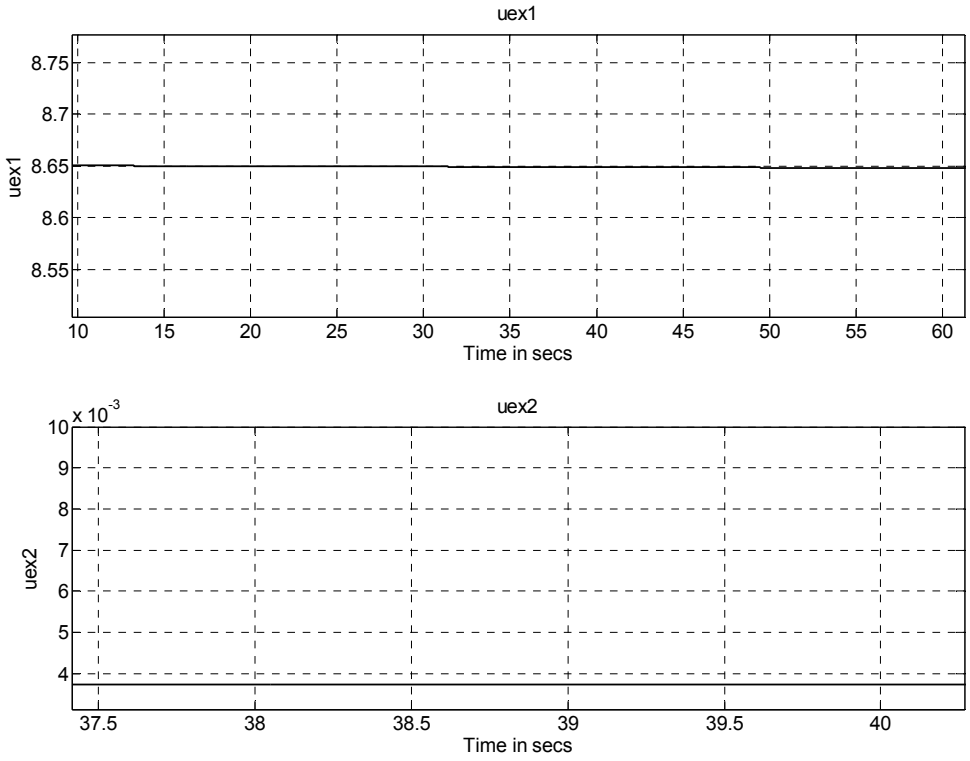

Figure 8.6 Magnified Plot of Extra Control Input to the Follower

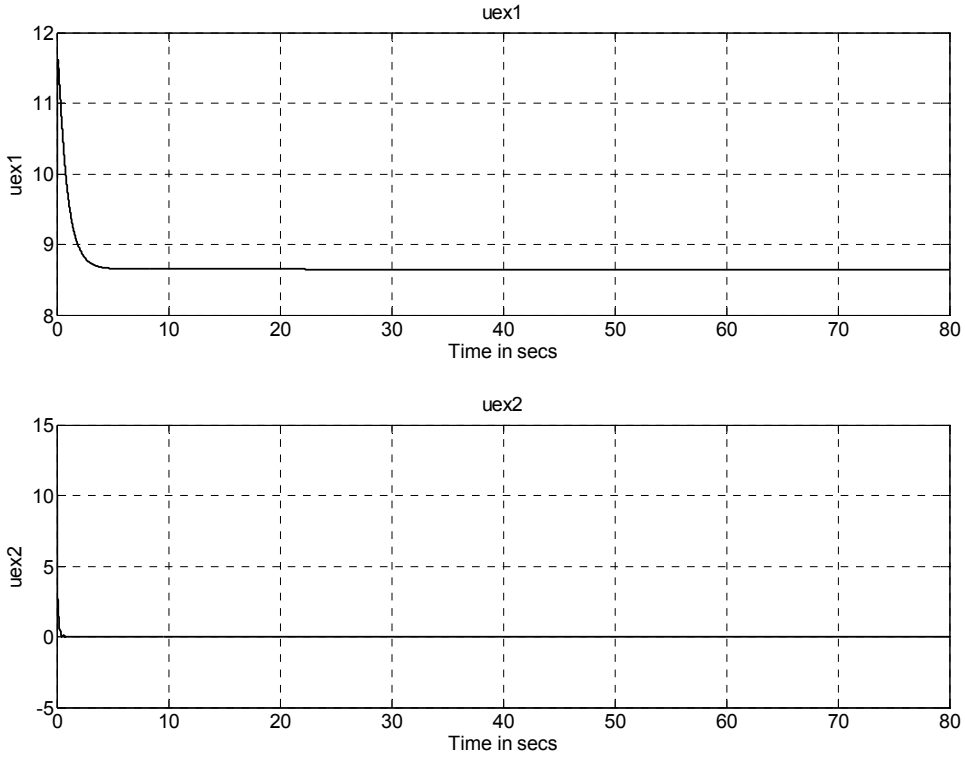

Figure 8.7 Extra Control Inputs to the Follower

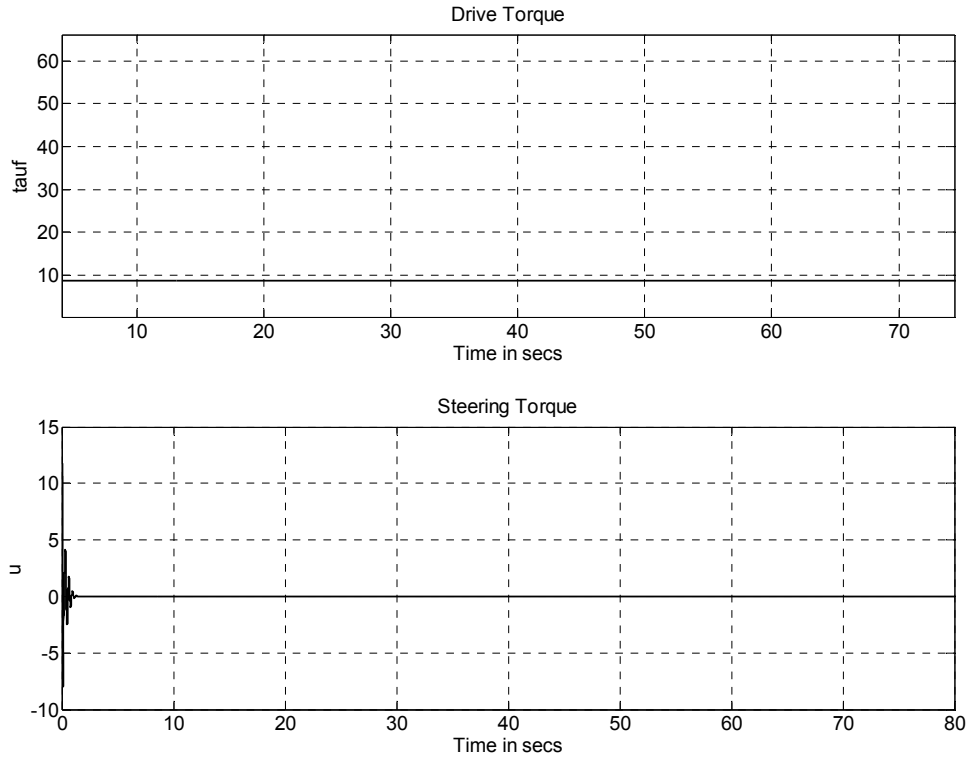

Figure 8.8 Drive Torque and Steering Torque of the Follower

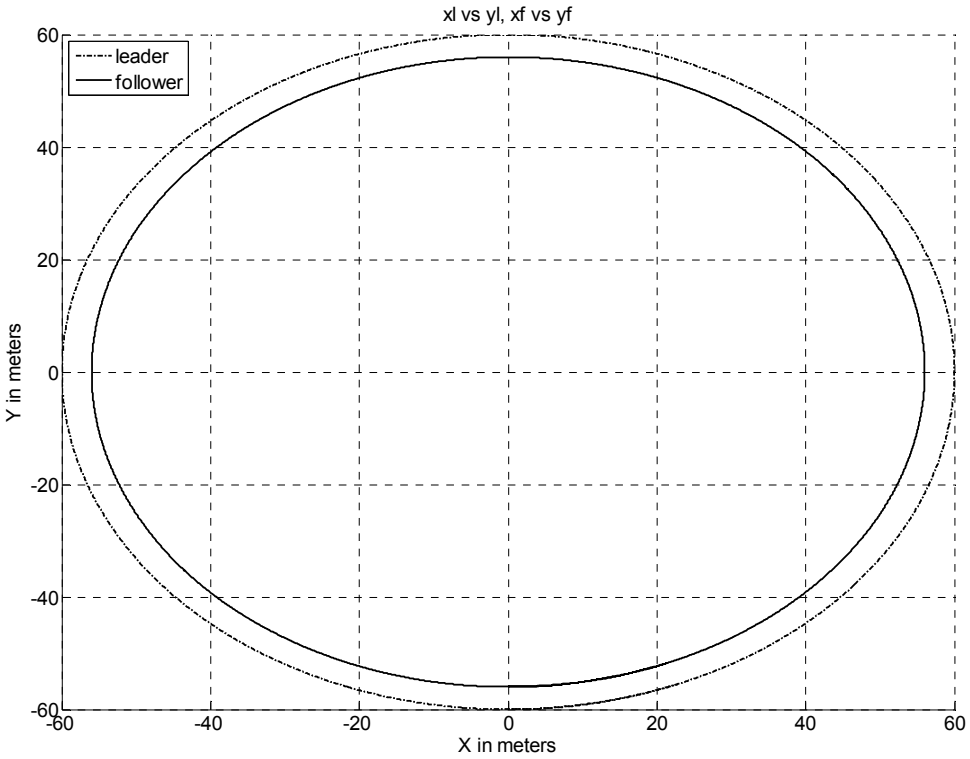

Figure 8.9 Leader and Follower Trajectories

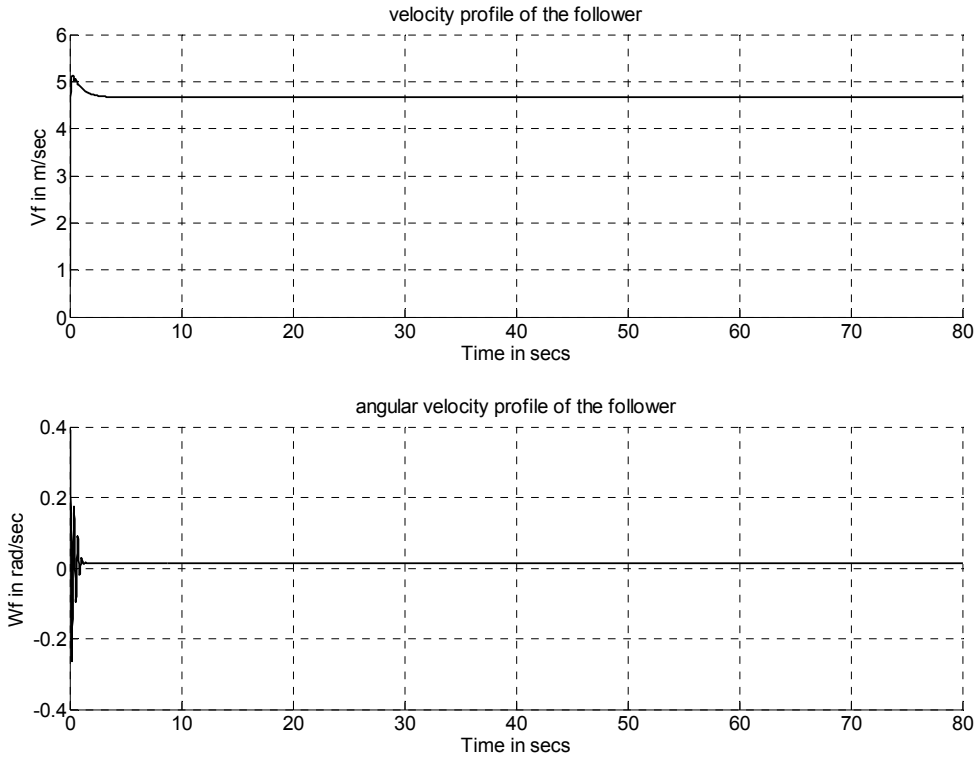

Figure 8.10 Velocity Profile of the Follower

From Figure 8.11 it can be inferred that the velocity tracking errors defined by the error system described by (113) also go to zero asymptotically. From Figure 8.12 and Figure 8.13 it can bee seen that both the neural networks are able to approximate $\mathbf{f}(\mathbf{x}_{Fnew1})$ and $\mathbf{f}(\mathbf{x}_{Fnew2})$ accurately. It is compared with the actual values of the estimated functions which is available to us during simulation runs and not during real-time implementation. Figure 8.14 shows the noisy input presented to the neural network. In the Figure 8.15 the boundedness of the neural network weights is shown. The relative distance and relative bearing angle plots are as shown in Figure 8.16.

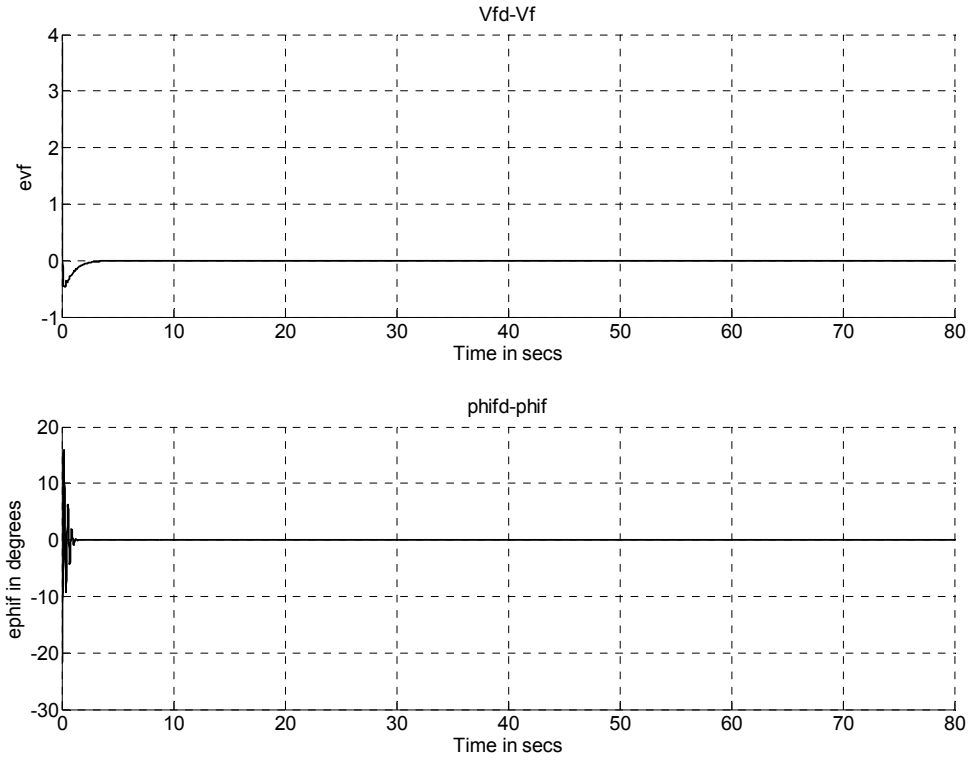

Figure 8.11 Velocity and Steering Angle Error Plots

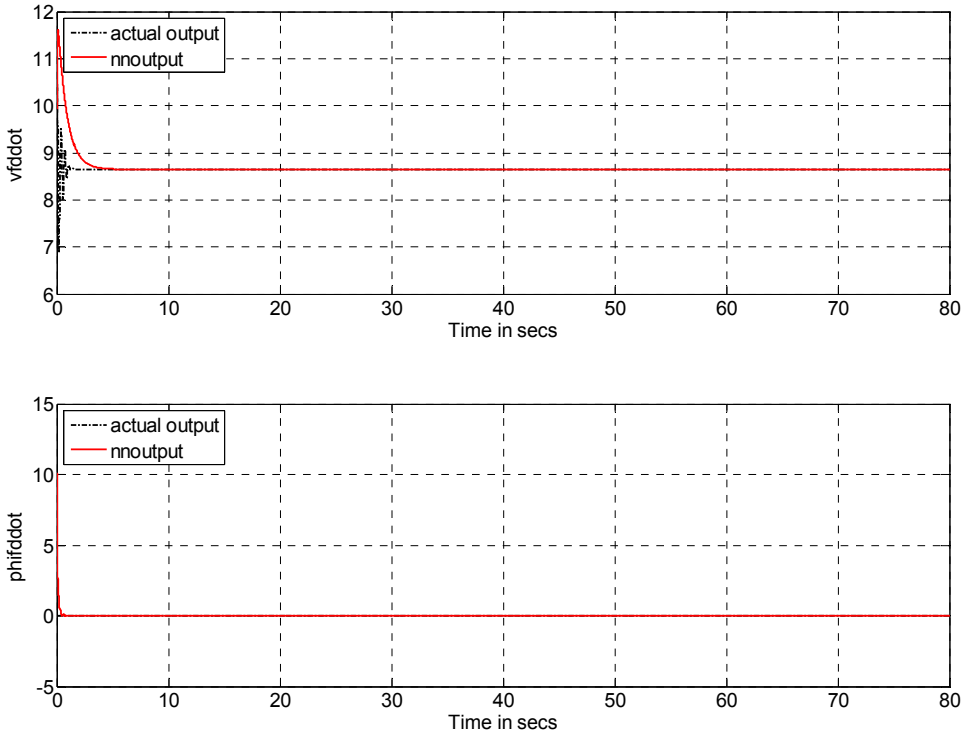

Figure 8.12 Neural Network Output

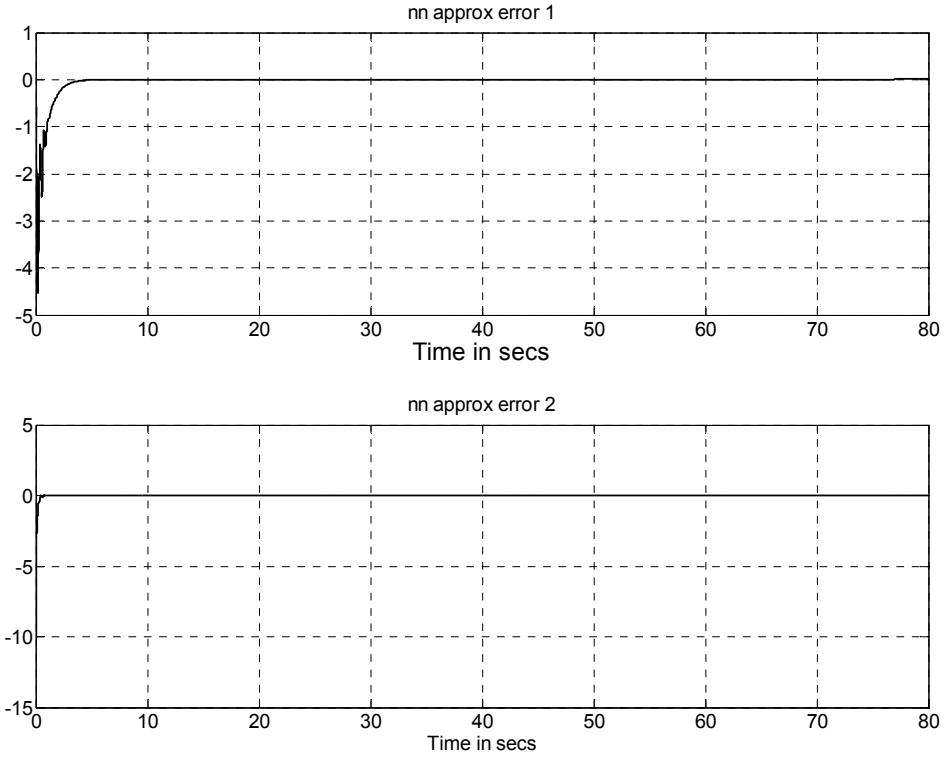

Figure 8.13 Neural Network Approximation Error

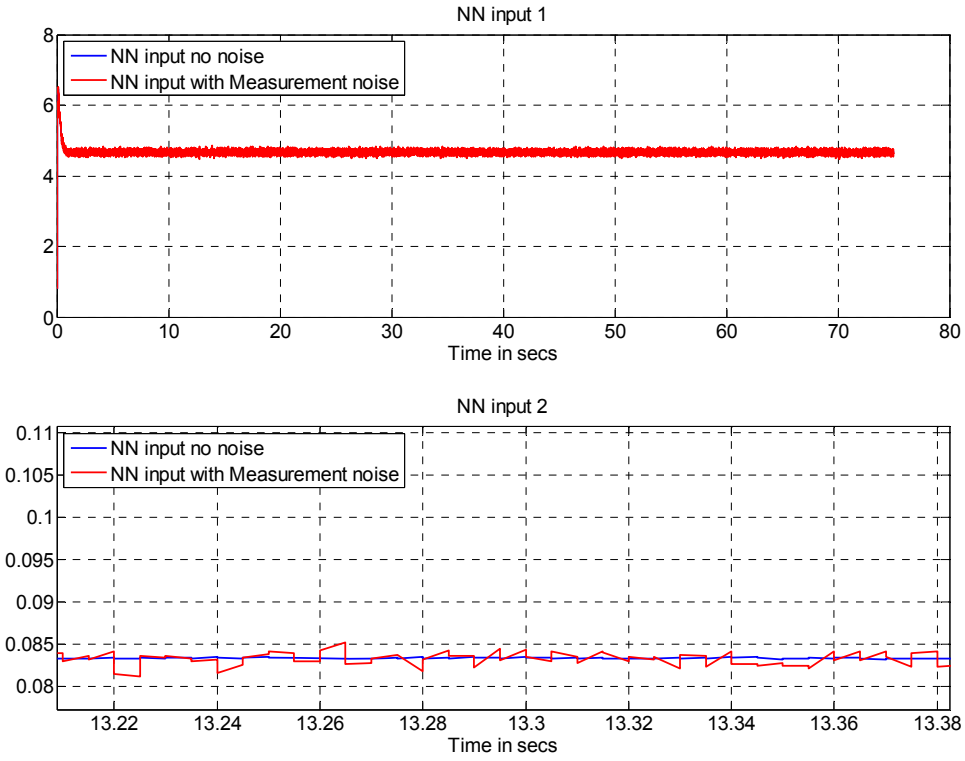

Figure 8.14 Magnified Plot of Noisy Inputs to the Neural Network

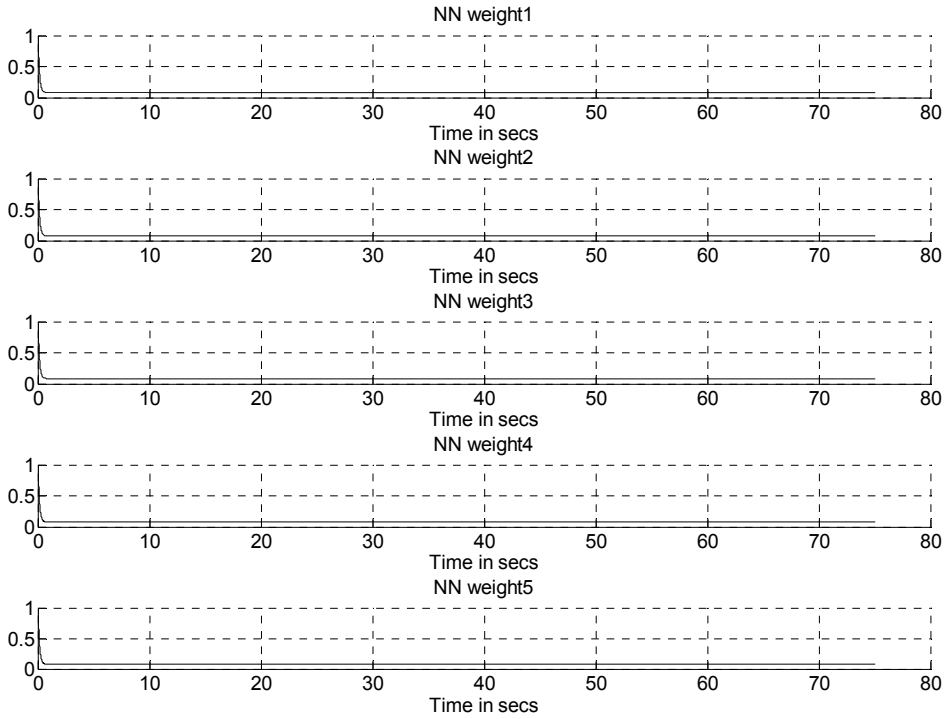

Figure 8.15 Plots Showing the Bounded-ness of Neural Network Weights

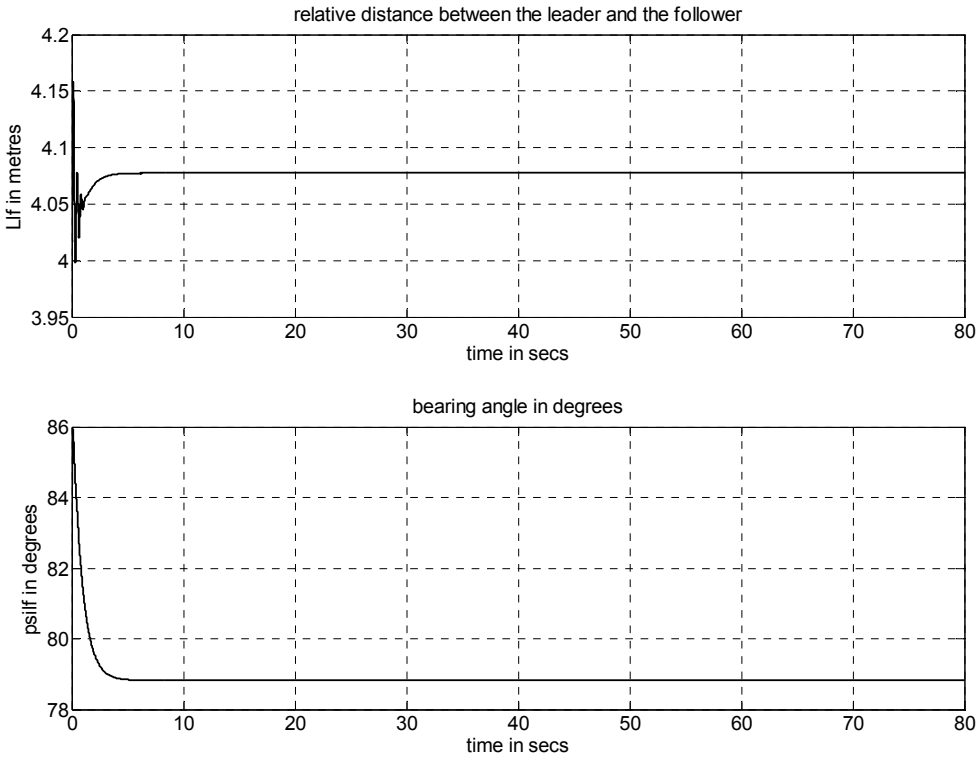

Figure 8.16 Relative Distance and Relative Bearing Angle of the Follower w.r.t. Leader

In this section the optimal control for the nominal system is obtained by using the SDARE approach. The nominal system is one without uncertainties. The uncertainties are compensated for by using extra control. The combination of the optimal and extra control inputs for the drive and steering system of a car-like follower mobile robot are used to maintain a desired relative distance and bearing angle between the leader and the follower.

Below the results for the case where the extra control is set to zero is presented. It can be found from the figures that the system response becomes oscillatory and the position and orientation errors do not go to zero. Figure 8.17 and Figure 8.18 show the orientation and position of the follower when there is no extra control. The error plots in both the body and inertial coordinates when the extra control is zero are as shown in

Figure 8.19 and Figure 8.20. The velocity profile and the velocity errors in the absence of extra control are as shown in Figure 8.21 and Figure 8.22.

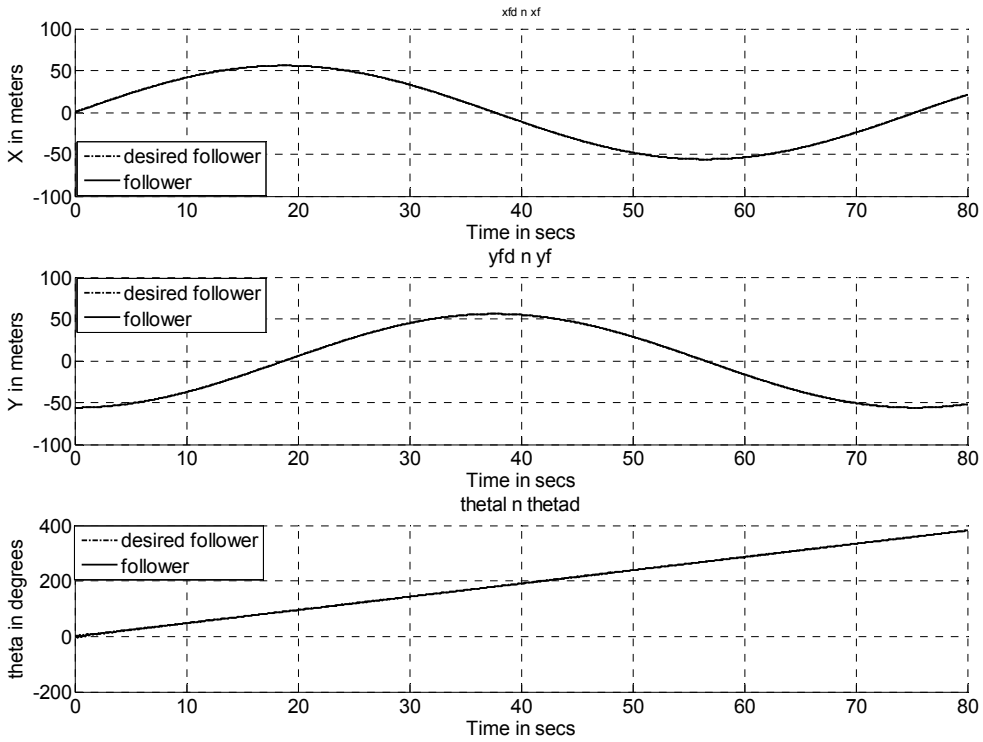

Figure 8.17 Actual and Desired Position and Orientation of the follower with $U_{EX} = 0$

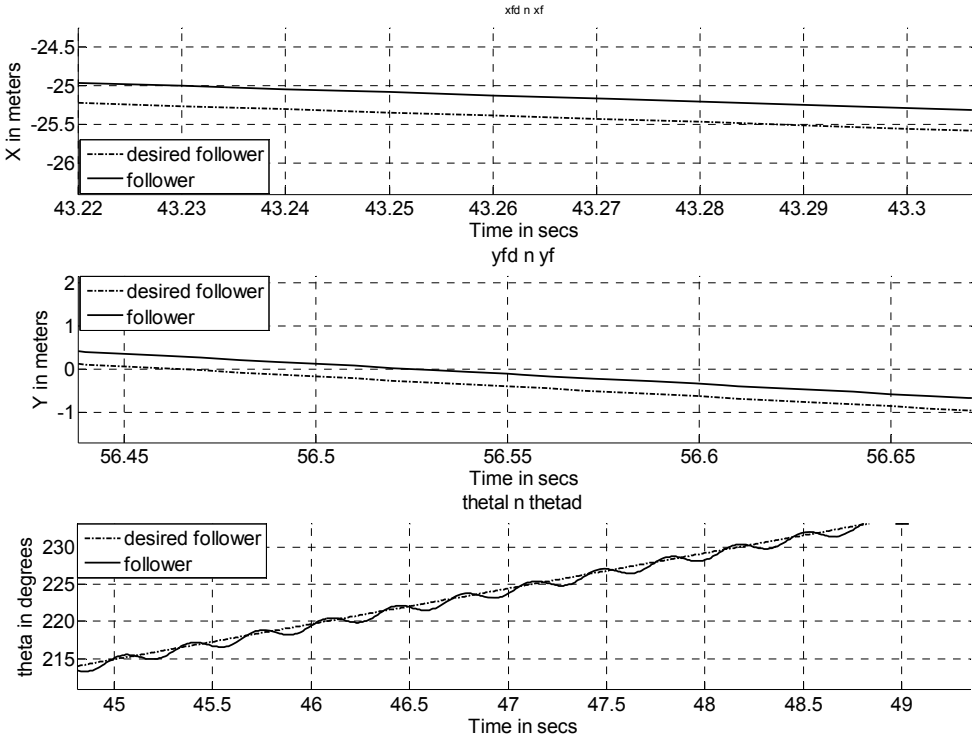

Figure 8.18 Magnified Actual and Desired Position and Orientation of the Follower with $U_{EX} = 0$

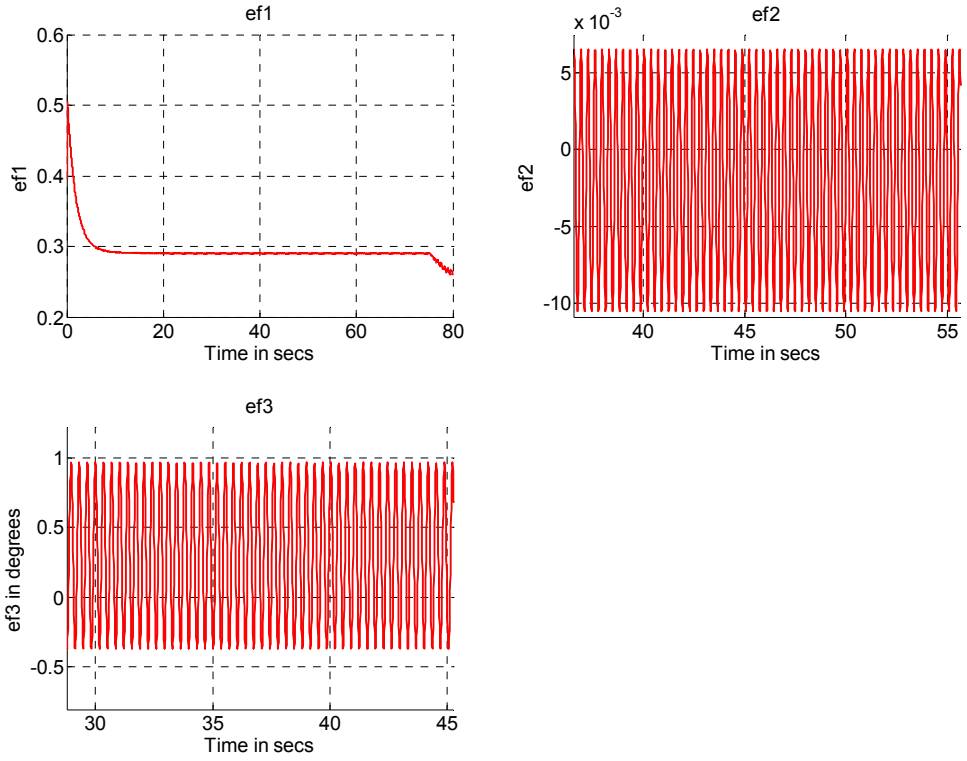

Figure 8.19 Magnified Position and Orientation Error Plots of the Follower with $U_{EX} = 0$

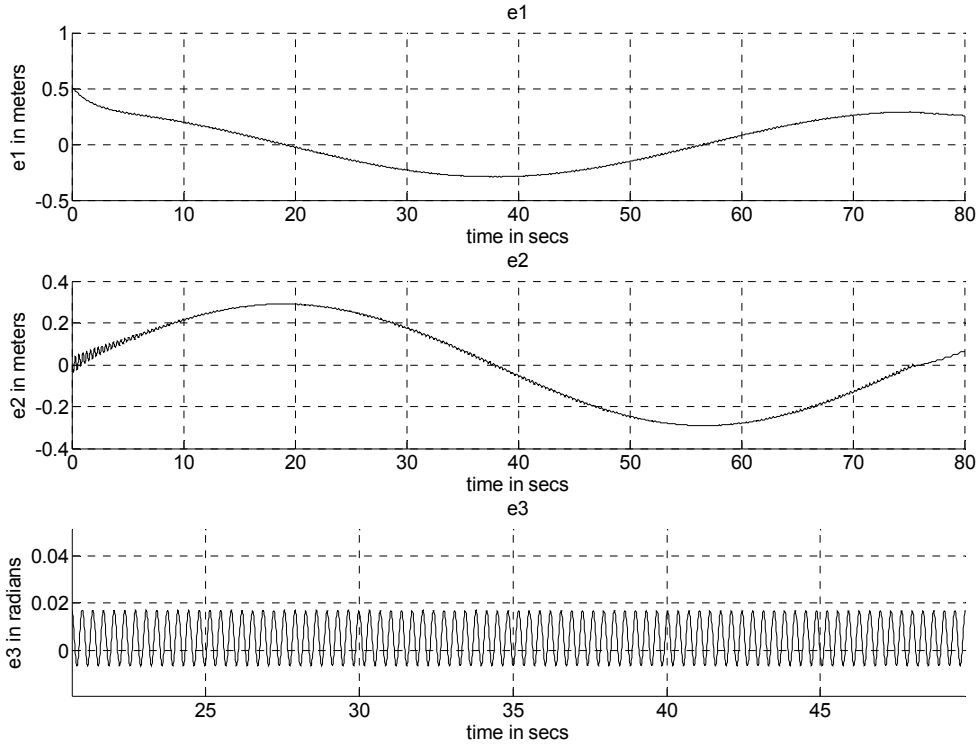

Figure 8.20 Magnified Position and Orientation Error Plots in Inertial Coordinates with $U_{EX} = 0$

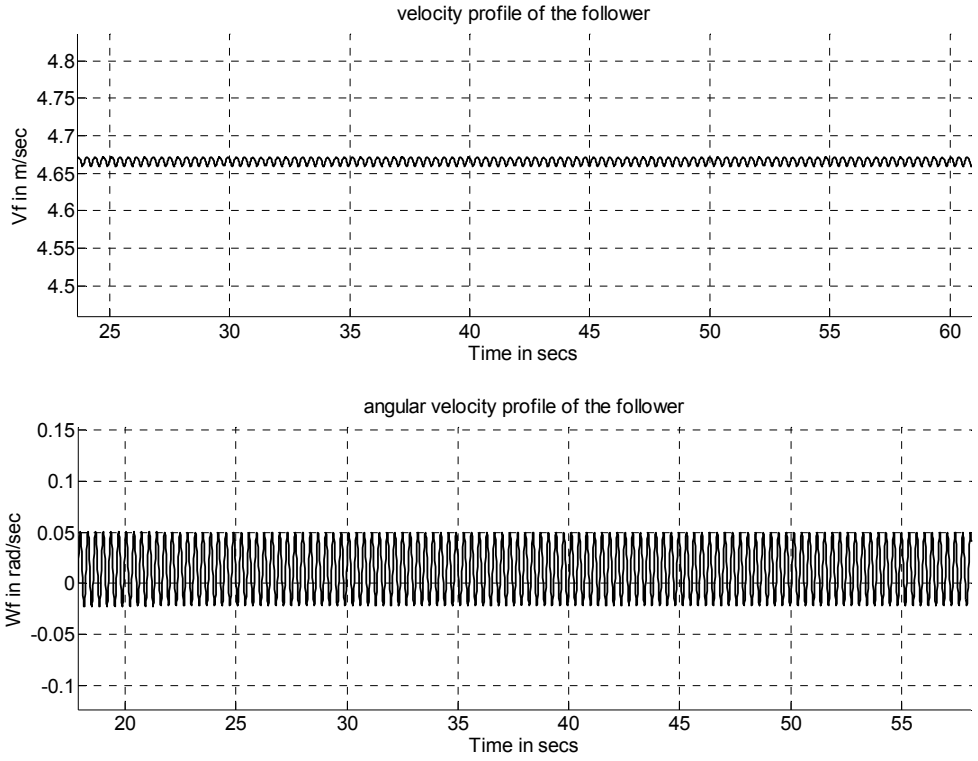

Figure 8.21 Magnified Linear and Angular Velocity Profile of the Follower with $U_{EX} = 0$

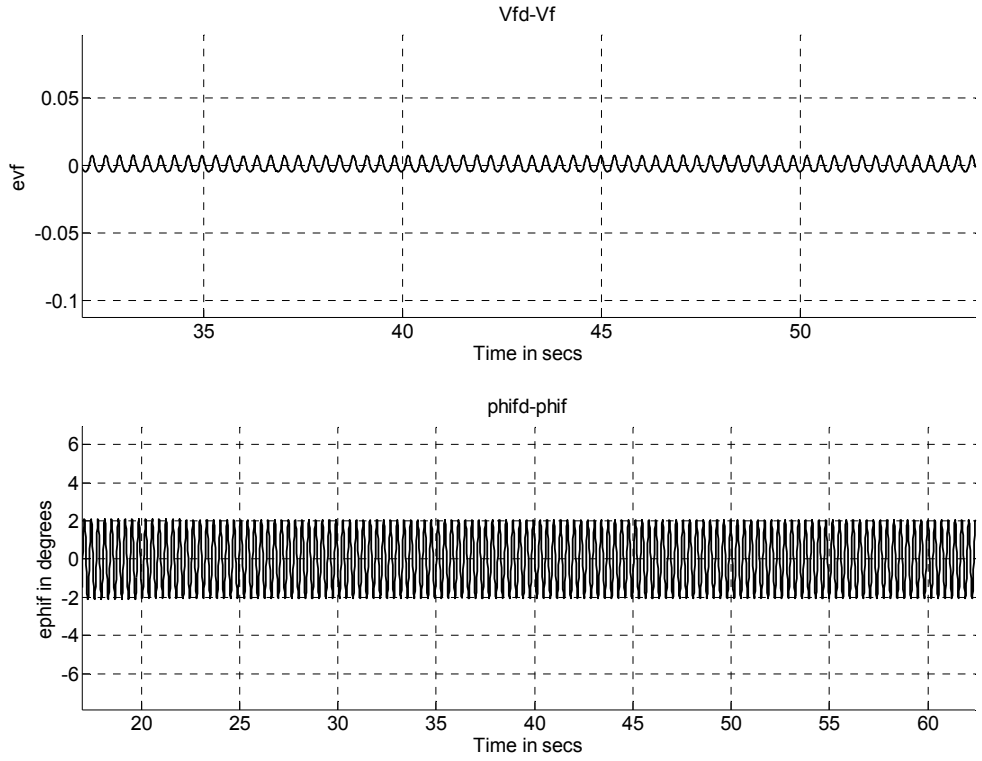

Figure 8.22 Magnified Velocity and Steering Angle Error Plots for the Follower with $U_{EX} = 0$

The relative distance and bearing angle plots shown in Figure 8.23 indicate that the formation is not kept. The optimal control plot in the absence of extra control is shown in Figure 8.24. Figure 8.25 shows the magnified drive and steering torque plots.

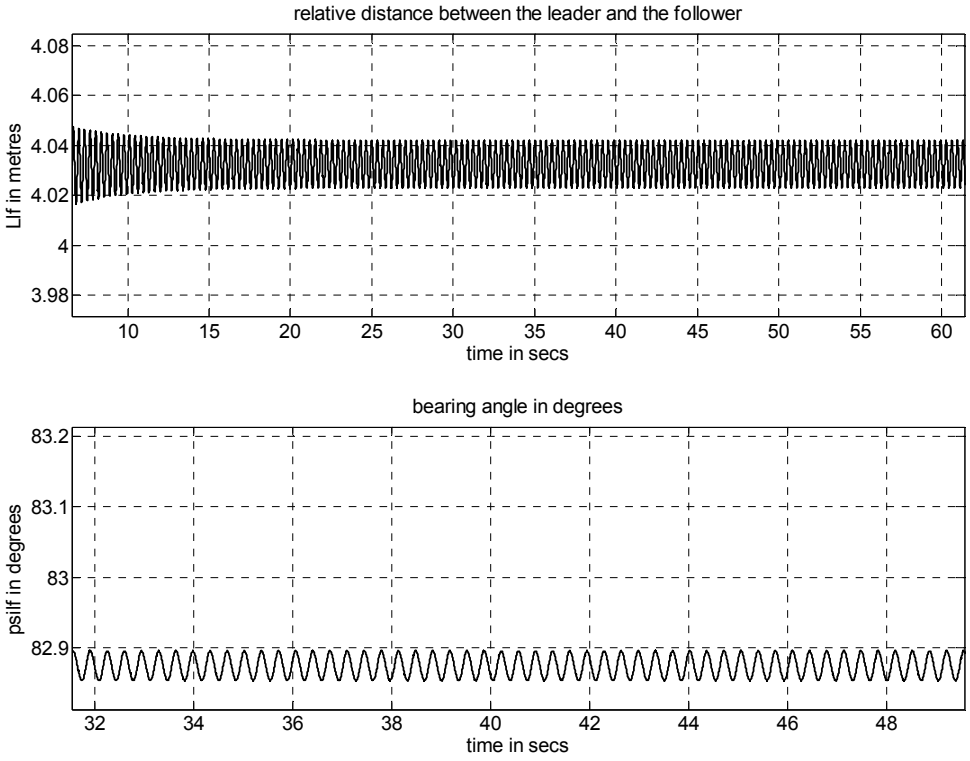

Figure 8.23 Magnified Relative Distance and Bearing Angle of the Follower w.r.t Leader with $U_{EX} = 0$

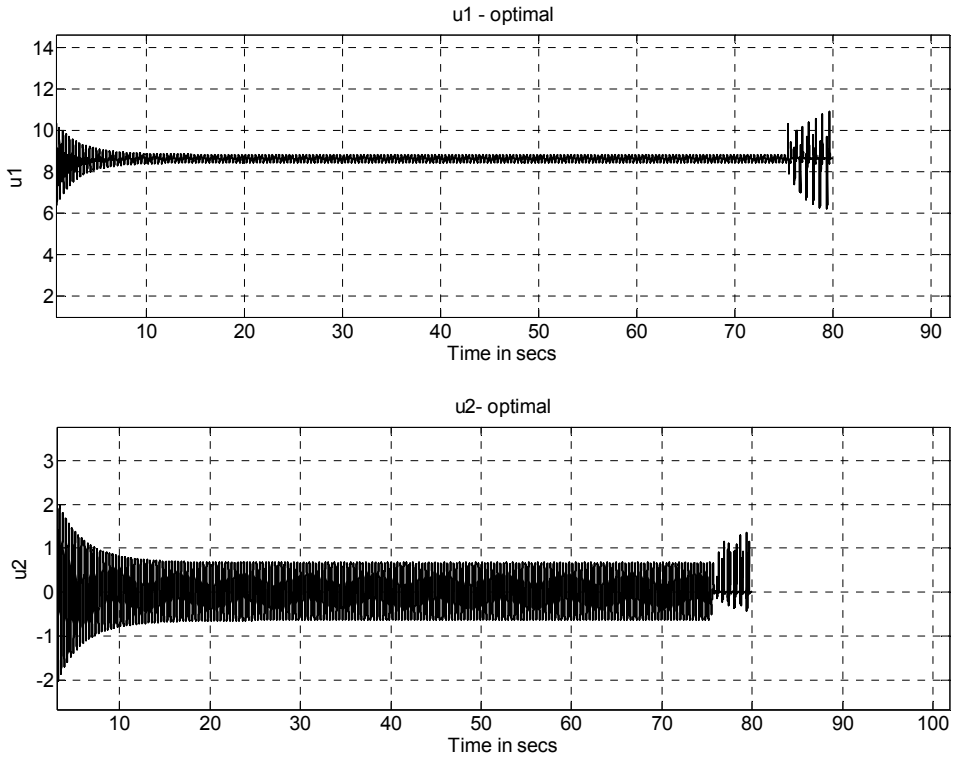

Figure 8.24 Magnified Optimal Control Inputs to the Follower with $U_{EX} = 0$

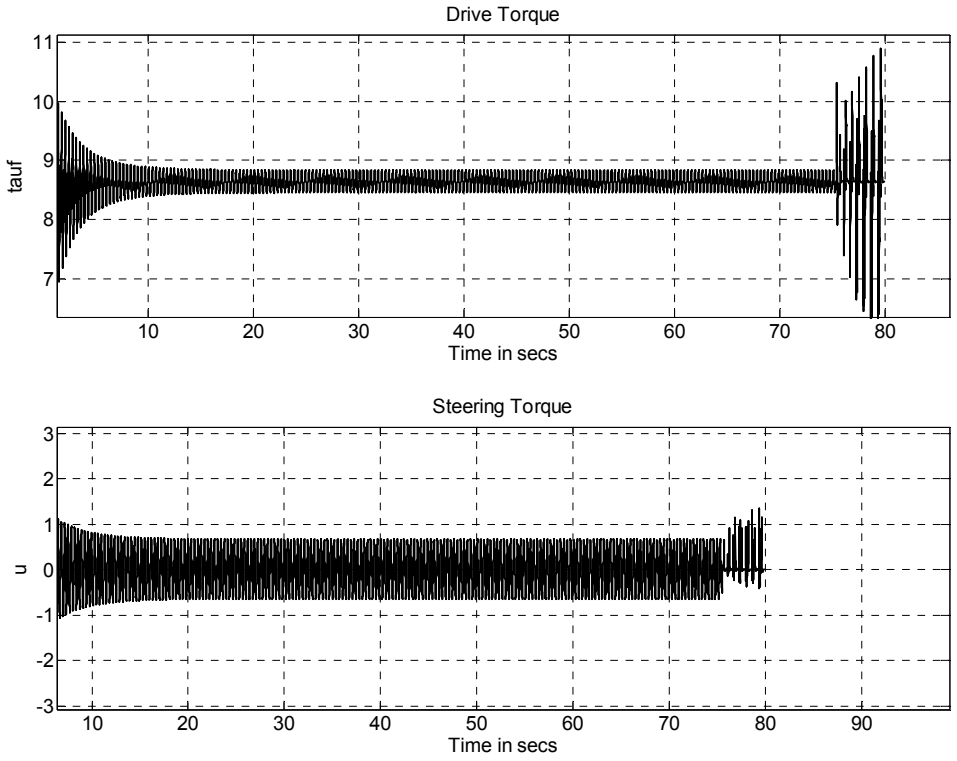

Figure 8.25 Magnified Plot of Drive and Steering Torque Inputs to the Follower with $U_{EX} = 0$

9. INTEGRATED TRACKING AND CONTROL DESIGN USING LYAPUNOV FUNCTION BASED APPROACH

The objective is to find torque control inputs to the follower for formation control of car-like mobile robots using the integrated tracking and control scheme. Initially a coupled framework is obtained wherein the follower error equations are combined with follower dynamics. Once the combined framework is obtained the state space equations thus obtained are used to design torque control inputs for the follower drive system as well as the steering system using Lyapunov function based approach so that the formation is maintained. It is assumed that the leader's motion is known.

9.1. CONTROLLER DESIGN

In order to stabilize the error system in (113) a torque controller is designed using the Lyapunov function based approach. Let the Lyapunov function candidate be

$$V = K_1 e_{F1}^2 + K_2 e_{F2}^2 + K_3(1-\cos e_{F3}) + K_4 e_{vF}^2 + K_5(1-\cos e_{\phi F}) \tag{306}$$

Differentiating (306) , $\dot{V}$ can be expressed as

$$\dot{V} = K_1 e_{F1}\dot{e}_{F1} + K_2 e_{F2}\dot{e}_{F2} + K_3 \sin e_{F3}\dot{e}_{F3} + K_4 e_{vF}\dot{e}_{vF} + K_5 \sin e_{\phi F}\dot{e}_{\phi F} \tag{307}$$

Each term on the right hand side (RHS) of (307) can be expanded as given below

$$K_1 e_{F1}\dot{e}_{F1} = K_1 e_{F1} v_L \cos e_{F3} - K_1 e_{F1} v_F - K_1 e_{F1} w_L L_{LF} \sin\gamma_F - K_1 e_{F1} e_{F2} w_L + K_1 e_{F1} e_{F2} w_F \tag{308}$$

$$K_2 e_{F2}\dot{e}_{F2} = \begin{pmatrix} K_2 e_{F2} v_L \sin e_{F3} + K_2 e_{F2} w_L L_{LF} \cos\gamma_F + K_2 e_{F1} e_{F2} w_L - K_2 e_{F1} e_{F2} w_F + K_2 e_{F2} w_F d \\ -K_2 e_{F2} w_L d - K_2 e_{F2} w_F L \end{pmatrix} \tag{309}$$

$$K_3\dot{e}_{F3}\sin e_{F3} = K_3 w_L \sin e_{F3} - K_3 w_F \sin e_{F3} \tag{310}$$

$$K_4 e_{vF}\dot{e}_{vF} = \begin{pmatrix} K_4 e_{vF} F_1 - \dfrac{K_4 e_{vF} d (v_{FD})^2 \tan^2\phi_F}{L^2} + \dfrac{K_4 (e_{vF})^2 2 d v_{FD} \tan^2\phi_F}{L^2} \\ -\dfrac{K_4 (e_{vF})^3 d \tan^2\phi_F}{L^2} - \dfrac{K_4 e_{vF}\tau_F}{rm} \end{pmatrix} \tag{311}$$

$$K_5\dot{e}_{\phi F}\sin e_{\phi F} = K_5 \sin e_{\phi F} F_2 + \frac{K_5 \sin e_{\phi F}\phi_{FD}}{\tau_S} - \frac{K_5 e_{\phi F}\sin e_{\phi F}}{\tau_S} - \frac{K_5 \sin e_{\phi F} u}{\tau_S} \tag{312}$$

From (108)

$$\begin{bmatrix} v_F & \phi_F \end{bmatrix}^T = \begin{bmatrix} (v_{FD} - e_{vF}) & (\phi_{FD} - e_{\phi F}) \end{bmatrix}^T \tag{313}$$

Taking $K_1 = K_2 = K$ and substituting (308) through (313) in (307) , $\dot{V}$ becomes

$$\dot{V} = \begin{pmatrix} Ke_{F1}v_L \cos e_{F3} - Ke_{F1}v_{FD} - Ke_{F1}w_L L_{LF} \sin\gamma_F + Ke_{F1}e_{vF} - Ke_{F2}w_L d + K_2 e_{F2}v_L \sin e_{F3} \\ +K_2 e_{F2}w_L L_{LF} \cos\gamma_F + \dfrac{Ke_{F2}v_{FD}\tan(\phi_{FD} - e_{\phi F})}{2} - \dfrac{Ke_{F2}e_{vF}\tan(\phi_{FD} - e_{\phi F})}{2} \\ +Ke_{F2}e_{vF}\tan(\phi_{FD} - e_{\phi F}) - Ke_{F2}v_{FD}\tan(\phi_{FD} - e_{\phi F}) + \dfrac{K_3 e_{vF}\sin e_{F3}\tan(\phi_{FD} - e_{\phi F})}{L} \\ +K_3 w_L \sin e_{F3} - \dfrac{K_3 v_{Fd}\sin e_{F3}\tan(\phi_{FD} - e_{\phi F})}{L} + K_4 e_{vF}F_1 - \dfrac{K_4 e_{vF}d(v_{FD})^2\tan^2\phi_F}{L^2} \\ + \dfrac{K_4(e_{vF})^2 v_{FD}\tan^2\phi_F}{L} - \dfrac{K_4(e_{vF})^3 d\tan^2\phi_F}{L^2} - \dfrac{K_4 e_{vF}\tau_F}{rm} + K_5 \sin e_{\phi F}F_2 + \dfrac{K_5 \sin e_{\phi F}\phi_{FD}}{\tau_S} \\ - \dfrac{K_5 e_{\phi F}\sin e_{\phi F}}{\tau_S} - \dfrac{K_5 \sin e_{\phi F}u}{\tau_S} \end{pmatrix} \tag{314}$$

Expanding the terms in (314) , $\dot{V}$ can be expressed as

$$\dot{V} = \begin{pmatrix} Ke_{F1}v_L \cos e_{F3} - Ke_{F1}v_{FD} - Ke_{F1}w_L L_{LF}\sin\psi_{LF}\cos e_{F3} - Ke_{F1}w_L L_{LF}\cos\psi_{LF}\sin e_{F3} \\ -Ke_{F2}w_L d + K_2 e_{F2}w_L L_{LF}\cos\psi_{LF}\cos e_{F3} - K_2 e_{F2}w_L L_{LF}\sin\psi_{LF}\sin e_{F3} + Ke_{F1}e_{vF} \\ - \dfrac{Ke_{F2}v_{FD}}{2}\left(\dfrac{\tan\phi_{FD}}{1+\tan\phi_{FD}\tan e_{\phi F}}\right) + \dfrac{Ke_{F2}v_{FD}}{2}\left(\dfrac{\tan e_{\phi F}}{1+\tan\phi_{FD}\tan e_{\phi F}}\right) + K_2 e_{F2}v_L \sin e_{F3} \\ + \dfrac{Ke_{F2}e_{vF}}{2}\left(\dfrac{\tan\phi_{FD}}{1+\tan\phi_{FD}\tan e_{\phi F}}\right) - \dfrac{Ke_{F2}e_{vF}}{2}\left(\dfrac{\tan e_{\phi F}}{1+\tan\phi_{FD}\tan e_{\phi F}}\right) \\ +K_3 w_L \sin e_{F3} + \dfrac{K_3 e_{vF}\sin e_{F3}}{L}\left(\dfrac{\tan\phi_{FD}}{1+\tan\phi_{FD}\tan e_{\phi F}}\right) - \dfrac{K_3 e_{vF}\sin e_{F3}}{L}\left(\dfrac{\tan e_{\phi F}}{1+\tan\phi_{FD}\tan e_{\phi F}}\right) \\ - \dfrac{K_3 v_{Fd}\sin e_{F3}}{L}\left(\dfrac{\tan\phi_{FD}}{1+\tan\phi_{FD}\tan e_{\phi F}}\right) + \dfrac{K_3 v_{Fd}\sin e_{F3}}{L}\left(\dfrac{\tan e_{\phi F}}{1+\tan\phi_{FD}\tan e_{\phi F}}\right) + K_4 e_{vF}F_1 \\ - \dfrac{K_4 e_{vF}d(v_{FD})^2\tan^2\phi_F}{L^2} + \dfrac{K_4(e_{vF})^2 v_{FD}\tan^2\phi_F}{L} - \dfrac{K_4(e_{vF})^3 d\tan^2\phi_F}{L^2} - \dfrac{K_4 e_{vF}\tau_F}{rm} \\ +K_5 \sin e_{\phi F}F_2 + \dfrac{K_5 \sin e_{\phi F}\phi_{FD}}{\tau_S} - \dfrac{K_5 e_{\phi F}\sin e_{\phi F}}{\tau_S} - \dfrac{K_5 \sin e_{\phi F}u}{\tau_S} \end{pmatrix} \tag{315}$$

Converting the equality in (315) into an inequality results in

$$\dot{V} < \left(\begin{array}{l} K\left|e_{F1}\right|v_L + K\left|-e_{F1}\right|v_{FD} + K\left|e_{F1}\right|w_L L_{LF}\left|\sin(-\psi_{LF})\right| + K\left|e_{F1}\right|w_L L_{LF}\left|\cos\psi_{LF}\right| \\ +K\left|-e_{F2}\right|w_L d + \dfrac{K\left|-e_{F2}\right|v_{FD}\left|\tan\phi_{FD}\right|}{2} + K_2\left|e_{F1}\right|v_L + K\left|e_{F2}\right|w_L L_{LF}\left|\cos\psi_{LF}\right| \\ +K\left|e_{F2}\right|w_L L_{LF}\left|\sin\psi_{LF}\right| + K_3 w_L + \dfrac{K_3 v_{Fd}\left|\tan\phi_{FD}\right|}{L} + \dfrac{Ke_{F2}e_{vF}}{2}\left(\dfrac{\tan\phi_{FD}}{1+\tan\phi_{FD}\tan e_{\phi F}}\right) \\ +\dfrac{K_3 e_{vF}\sin e_{F3}}{L}\left(\dfrac{\tan\phi_{FD}}{1+\tan\phi_{FD}\tan e_{\phi F}}\right) - \dfrac{\alpha K_3 e_{vF}\sin e_{F3}}{L}\left(\dfrac{\tan e_{\phi F}}{1+\tan\phi_{FD}\tan e_{\phi F}}\right) + Ke_{F1}e_{vF} \\ -\dfrac{(1-\alpha)K_3 e_{vF}\sin e_{F3}}{L\cos e_{\phi F}}\left(\dfrac{\sin e_{\phi F}}{1+\tan\phi_{FD}\tan e_{\phi F}}\right) + K_4 e_{vF}F_1 - \dfrac{K_4 e_{vF} d(v_{FD})^2\tan^2\phi_F}{L^2} \\ +\dfrac{K_4(e_{vF})^2 v_{FD}\tan^2\phi_F}{L} - \dfrac{K_4(e_{vF})^3 d\tan^2\phi_F}{L^2} - \dfrac{K_4 e_{vF}\tau_F}{rm} + \dfrac{Ke_{F2}v_{FD}}{2\cos e_{\phi F}}\left(\dfrac{\sin e_{\phi F}}{1+\tan\phi_{FD}\tan e_{\phi F}}\right) \\ +\dfrac{K_3 v_{Fd}\sin e_{F3}}{L\cos e_{\phi F}}\left(\dfrac{\sin e_{\phi F}}{1+\tan\phi_{FD}\tan e_{\phi F}}\right) + K_5\sin e_{\phi F}F_2 + \dfrac{K_5\sin e_{\phi F}\phi_{FD}}{\tau_S} - \dfrac{K_5 e_{\phi F}\sin e_{\phi F}}{\tau_S} \\ -\dfrac{K_5\sin e_{\phi F}u}{\tau_S} - \dfrac{\alpha Ke_{F2}e_{vF}}{2}\left(\dfrac{\tan e_{\phi F}}{1+\tan\phi_{FD}\tan e_{\phi F}}\right) - \dfrac{(1-\alpha)Ke_{F2}e_{vF}}{2\cos e_{\phi F}}\left(\dfrac{\sin e_{\phi F}}{1+\tan\phi_{FD}\tan e_{\phi F}}\right) \end{array} \right) \quad (316)$$

By choosing the drive torque control input as

$$\tau_F = \left(\begin{array}{l} rm\left(\begin{array}{l} \dfrac{Ke_{F1}}{K_4} + \dfrac{Ke_{F2}}{2K_4}\left(\dfrac{\tan\phi_{FD}}{1+\tan\phi_{FD}\tan e_{\phi F}}\right) + \dfrac{K_3\sin e_{F3}}{K_4 L}\left(\dfrac{\tan\phi_{FD}}{1+\tan\phi_{FD}\tan e_{\phi F}}\right) \\ -\dfrac{\alpha K_3\sin e_{F3}}{K_4 L}\left(\dfrac{\tan e_{\phi F}}{1+\tan\phi_{FD}\tan e_{\phi F}}\right) + F_1 - \dfrac{d(v_{FD})^2\tan^2\phi_F}{L^2} + \dfrac{e_{vF}v_{FD}\tan^2\phi_F}{L} \\ -\dfrac{(e_{vF})^2 d\tan^2\phi_F}{L^2} + k_1 e_{vF} - \dfrac{\alpha Ke_{F2}}{2K_4}\left(\dfrac{\tan e_{\phi F}}{1+\tan\phi_{FD}\tan e_{\phi F}}\right) \end{array} \right) \\ +\dfrac{rm}{K_4\left|e_{vF}\right|}\left(\begin{array}{l} Kk_2(e_{F1})^2 + Kk_3(e_{F2})^2 + Kk_4\sin^2 e_{F3} + K\left|e_{F1}\right|v_L + K\left|-e_{F1}\right|v_{FD} \\ +K\left|e_{F1}\right|w_L L_{LF}\left|\sin(-\psi_{LF})\right| + K\left|e_{F1}\right|w_L L_{LF}\left|\cos\psi_{LF}\right| + K\left|-e_{F2}\right|w_L d \\ +\dfrac{K\left|-e_{F2}\right|v_{FD}\left|\tan\phi_{FD}\right|}{2} + K_2\left|e_{F1}\right|v_L + K\left|e_{F2}\right|w_L L_{LF}\left|\cos\psi_{LF}\right| \\ +K\left|e_{F2}\right|w_L L_{LF}\left|\sin\psi_{LF}\right| + K_3 w_L + \dfrac{K_3 v_{Fd}\left|\tan\phi_{FD}\right|}{L} \end{array} \right) \end{array} \right) \quad (317)$$

And the steering torque control input as

$$u=\begin{pmatrix} \tau_S F_2+\phi_{FD}-e_{\phi F}+k_5\sin e_{\phi F}-\dfrac{\tau_S}{K_5}\dfrac{(1-\alpha)K_3 e_{vF}\sin e_{F3}}{L\cos e_{\phi F}}\left(\dfrac{1}{1+\tan\phi_{FD}\tan e_{\phi F}}\right) \\ +\dfrac{\tau_S}{K_5}\dfrac{Ke_{F2}v_{FD}}{2\cos e_{\phi F}}\left(\dfrac{1}{1+\tan\phi_{FD}\tan e_{\phi F}}\right)+\dfrac{\tau_S}{K_5}\dfrac{K_3 v_{FD}\sin e_{F3}}{L\cos e_{\phi F}}\left(\dfrac{1}{1+\tan\phi_{FD}\tan e_{\phi F}}\right) \\ -\dfrac{\tau_S}{K_5}\dfrac{(1-\alpha)Ke_{F2}e_{vF}}{2\cos e_{\phi F}}\left(\dfrac{1}{1+\tan\phi_{FD}\tan e_{\phi F}}\right) \end{pmatrix} \tag{318}$$

and substituting (317) and (318) in (316), the expression for $\dot{V}$ becomes

$$\dot{V}<\left(-k_1K_4(e_{vF})^2-k_5K_5\sin^2 e_{\phi F}-k_2K(e_{F1})^2-k_3K(e_{F2})^2-k_4K_3\sin^2 e_{F3}\right) \tag{319}$$

With $K_1=K_2=K$ and $K,K_3,K_4,K_5,k_1,k_2,k_3,k_4,k_5>0$ we have $\dot{V}<0$. Therefore the torque control inputs in (317) and (318) provides asymptotic stability to the error system in (113) i.e. $e\to 0 \text{ as } t\to\infty$.

9.2. USE OF NEURAL NETWORK FOR CONTROLLER DESIGN, WEIGHT UPDATE RULE AND PROOF OF BOUNDED-NESS OF WEIGHTS

Two single layer functional link neural networks (FLNN) are used for the approximation of the terms F_1 and F_2 in(113). These terms involve the friction terms and desired accelerations terms that cannot be computed in real life accurately. Hence, online neural networks will be used to estimate F_1 and F_2, and they are defined as follows

$$F_1=\mathbf{f}(\mathbf{x}_{Fnew1}) \tag{320}$$

$$F_1=\mathbf{f}(\mathbf{x}_{Fnew2}) \tag{321}$$

The activation functions $\phi(\mathbf{x}_{Fnew1}),\phi(\mathbf{x}_{Fnew2})$ can be chosen as a basis set for the universal approximation property to hold for single layer FLNN. Then there exists weights W_1 and W_2 such that

$$\mathbf{f}(\mathbf{x}_{Fnew1})=W_1^T\phi(\mathbf{x}_{Fnew1})+\varepsilon_1 \tag{322}$$

$$\mathbf{f}(\mathbf{x}_{Fnew2})=W_2^T\phi(\mathbf{x}_{Fnew2})+\varepsilon_2 \tag{323}$$

with the estimation errors ε_1 and ε_2 bounded. The bounds are given by $\|\varepsilon_1\| < \varepsilon_{1N}$ and $\|\varepsilon_2\| < \varepsilon_{2N}$. The ideal approximating weights are unknown and nonunique. So an assumption is made that $\|W_1\|_F < W_{1B}$ and $\|W_2\|_F < W_{2B}$ with the bounds W_{1B} and W_{2B} known. The Forbenius norm is denoted by $\|\ \|_F$. Then estimates of $\mathbf{f}(\mathbf{x}_{Fnew1})$ and $\mathbf{f}(\mathbf{x}_{Fnew2})$ are given by

$$\hat{F}_1 = \hat{\mathbf{f}}(\mathbf{x}_{Fnew1}) = \hat{W}_1^T \phi(\mathbf{x}_{Fnew1}) \tag{324}$$

$$\hat{F}_2 = \hat{\mathbf{f}}(\mathbf{x}_{Fnew2}) = \hat{W}_2^T \phi(\mathbf{x}_{Fnew2}) \tag{325}$$

with $\hat{W}_1$ and $\hat{W}_2$ being the weights of the two neural networks.

Now let the new drive and steering torque control inputs be given by

$$\tau_{FNEW} = \left(rm \left(\begin{array}{l} \frac{Ke_{F1}}{K_4} + \frac{Ke_{F2}}{2K_4}\left(\frac{\tan\phi_{FD}}{1+\tan\phi_{FD}\tan e_{\phi F}}\right) + \frac{K_3 \sin e_{F3}}{K_4 L}\left(\frac{\tan\phi_{FD}}{1+\tan\phi_{FD}\tan e_{\phi F}}\right) \\ -\frac{\alpha K_3 \sin e_{F3}}{K_4 L}\left(\frac{\tan e_{\phi F}}{1+\tan\phi_{FD}\tan e_{\phi F}}\right) + \hat{W}_1^T \phi(\mathbf{x}_{Fnew1}) \\ -\frac{\alpha K e_{F2}}{2K_4}\left(\frac{\tan e_{\phi F}}{1+\tan\phi_{FD}\tan e_{\phi F}}\right) + \frac{e_{vF} v_{FD}\tan^2\phi_F}{L} - \frac{(e_{vF})^2 d\tan^2\phi_F}{L^2} \\ +k_1 e_{vF} - \frac{d(v_{FD})^2\tan^2\phi_F}{L^2} \end{array} \right) \right.$$
$$\left. + \frac{rm}{K_4|e_{vF}|}\left(\begin{array}{l} Kk_2(e_{F1})^2 + Kk_3(e_{F2})^2 + Kk_4\sin^2 e_{F3} + K|e_{F1}|v_L + K|-e_{F1}|v_{FD} \\ +K|e_{F1}|w_L L_{LF}|\sin(-\psi_{LF})| + K|e_{F1}|w_L L_{LF}|\cos\psi_{LF}| \\ +\frac{K|-e_{F2}|v_{FD}|\tan\phi_{FD}|}{2} + K_2|e_{F1}|v_L + K|e_{F2}|w_L L_{LF}|\cos\psi_{LF}| \\ +K|e_{F2}|w_L L_{LF}|\sin\psi_{LF}| + K_3 w_L + \frac{K_3 v_{Fd}|\tan\phi_{FD}|}{L} + K|-e_{F2}|w_L d \end{array} \right) \right) \tag{326}$$

$$u_{NEW} = \left(\begin{array}{l} \tau_S \hat{W}_2^T \phi(\mathbf{x}_{Fnew2}) - \frac{\tau_S}{K_5}\frac{(1-\alpha)K_3 e_{vF}\sin e_{F3}}{L\cos e_{\phi F}}\left(\frac{1}{1+\tan\phi_{FD}\tan e_{\phi F}}\right) \\ +\frac{\tau_S}{K_5}\frac{Ke_{F2}v_{FD}}{2\cos e_{\phi F}}\left(\frac{1}{1+\tan\phi_{FD}\tan e_{\phi F}}\right) + \frac{\tau_S}{K_5}\frac{K_3 v_{FD}\sin e_{F3}}{L\cos e_{\phi F}}\left(\frac{1}{1+\tan\phi_{FD}\tan e_{\phi F}}\right) \\ -\frac{\tau_S}{K_5}\frac{(1-\alpha)Ke_{F2}e_{vF}}{2\cos e_{\phi F}}\left(\frac{1}{1+\tan\phi_{FD}\tan e_{\phi F}}\right) + \phi_{FD} - e_{\phi F} + k_5 \sin e_{\phi F} \end{array} \right) \tag{327}$$

Define $\tilde{\mathbf{f}}(\mathbf{x}_{Fnew1})$ and $\tilde{\mathbf{f}}(\mathbf{x}_{Fnew2})$ as

$$\tilde{\mathbf{f}}(\mathbf{x}_{Fnew1}) = \mathbf{f}(\mathbf{x}_{Fnew1}) - \hat{\mathbf{f}}(\mathbf{x}_{Fnew1}) \tag{328}$$

$$\tilde{\mathbf{f}}(\mathbf{x}_{Fnew2}) = \mathbf{f}(\mathbf{x}_{Fnew2}) - \hat{\mathbf{f}}(\mathbf{x}_{Fnew2}) \tag{329}$$

An online weight update rule is now developed to guarantee stable tracking and yet guarantee bounded-ness of weights. The weight estimation error is defined as

$$\tilde{W_1} = W_1 - \hat{W_1} \tag{330}$$

$$\tilde{W_2} = W_2 - \hat{W_2} \tag{331}$$

Let the Lyapunov candidate function in (306) be denoted by V_{OLD}. The new Lyapunov candidate function is chosen as

$$V_{NEW} = V_{OLD} + \frac{1}{2} tr\left\{\tilde{W_1}^T L_1^{-1} \tilde{W_1}\right\} + \frac{1}{2} tr\left\{\tilde{W_2}^T L_2^{-1} \tilde{W_2}\right\} \tag{332}$$

On differentiating (332) and substituting the new drive and steering control torque expressions from (326) and (327) , the expression for $\dot{V}_{NEW}$ is given by

$$\dot{V}_{NEW} = \begin{pmatrix} -k_1 K_4 (e_{vF})^2 - k_5 K_5 \sin^2 e_{\phi F} - k_2 K (e_{F1})^2 - k_3 K (e_{F2})^2 - k_4 K_3 \sin^2 e_{F3} \\ +K_5 \sin e_{\phi F} \tilde{\mathbf{f}}(\mathbf{x}_{Fnew2}) + K_4 e_{vF} \tilde{\mathbf{f}}(\mathbf{x}_{Fnew1}) + tr\left\{\tilde{W_1}^T L_1^{-1} \dot{\tilde{W}}_1\right\} + tr\left\{\tilde{W_2}^T L_2^{-1} \dot{\tilde{W}}_2\right\} \end{pmatrix} \tag{333}$$

where L_1, L_2 are user defined tuning matrices.

Using (328) through (331) in (333), $\dot{V}_{NEW}$ becomes

$$\dot{V}_{NEW} = \begin{pmatrix} -k_1 K_4 (e_{vF})^2 - k_5 K_5 \sin^2 e_{\phi F} - k_2 K (e_{F1})^2 - k_3 K (e_{F2})^2 - k_4 K_3 \sin^2 e_{F3} \\ +K_5 \sin e_{\phi F} \tilde{W}_2^T \phi(\mathbf{x}_{Fnew2}) + K_4 e_{vF} \tilde{W}_1^T \phi(\mathbf{x}_{Fnew1}) + tr\left\{\tilde{W_1}^T L_1^{-1} \dot{\tilde{W}}_1\right\} + tr\left\{\tilde{W_2}^T L_2^{-1} \dot{\tilde{W}}_2\right\} \end{pmatrix} \tag{334}$$

Rearranging (334) results in

$$\dot{V}_{NEW} = \begin{pmatrix} -k_1 K_4 (e_{vF})^2 - k_5 K_5 \sin^2 e_{\phi F} - k_2 K (e_{F1})^2 - k_3 K (e_{F2})^2 - k_4 K_3 \sin^2 e_{F3} \\ +tr\left\{\tilde{W_1}^T \left(L_1^{-1} \dot{\tilde{W}}_1 + \phi(\mathbf{x}_{Fnew1}) K_4 e_{vF}\right)\right\} + tr\left\{\tilde{W_2}^T \left(L_2^{-1} \dot{\tilde{W}}_2 + \phi(\mathbf{x}_{Fnew2}) K_5 \sin e_{\phi F}\right)\right\} \end{pmatrix} \tag{335}$$

Selecting the weight tuning laws as

$$\dot{\hat{W}}_1 = L_1 \phi(\mathbf{x}_{Fnew1}) K_4 e_{vF} - k_{NEW1} L_1 \left\|\mathbf{e}_{vF}\right\| \hat{W}_1 \tag{336}$$

$$\dot{\hat{W}}_2 = L_2 \phi(\mathbf{x}_{Fnew2}) K_5 \sin e_{\phi F} - k_{NEW2} L_2 \left\|\sin e_{\phi F}\right\| \hat{W}_2 \tag{337}$$

Substituting (336) and (337) in (335) $\dot{V}_{NEW}$ can be written as

$$\dot{V}_{NEW} = \begin{pmatrix} -k_1 K_4 (e_{vF})^2 - k_5 K_5 \sin^2 e_{\phi F} - k_2 K (e_{F1})^2 - k_3 K (e_{F2})^2 - k_4 K_3 \sin^2 e_{F3} \\ +k_{NEW1} \left\| e_{vF} \right\| tr\left\{ \tilde{W}_1^T \left(W_1 - \hat{W}_1 \right) \right\} + k_{NEW2} \left\| \sin e_{\phi F} \right\| tr\left\{ \tilde{W}_2^T \left(W_2 - \hat{W}_2 \right) \right\} \end{pmatrix} \tag{338}$$

Also from [20]

$$tr\left\{ \tilde{W}^T (W - \hat{W}) \right\} = \left\langle \tilde{W}, W \right\rangle_F - \left\| \tilde{W} \right\|_F^2 \le \left\| \tilde{W} \right\|_F \left\| W \right\|_F - \left\| \tilde{W} \right\|_F^2 \tag{339}$$

Using (339) and further simplifying (338)

$$\dot{V}_{NEW} \le \begin{pmatrix} -k_2 K (e_{F1})^2 - \left\| e_{vF} \right\| \left\{ k_1 K_4 \left\| e_{vF} \right\| + k_{NEW1} \left\| \tilde{W}_1 \right\|_F \left(\left\| \tilde{W}_1 \right\|_F - W_{1B} \right) \right\} - k_3 K (e_{F2})^2 \\ - \left\| \sin e_{\phi F} \right\| \left\{ k_5 K_5 \left\| \sin e_{\phi F} \right\| + k_{NEW2} \left\| \tilde{W}_2 \right\|_F \left(\left\| \tilde{W}_2 \right\|_F - W_{2B} \right) \right\} - k_4 K_3 \sin^2 e_{F3} \end{pmatrix} \tag{340}$$

The term given by

$$k_1 K_4 \left\| e_{vF} \right\| + k_{NEW1} \left\| \tilde{W}_1 \right\|_F \left(\left\| \tilde{W}_1 \right\|_F - W_{1B} \right) = k_{NEW1} \left(\left\| \tilde{W}_1 \right\|_F - \frac{W_{1B}}{2} \right)^2 - \frac{k_{NEW1} W_{1B}^2}{4} + k_1 K_4 \left\| e_{vF} \right\| \tag{341}$$

is guaranteed positive as long as

$$\left\| e_{vF} \right\| \ge \frac{k_{NEW1} W_{1B}^2}{4 k_1 K_4} \equiv b_{e_{FD1}} \; or \; \left\| \tilde{W}_1 \right\|_F > \frac{W_{1B}}{2} + \sqrt{\frac{W_{1B}^2}{4}} \equiv b_{W1} \tag{342}$$

The term given by

$$k_5 K_5 \left\| \sin e_{\phi F} \right\| + k_{NEW2} \left\| \tilde{W}_2 \right\|_F \left(\left\| \tilde{W}_2 \right\|_F - W_{2B} \right) = \begin{pmatrix} k_{NEW2} \left(\left\| \tilde{W}_2 \right\|_F - \frac{W_{2B}}{2} \right)^2 - \frac{k_{NEW2} W_{2B}^2}{4} \\ +k_5 K_5 \left\| \sin e_{\phi F} \right\| \end{pmatrix} \tag{343}$$

is guaranteed positive as long as

$$\left\| \sin e_{\phi F} \right\| \ge \frac{k_{NEW2} W_{2B}^2}{4 k_5 K_5} \equiv b_{e_{FD2}} \; or \; \left\| \tilde{W}_2 \right\|_F > \frac{W_{2B}}{2} + \sqrt{\frac{W_{2B}^2}{4}} \equiv b_{W2} \tag{344}$$

So, $\dot{V}_{NEW}$ is negative outside a compact set. Let the NN function approximation property holds for $\mathbf{f}(\mathbf{x}_{Fnew1})$ and $\mathbf{f}(\mathbf{x}_{Fnew2})$ with an accuracy of ε_{N1} and ε_{N2} respectively for all $\mathbf{x}_{Fnew1}$ and $\mathbf{x}_{Fnew2}$ in the compact sets $S_{Fnew1} \equiv \{x_{Fnew1} \mid \left\| x_{Fnew1} \right\| < b_{x_{Fnew1}}\}$ and $S_{Fnew2} \equiv \{x_{Fnew2} \mid \left\| x_{Fnew2} \right\| < b_{x_{Fnew2}}\}$ with $b_{x_{Fnew1}} > e_{vFB}$ and $b_{x_{Fnew2}} > \sin e_{\phi FB}$ where e_{vFB} and $\sin e_{\phi FB}$ are the bounds on the desired trajectory e_{vFD} and $\sin e_{\phi FD}$.

Define $S_{e_{VF}} \equiv \{e_{vF} \mid \left\| e_{VF} \right\| < (b_{x_{Fnew1}} - e_{vFB}) / (c_0 + c_1)\}$ (345)

$$S_{e_{\phi F}} \equiv \{\sin e_{\phi F} \mid \left\|\sin e_{\phi F}\right\| < (b_{x_{Fnew2}} - \sin e_{\phi FB})/(c_2 + c_3)\} \tag{346}$$

Now selecting the gains

$$k_1 K_4 > \frac{k_{NEW1} W_{1B}^2 (c_0 + c_1)}{4(b_{x_{Fnew1}} - e_{vFB})} \tag{347}$$

$$k_5 K_5 > \frac{k_{NEW2} W_{2B}^2 (c_2 + c_3)}{4(b_{x_{Fnew2}} - \sin e_{\phi FB})} \tag{348}$$

ensures that the compact sets defined by $\left\|e_{vF}\right\| < b_{e_{FD1}}$ and $\left\|\sin e_{\phi F}\right\| < b_{e_{FD2}}$ are contained in S_{evF} and $S_{e\phi F}$. This guarantees that the error $e_{vF}, e_{\phi F}$ and the NN weight estimates $\hat{W}_1$ and $\hat{W}_2$ are uniformly ultimately bounded (UUB) [20] with bounds given by (342) and (344).

9.3. FORMATION STABILITY

Consider a formation of $N+1$ robots consisting of a leader "l_i" and N followers. Let the torque control inputs $\begin{bmatrix}\tau_L & u_L\end{bmatrix}^T$ be applied to the leader such that the leader tracks a virtual reference robot. The torque control inputs for the leader can be derived in a similar way as the torque control inputs for the follower. It is assumed that the leader's motion is known i.e. there exists a control law that drives the leader independently to its desired trajectory. The torque control inputs by (326) and(327). Then the origin given by $E = \begin{bmatrix} e_{l_1} & e_{l_2} & e_{l_3} & e_{vl} & e_{\phi l} & e_{F1i}^T & e_{F2i}^T & e_{F3i}^T & e_{vFi}^T & e_{\phi Fi}^T \end{bmatrix}^T$ where $E \in \Box^{(5(N+1))X1}$, which represents the augmented position, orientation and velocity tracking error systems for the leader "l_i" and N followers, respectively, is asymptotically stable in the presence of uncertainties and noise is proved below.

Consider the following Lyapunov candidate function

$$V_{Formation} = \sum_{1}^{N} V_{NEWi} + V_{l_1} \tag{349}$$

where V_{NEWi} is given by (332) and

$$V_{l_1} = e_{l_1}^2 + e_{l_2}^2 + e_{l_3}^2 + e_{vl}^2 + e_{\phi l}^2 \tag{350}$$

Also (349) is positive for $E = \begin{bmatrix} e_{l_1} & e_{l_2} & e_{l_3} & e_{vl} & e_{\phi l} & e_{F1i}^T & e_{F2i}^T & e_{F3i}^T & e_{vFi}^T & e_{\phi Fi}^T \end{bmatrix}^T \neq 0$. Differentiating (349) yields

$$\dot{V}_{Formation} = \sum_{1}^{N} \dot{V}_{NEWi} + \dot{V}_{l_1} \tag{351}$$

In the previous subsection it has been proved that V_{NEWi} for all $i = 1 to N$ individually is negative outside a compact set and that the errors and the NN weight estimates $\hat{W}_1$ and $\hat{W}_2$ are uniformly ultimately bounded (UUB). Hence, when $\dot{V}_{NEWi} < 0$ for all $i = 1 to N$, so it automatically follows that $\sum_{1}^{N} \dot{V}_{NEWi} < 0$. Also, the leader torque control inputs are designed such that the errors go to zero asymptotically and hence, $\dot{V}_{l_1}$ is negative. Therefore, $\dot{V}_{Formation} < 0$, and the entire formation is asymptotically stable.

9.4. RESULTS AND DISCUSSION

A single leader single follower scenario is considered and the simulations are carried out using MATLAB for the same. The leader executes a circular trajectory with radius = 60 m, linear velocity of 5 m/sec and an angular velocity ~ 0.08 rad/sec. It is desired for the follower to execute a circle of radius = 56 m being parallel to the leader at all times. So the desired relative distance to be maintained is 4.0774 m and a relative bearing angle of 78.8199 degrees. The gains used during simulation are $K = 1$, $K_3 = 5.5$, $K_4 = 45$, $K_5 = 45$, $k_1 = 20$, $k_2 = 5$, $k_3 = 2.1$, $k_4 = 40$ and $k_5 = 1$. The results obtained are presented below.

Figure 9.1 shows the position and orientation of the follower. The trajectories traced by the leader and follower are shown in Figure 9.2. The drive and steering torque plot is given in Figure 9.3. From the Figure 9.4, Figure 9.5 and Figure 9.6 it can be seen that the position errors and the velocity error do not go to zero. This is reflected in the follower not being able to keep the formation which can be observed from Figure 9.7. Figure 9.8 shows the error rate plots and Figure 9.9 shows the velocity profile of the

follower. The optimal set of gains that will make the errors go to zero could not be arrived at.

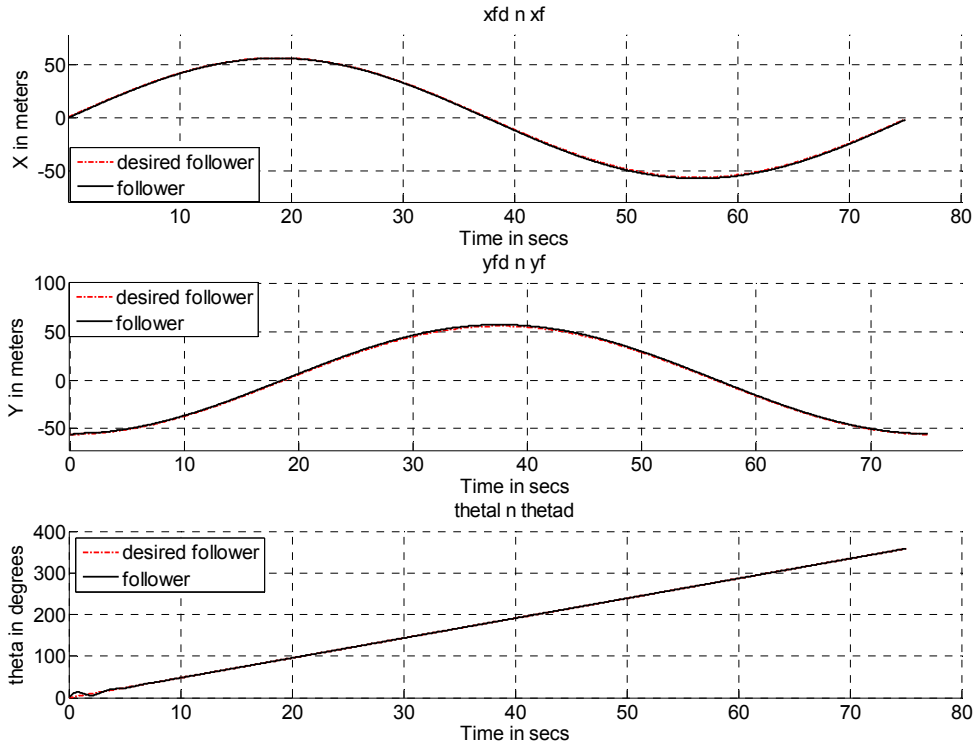

Figure 9.1 Actual and Desired Position and Orientation of the Follower

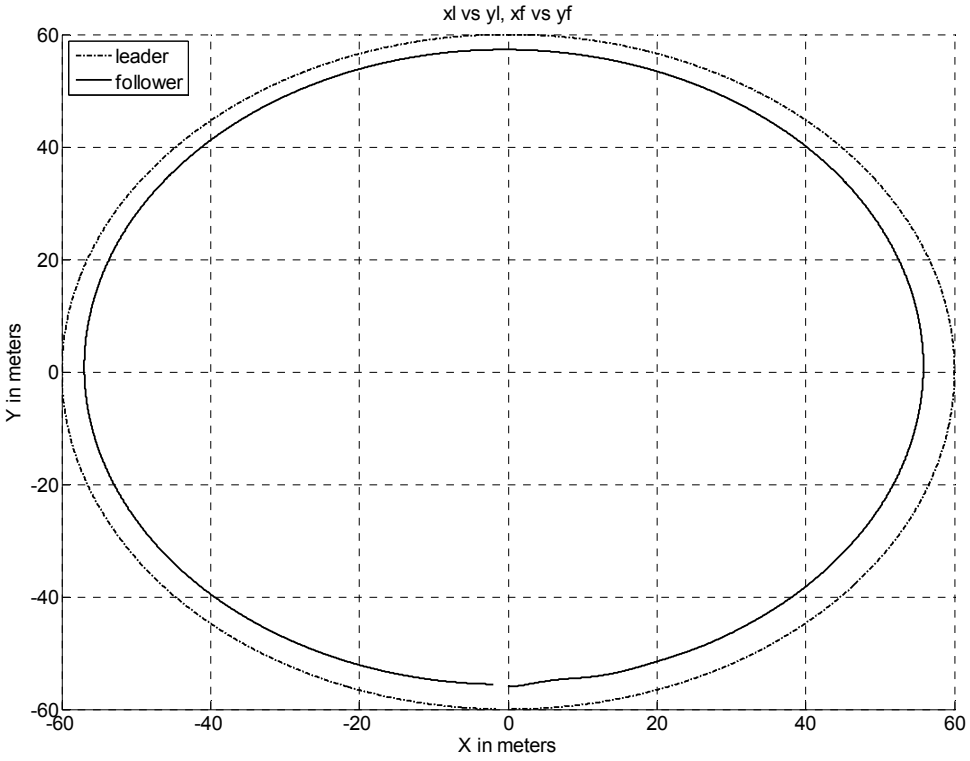

Figure 9.2 Leader and Follower Trajectories

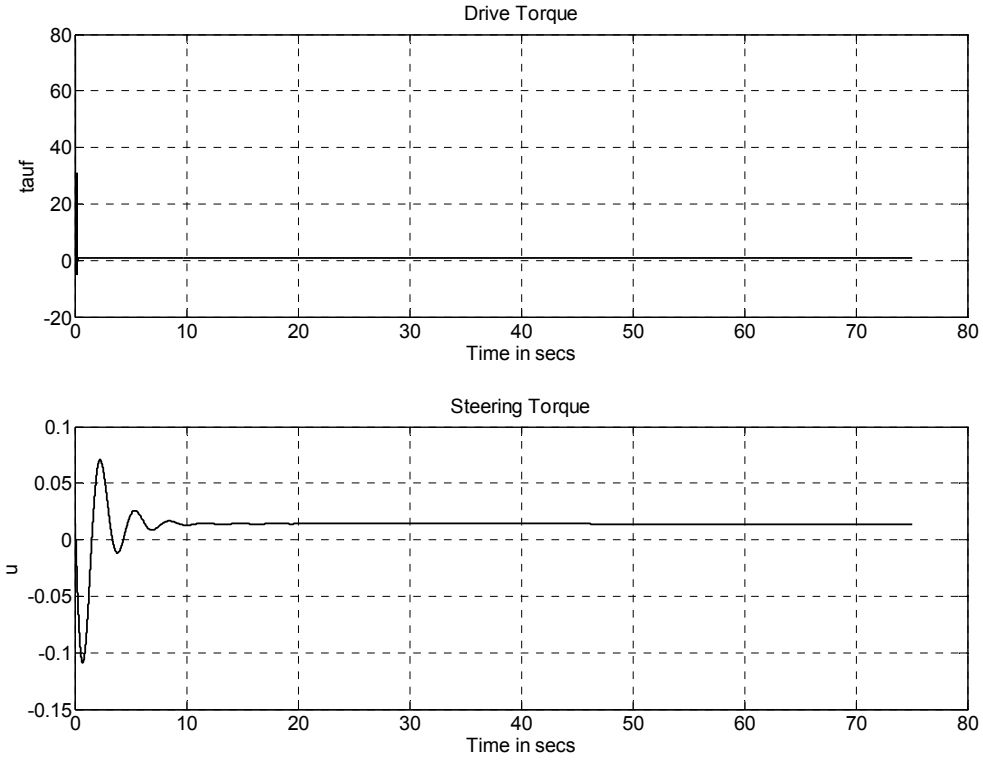

Figure 9.3 Drive and Steering Torques

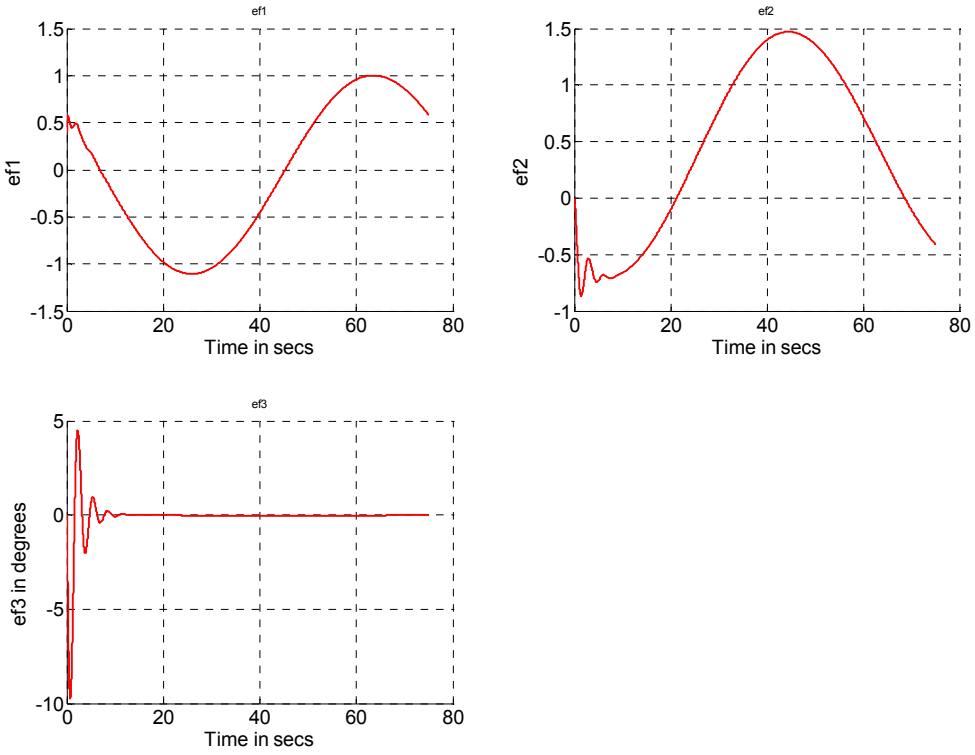

Figure 9.4 Position and Orientation Errors in Body Coordinates

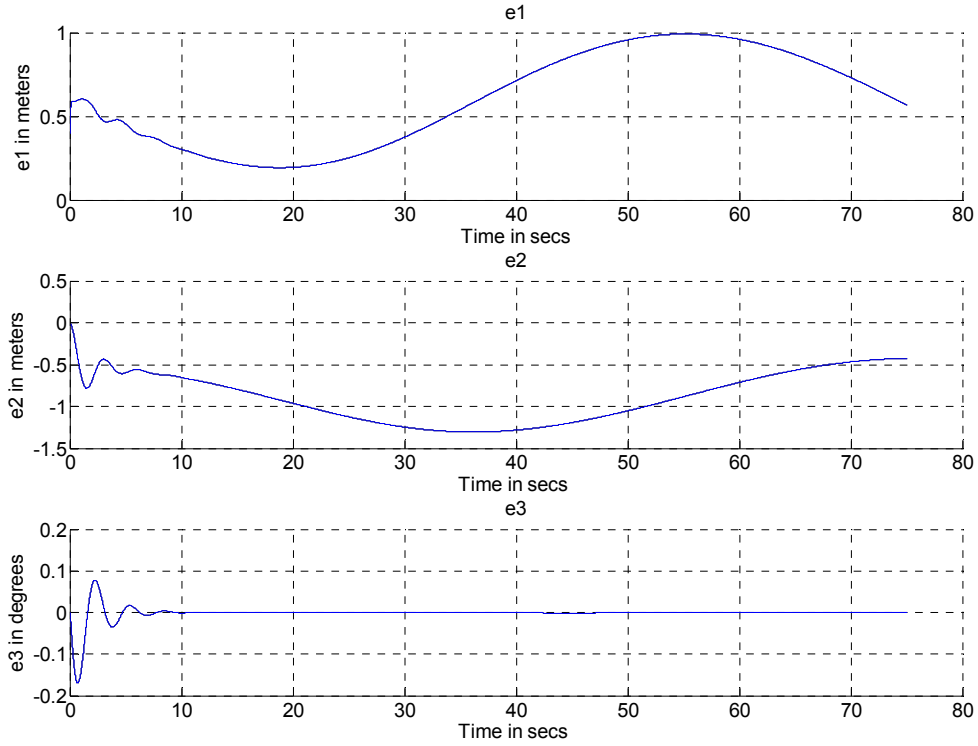

Figure 9.5 Position and Orientation Errors in Inertial Coordinates

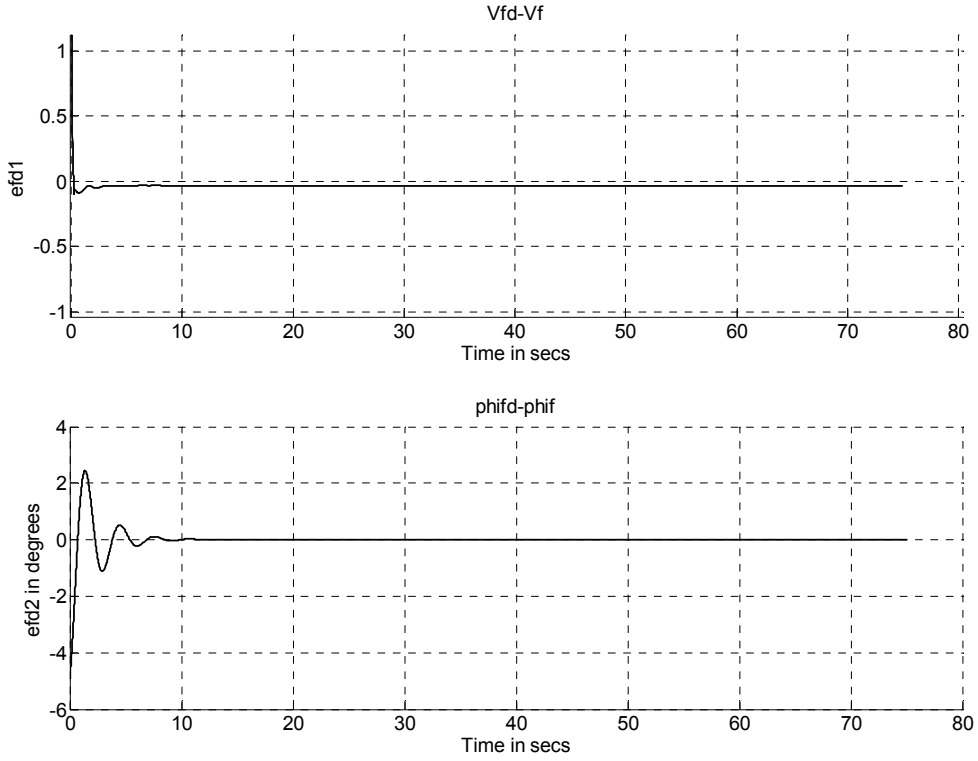

Figure 9.6 Velocity and Steering Angle Error Plots

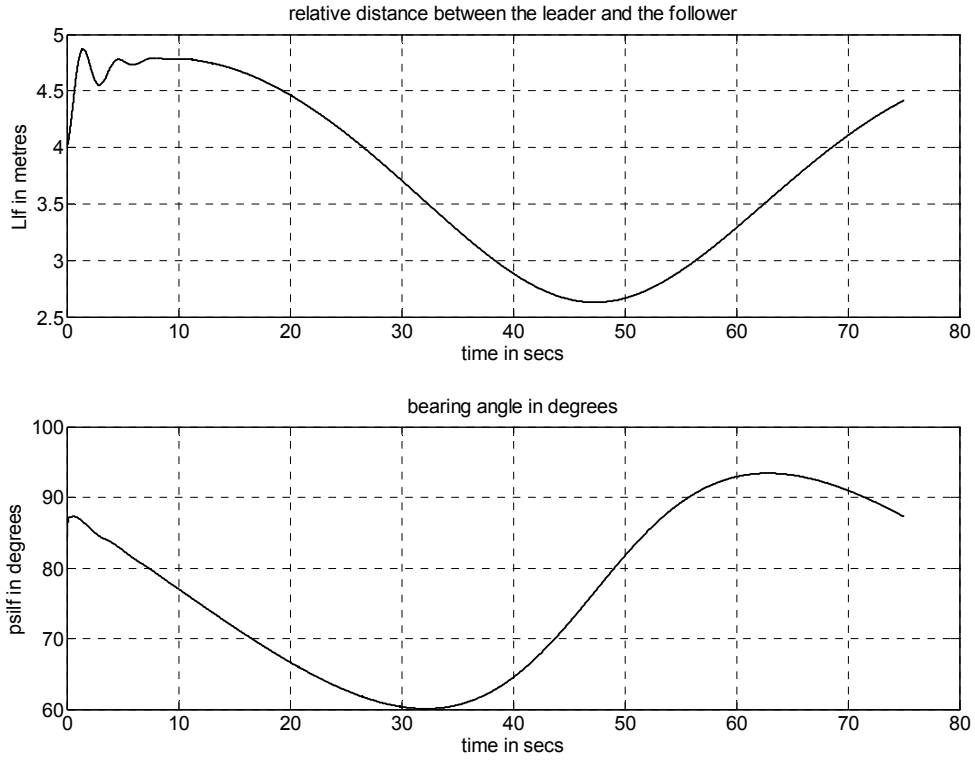

Figure 9.7 Relative Distance and Relative Bearing of the Follower w.r.t. Leader

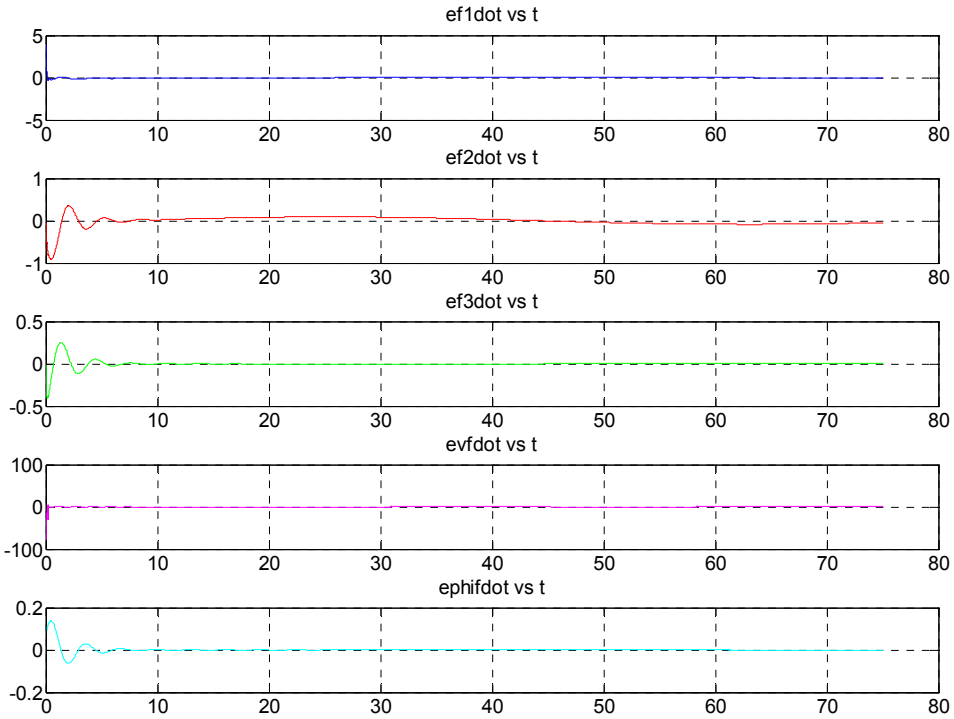

Figure 9.8 Error Rate Plots

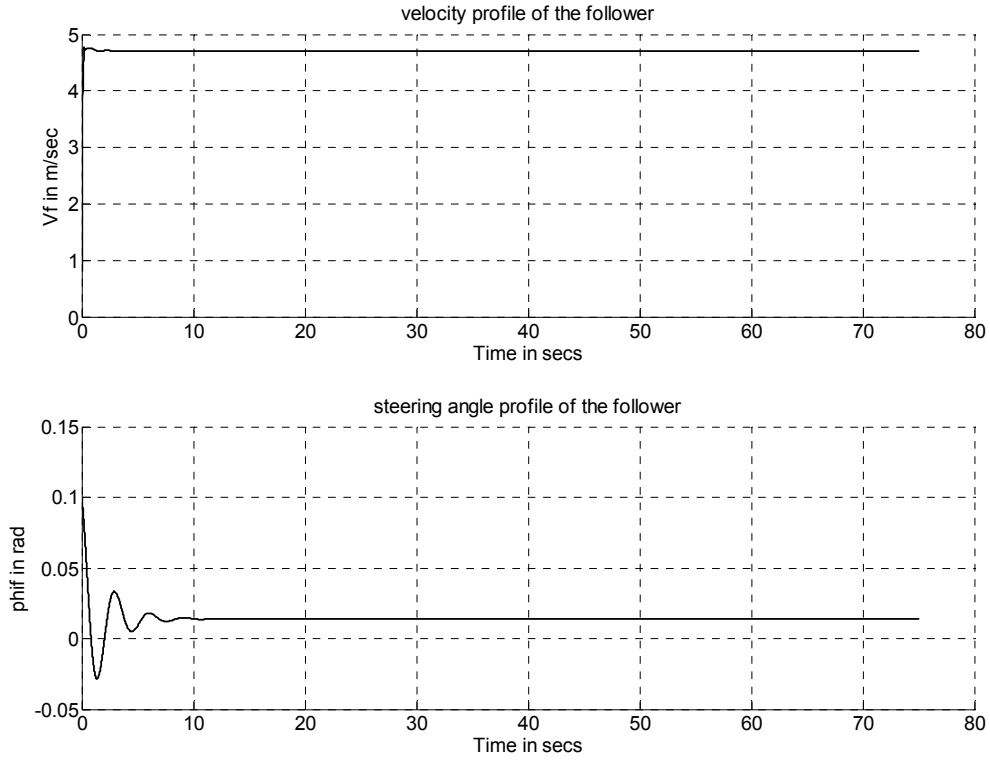

Figure 9.9 Linear and Angular Velocity Profile of the Follower

BIBLIOGRAPHY

[1] J.Shao, G.Xie and L.Wang , " Leader-Following Formation Control of Multiple Mobile Vehicles," *IET Control Theory and Appln*, vol.1 , no.2, pp 545-552 , March 2007 .

[2] E.N. Moret , "Dynamic Modeling and Control of a Car-like Robot," *Thesis Dissertation* , Virginia Tech , Feb 2003.

[3] De Luca, G. Oriolo and C. Samson, "*Robot Motion Planning and Control*," Chapter 4, http://www.laas.fr/ jpl/book.html. Dec. 1999.

[4] R. Fierro and F.L. Lewis, "Control of a Nonholonomic Mobile Robot: Backstepping Kinematics Into Dynamics," *Proc. IEEE Conf. on Decision and Contr.*,Kobe, Japan, 1996, pp. 1722-1727.

[5] M. Egerstedt, X. Hu, and A. Stotsky, "Control of Mobile Platforms Using a Virtual Vehicle Approach," *IEEE Transactions on Automatic Control*, vol. 46, pp 1777-1782, November 2001.

[6] R. Fierro and F. L. Lewis, "Control of a Nonholonomic Mobile Robot Using Neural Networks", *IEEE Transactions on Neural Networks*, vol. 8, pp589-600, July1998.

[7] Y. Kanayama, Y. Kimura, F. Miyazaki, and T. Noguchi, "A Stable Tracking Control Method for an Autonomous Mobile Robot," *Proc. IEEE International Conference on Robotics and Automation*, vol. 1, pp384-389, May 1990.

[8] T. Fukao, H. Nakagawa, and N. Adachi, "Adaptive Tracking Control of a Nonholonomic Mobile Robot," *IEEE Transactions on Robotics and Automation*, vol.16, pp 609-615, October 2000.

[9] J.Shao, G.Xie and L.Wang , " Leader-Following Formation Control of Multiple Mobile Vehicles," *IET Control Theory and Appln*, vol.1 , no.2, pp 545-552 , March 2007 .

[10] X. Li, J. Xiao, and Z. Cai, "Backstepping Based Multiple Mobile Robots Formation Control," *Proc. IEEE International Conference on Intelligent Robots and Systems*, pp 887-892, August 2005.

[11] T. Dierks and S. Jagannathan, "Control of Nonholonomic Mobile Robot Formations: Backstepping Kinematics into Dynamics," *Thesis Dissertation*, UMR, 2007.

[12] J. Fredslund and M. Mataric, "A General Algorithm for Robot Formations Using Local Sensing and Minimal Communication," *IEEE Transactions on Robotics and Automation*, vol. 18, pp 837-846, October 2002.

[13] G. L. Mariottini, G. Pappas, D. Prattichizzo, and K. Daniilidis, "Vision-based Localization of Leader-Follower Formations," *Proc. IEEE European Control Conference on Decision and Control*, pp 635-640,December2005.

[14] K. H. Tan and M. A. Lewis, "Virtual Structures for High-Precision Cooperative Mobile Robotic Control," *Proceedings of the 1996 IEEE/RSJ International Conference Intelligent Robots and Systems*, vol. 1, pp. 132–139, November 1996

[15] P. Ogren, M. Egerstedt, and X. Hu, "A Control Lyapunov Function Approach to Multiagent Coordination," *IEEE Transactions on Robotics and Automation*, vol.18,pp 847-851, October 2002.

[16] T. Balch and R. Arkin, "Behavior-Based Formation Control for Multirobot Teams," *IEEE Transaction on Robotics and Automation*, vol. 15, pp 926-939,December 1998.

[17] J. Lawton, R. Bear, and B. Young, "A Decentralized Approach to Formation Maneuvers," *IEEE Transactions on Robotics and Automation*, vol. 19, pp 933 - 941,December 2003

[18] J.P.Desai, J.P.Ostrowski and V.J.Kumar, "Modeling and Control of Formations of Nonholonomic Mobile Robots," *IEEE Trans. Robot Automation*, vol 17, pp 905-908 , 2001.

[19] M.Xin and S.N.Balakrishnan, "Integrated Guidance and Control of Missiles with $\theta - D$ Method ," *IEEE Transactions on Control Systems Technology*, vol. 14, no. 6, pp 981-992, November 2006.

[20] J.R. Cloutier and D.T.Stansbery, "The Capabilities and Art of State-Dependent Riccati Equation-Based Design," *Proc. Of American Control Conference*, Anchorage, AK, May 2002, pp. 86-91.

[21] R.A. Hull , J.R. Cloutier, C.P. Mracek and D.T.Stansbery, "State-Dependent Riccati Equation Solution of the Toy Nonlinear Optimal Control Problem," *Proc. Of American Control Conference*, Philadelphia, Pennsylvania, Jun. 1998, pp. 1658-1662.

[22] J.R. Cloutier, "State-dependent Riccati equation techniques: an overview," *Proc. of the American Control Conference*, Albuquerque, New Mexico, Jun. 1997, pp. 932- 936.

[23] E.B. Erdem and A.G. Alleyne, "Design of a class of nonlinear controllers via state dependent Riccati equations," *IEEE Trans. On Control Systems Technology*, vol. 12, no. 1, Jan. 2004, pp.133-137

[24] C. P. Mracek and J. R. Cloutier, "Control designs for the nonlinear benchmark problem via the State-Dependent Riccati Equation method," I*nt. J. Robust Nonlinear Control*, vol. 8, no. 4/5, pp. 401–433, 1998.

[25] J.R.Cloutier and J.C.Cockburn, "The state-dependent nonlinear regulator with state constraints," *Proc. Of American Control Conference*, vol.1, 2001 pp. 390-395 .

[26] V.Yadav, R.Padhi and S.N.Balakrishnan, "Robust/Optimal Temperature Profile Control of a High-Speed Aerospace Vehicle Using Neural Networks," *IEEE Transactionsons on Neural Networks*, vol 18, no. 4, pp 1115 – 1128, July 2007.]

[27] F.L.Lewis, S. Jagannathan and A.Yesildirek, "*Neural Network Control of Robot Manipulators and Nonlinear Systems*," Taylor and Francis, 1999.

[28] B.Friedland, "Control *Systems Design: An Introduction to State Space Methods*," Dover Books on Engineering.

[29] F. L. Lewis "*Applied Optimal Control and Estimation*", Prentice Hall 1992, ch.3.

[30] Z. Qu and J.R. Cloutier, "A New Suboptimal Control Design for Cascaded Non-linear Systems," *Proc. Of American Control Conference*, Chicago, Illinois, Jun. 2000, pp. 3903-3907.

VITA

Shweta Annapurani Panimadai Ramaswamy was born in Bellary, India on August 21, 1983. She earned a Bachelor of Engineering degree in Electrical and Electronics Engineering while attending SSN College of Engineering affiliated to the Anna University, India in May of 2005. While attending the Missouri University of Science and Technology she earned a Master of Science degree in Electrical Engineering in May of 2008.